

IEEE Recommended Practice for Radio-Frequency (RF) Absorber Evaluation in the Range of 30 MHz to 5 GHz

Sponsor

**Standards Committee
of the
IEEE Electromagnetic Compatibility Society**

Approved 13 January 1998

IEEE Standards Board

Abstract: Realistic and repeatable criteria, as well as recommended test methods, for characterizing the absorption properties of typical anechoic chamber linings applied to a metallic surface are described. Parameters and test procedures are described for the evaluation of RF absorbers to be used for radiated emissions and radiated susceptibility testing of electronic products, in the absorber manufacturer and/or absorber user environment, over the frequency range of 30 MHz to 5 GHz.

Keywords: anechoic chamber, radiated emissions, RF absorber, semianechoic chamber

The Institute of Electrical and Electronics Engineers, Inc.
345 East 47th Street, New York, NY 10017-2394, USA

Copyright © 1998 by the Institute of Electrical and Electronics Engineers, Inc.
All rights reserved. Published 1998. Printed in the United States of America.

ISBN 1-55937-986-3

No part of this publication may be reproduced in any form, in an electronic retrieval system or otherwise, without the prior written permission of the publisher.

IEEE Standards documents are developed within the IEEE Societies and the Standards Coordinating Committees of the IEEE Standards Board. Members of the committees serve voluntarily and without compensation. They are not necessarily members of the Institute. The standards developed within IEEE represent a consensus of the broad expertise on the subject within the Institute as well as those activities outside of IEEE that have expressed an interest in participating in the development of the standard.

Use of an IEEE Standard is wholly voluntary. The existence of an IEEE Standard does not imply that there are no other ways to produce, test, measure, purchase, market, or provide other goods and services related to the scope of the IEEE Standard. Furthermore, the viewpoint expressed at the time a standard is approved and issued is subject to change brought about through developments in the state of the art and comments received from users of the standard. Every IEEE Standard is subjected to review at least every five years for revision or reaffirmation. When a document is more than five years old and has not been reaffirmed, it is reasonable to conclude that its contents, although still of some value, do not wholly reflect the present state of the art. Users are cautioned to check to determine that they have the latest edition of any IEEE Standard.

Comments for revision of IEEE Standards are welcome from any interested party, regardless of membership affiliation with IEEE. Suggestions for changes in documents should be in the form of a proposed change of text, together with appropriate supporting comments.

Interpretations: Occasionally questions may arise regarding the meaning of portions of standards as they relate to specific applications. When the need for interpretations is brought to the attention of IEEE, the Institute will initiate action to prepare appropriate responses. Since IEEE Standards represent a consensus of all concerned interests, it is important to ensure that any interpretation has also received the concurrence of a balance of interests. For this reason, IEEE and the members of its societies and Standards Coordinating Committees are not able to provide an instant response to interpretation requests except in those cases where the matter has previously received formal consideration.

Comments on standards and requests for interpretations should be addressed to:

Secretary, IEEE Standards Board
445 Hoes Lane
P.O. Box 1331
Piscataway, NJ 08855-1331
USA

Note: Attention is called to the possibility that implementation of this standard may require use of subject matter covered by patent rights. By publication of this standard, no position is taken with respect to the existence or validity of any patent rights in connection therewith. The IEEE shall not be responsible for identifying patents for which a license may be required by an IEEE standard or for conducting inquiries into the legal validity or scope of those patents that are brought to its attention.

Authorization to photocopy portions of any individual standard for internal or personal use is granted by the Institute of Electrical and Electronics Engineers, Inc., provided that the appropriate fee is paid to Copyright Clearance Center. To arrange for payment of licensing fee, please contact Copyright Clearance Center, Customer Service, 222 Rosewood Drive, Danvers, MA 01923 USA; (508) 750-8400. Permission to photocopy portions of any individual standard for educational classroom use can also be obtained through the Copyright Clearance Center.

Introduction

[This introduction is not part of IEEE Std 1128-1998, IEEE Recommended Practice for Radio-Frequency (RF) Absorber Evaluation in the Range of 30 MHz to 5 GHz.]

Interest in materials that absorb radio-frequency energy has existed for many years. The recent increased regulation of sources of radio waves and equipment immunity levels has led to the need for a more accurate determination of electromagnetic field intensity. As modern measuring antennas and receivers have increased measurement accuracy, the problem of making accurate measurements in less than optimum open-area test sites has become a more important part of the overall measurement procedures. The practice of placing absorbing materials on the walls and ceilings of measuring sites to reduce reflections from these surfaces has become common. Claims for the efficacy of various absorbing materials, however, have led to conflicting reports in the literature, which confuse many potential purchasers of absorbing material. An effort to end that confusion led to the development of a draft recommended practice in 1986. Following several years of work, the current recommended practice was developed.

At the time this recommended practice was completed, the working group had the following membership:

Anatoly Tsailovich, <i>Vice Chair</i>	Jose Perini, <i>Chair</i>	Ferdy Mayer, <i>Secretary</i>
Paul Anderson	H. R. Hofmann	Walter D. Mc Kerchar
Edwin L. Bronaugh	Motohisa Kanda	Fernando Mendoza
Frederic J. Broyde	Keneth K. Kimura	John D. Osburn
Donald E. Clark	James C. Klouda	Barry Pate
Larry S. Cohen	Brian F. Lawrence	Ghery S. Petit
William E. Cory	Ming-Chiang Li	Hugo Pues
Heinrich Garn	Kefeng Liu	Scott Roleson
David Giangiulli	L. Van De Looverbosch	Gabriel A. Sanchez
Franz Gisin	Atsuya Maeda	Verner Schaefer
Diethard Hansen	Luc Martens	James R. Stidman
	William H. McGinnis	

The following individuals have contributed reviews and comments and have attended meetings:

Randy Anderson	Donald N. Heirman	Detlef Ristan
J. P. Chaumat	John Howard	M. Sekimoto
Tim D'Arcangelis	Edward F. Kuester	Shrish Shah
Hugh W. Denny	Robert Martens	K. Shinada
Michael Foegelle	D. Mc Nulty	James Royal
Tim Harrington	Monika Neufingeri	Gary F. E. Vrooman
Grahme Harveyu		Donald A. Weber

The following persons were on the balloting committee:

Stephen H. Berger	Donald N. Heirman	A. Piper
Edwin L. Bronaugh	Daniel D. Hoolihan	J. H. Pluck
Frederic J. Broyde	Atsuya Maeda	Scott Roleson
Joseph E. Butler	Ferdy Mayer	David Seabury
Donald E. Clark	John D. Osburn	Ralph M. Showers
William E. Cory	Jose Perini	Donald L. Sweeney
Hugh W. Denny	Ghery Pettit	David L. Traver
Heinrich Garn		Graham Wilson

The final conditions for approval of this recommended practice were met on 13 January 1998. This recommended practice was conditionally approved by the IEEE Standards Board on 9 December 1997, with the following membership:

Donald C. Loughry, *Chair*

Richard J. Holleman, *Vice Chair*

Andrew G. Salem, *Secretary*

Clyde R. Camp
Stephen L. Diamond
Harold E. Epstein
Donald C. Fleckenstein
Jay Forster*
Thomas F. Garrity
Donald N. Heirman
Jim Isaak
Ben C. Johnson

Lowell Johnson
Robert Kennelly
E. G. "Al" Kiener
Joseph L. Koepfinger*
Stephen R. Lambert
Lawrence V. McCall
L. Bruce McClung
Marco W. Migliaro

Loius-François Pau
Gerald H. Peterson
John W. Pope
Jose R. Ramos
Ronald H. Reimer
Ingo Rüsck
John S. Ryan
Chee Kiow Tan
Howard L. Wolfman

*Member Emeritus

Also included are the following nonvoting IEEE Standards Board liaisons:

Satish K. Aggarwal
Alan H. Cookson

Contents

1.	Introduction.....	1
1.1	Scope.....	1
1.2	Applications.....	1
2.	References.....	2
3.	Definitions and acronyms.....	2
3.1	Definitions.....	2
3.2	Acronyms.....	4
4.	Measurement instrumentation.....	5
4.1	Spectrum analyzers.....	5
4.2	Spectrum analyzer and tracking generator.....	8
4.3	Electromagnetic interference (EMI) receiver.....	11
4.4	Vector network analyzers.....	13
4.5	Scalar network analyzers.....	13
4.6	Vector voltmeter.....	14
4.7	Time-domain reflectometer.....	15
4.8	EMC antennas.....	16
5.	Test environment parameter guidelines.....	17
6.	Material bulk-parameter evaluation.....	17
6.1	Background.....	18
6.2	Bulk-parameter measurement procedures.....	21
7.	Evaluation of the reflectivity of RF absorbers.....	26
7.1	Background.....	26
7.2	RF absorber reflectivity measurement procedures.....	28
8.	RF absorber performance in ATS, ALC, and semianechoic absorber-lined chambers (SALC).....	49
8.1	Background.....	49
8.2	ATS and ALC measurement procedure.....	50
8.3	Semianechoic chamber measurement procedure.....	55
9.	Test reports.....	57
9.1	Test report content.....	57
9.2	Test report disposition.....	57
10.	Bibliography.....	57

IEEE Recommended Practice for Radio-Frequency (RF) Absorber Evaluation in the Range of 30 MHz to 5 GHz

1. Introduction

1.1 Scope

The purpose of this recommended practice is to recommend realistic and repeatable criteria, as well as recommended test methods, to characterize the absorption properties of typical anechoic chamber linings applied to a metallic surface. This recommended practice covers the parameters and test procedures for the evaluation of radio-frequency (RF) absorbers to be used for radiated emissions and radiated susceptibility testing of electronic products, in the absorber manufacturer and/or absorber user environment, over the frequency range of 30 MHz to 5 GHz.

The recommended methods approach the RF absorber evaluation at three levels:

- a) RF absorber materials bulk parameters
- b) Arrays of commercially available RF absorbers
- c) RF absorbers in actual applications, as in anechoic or semianechoic chambers and lined open-area test sites.

The evaluation measurements can be performed in frequency and/or time domain. This recommended practice, however, does not address the accuracy and limitations of the different evaluation methods. These issues will be addressed in future revisions of this recommended practice.

1.2 Applications

With the proliferation of RF absorber-lined shielded rooms, and their wide utilization for testing equipment for radiated emissions and radiated susceptibility, there is a need to provide repeatable and realistic performance figures of such RF absorbers in the frequency range of 30 MHz to 5 GHz and higher.

Up until now, the data provided by many manufacturers usually has been for normal incidence only. This data eliminates the effect of polarization on the RF absorber performance. For RF absorbers that use a pyramidal structure, the reflection coefficient is also a function of the alignment of the incident wave with the pyramidal structure, especially for high frequencies and for large angles of incidence. Furthermore, only the magnitude of the reflection coefficient typically is provided by the manufacturers. The lack of these kinds of data precludes the accurate calculation of the performance of RF absorber materials in the great majority of applications.

This recommended practice is intended as an aid to RF absorber users and manufacturers. It indicates the type of data that is required by the design engineer and the various methods that may be used to obtain such data. It is hoped that, in the future, both manufacturers and users will utilize the same or accepted equivalent methods to estimate the performance of RF absorbers.

2. References

This recommended practice should be used in conjunction with the following documents:

ANSI C63.2-1996, American National Standard for Electromagnetic Noise and Field Strength Instrumentation, 10 kHz to 40 GHz Specifications.¹

ANSI C63.4-1992, American National Standard for Methods of Measurement of Radio-Noise Emissions from Low-Voltage Electrical and Electronic Equipment in the Range of 9 kHz to 40 GHz.

IEC/CISPR 16-1 (1993-08), Specifications for radio disturbance and immunity measuring apparatus and methods—Part 1: Radio disturbance and immunity measuring apparatus.²

3. Definitions and acronyms

3.1 Definitions

For the purposes of this recommended practice, the following terms and definitions shall apply.

3.1.1 absorber-lined chamber (ALC): A room or enclosure (either shielded or unshielded) with all of its surfaces lined with radio-frequency (RF) absorber material. Commonly referred to as an anechoic chamber.

3.1.2 absorber-lined open-area test site (ATS): An open-area test site (OATS) in which the ground plane is covered with radio-frequency (RF) absorber to suppress ground reflections. *See also: open-area test site (OATS).*

3.1.3 angle of incidence: At a point on a surface, the acute angle between the normal to this surface and the direction of propagation of an incident wave.

3.1.4 antenna factor: a) Quantity relating the strength of the field in which an antenna is immersed to the output voltage across the load connected to the antenna. b) A factor that, when properly applied to the voltage meter reading of the measuring instrument, yields the electric field strength in volts/meter or the magnetic field strength in amperes/meter.

NOTES

¹—This factor includes the effects of antenna effective length and mismatch and may include transmission line loss.

²—The factor for the electric field strength is not necessarily the same as the factor for the magnetic field strength.

³—The antenna factor, as determined in ANSI C63.5-1988, is very nearly equal to the free-space antenna factor.

3.1.5 bistatic reflectivity: The reflectivity when the reflected wave is in any specified direction other than back toward the transmit antenna. The transmit and receive antennas are at different locations.

¹ANSI C63 publications are available from the Institute of Electrical and Electronics Engineers, 445 Hoes Lane, P.O. Box 1331, Piscataway, NJ 08855-1331, USA; or from the Sales Department, American National Standards Institute, 11 West 42nd Street, 13th Floor, New York, NY 10036, USA.

²CISPR documents are available from the International Electrotechnical Commission, 3, rue de Varembe, Case Postale 131, CH 1211, Genève 20, Switzerland/Suisse. They are also available in the United States from the Sales Department, American National Standards Institute, 11 West 42nd Street, 13th Floor, New York, NY 10036, USA.

3.1.6 bulk parameters: Complex permittivity, complex permeability, and conductivity properties of the bulk material used in the radio-frequency (RF) absorber. The conductivity may be included in the imaginary part of the complex permittivity.

3.1.7 diffuse scattering: Scattering of incident electromagnetic energy over a range of angles other than the specular direction.

3.1.8 equipment under test (EUT): The equipment being measured or tested, as opposed to support or ancillary equipment.

3.1.9 equivalent reflection coefficient (ERC): The measure of the reflection coefficient of an actual radio-frequency (RF) absorber-lined reflecting surface. The ERC includes not only the RF absorber reflection, but other effects such as mounting fixtures, adhesive, and any air space between the RF absorber and the reflecting surface.

3.1.10 frequency domain: A function in which frequency is the independent variable.

3.1.11 gigahertz transverse electromagnetic (GTEM) cell: A tapered transverse electromagnetic (TEM) cell with an absorber-lined end wall terminated with an absorber load.

3.1.12 intrinsic impedance: For a monochromatic (time harmonic) electromagnetic wave propagating in a homogenous medium, the ratio of the complex amplitude of the electric field to that of the magnetic field.

NOTE—The intrinsic impedance of a medium is sometimes referred to as the characteristic impedance of the medium.

3.1.13 monostatic reflectivity: Reflectivity in which the reflected and incident waves follow the same path but in opposite directions. The transmit and receive antennas are in the same location, and normal incidence occurs at the reflecting surface.

3.1.14 open-area test site (OATS): A site that meets specified requirements for measuring radio-interference fields radiated by an equipment under test (EUT).

3.1.15 parallel polarization: The polarization of a wave for which the electric field vector lies in the plane of incidence.

NOTE—This is sometimes called vertical or transverse magnetic (TM) polarization.

3.1.16 perpendicular polarization: The polarization of a wave for which the electric field is perpendicular to the plane of incidence.

NOTE—This is sometimes called horizontal or transverse electric (TE) polarization.

3.1.17 plane of incidence: The plane containing the normal to the surface of a boundary and the phase vector (β) of the incident wave.

3.1.18 quiet zone: A described volume within an anechoic chamber where electromagnetic waves reflected from the walls, floor, and ceiling are stated to be below a certain specified minimum. The quiet zone may have a spherical, cylindrical, rectangular, etc., shape depending on the chamber characteristics.

3.1.19 radio-frequency (RF) absorber: A material designed to absorb electromagnetic energy. The material may have a flat face or may be formed into pyramids, wedges, or cones. Radar absorber material is commonly referred to as RAM.

3.1.20 reflectivity (R): For a radio-frequency (RF) absorber, the ratio of the plane wave reflected power density (P_r) to the plane wave incident power density (P_i) at a reference point in space. It is expressed in dB as $R = 10 \log_{10}(P_r/P_i)$.

3.1.21 reflectometer, time-domain: An instrument designed to indicate and to measure reflection characteristics of a transmission system connected to the instrument by monitoring the step-formed signals entering the test object and the superimposed reflected transient signals on an oscilloscope that is equipped with a suitable time-based sweep. The measuring system basically consists of a fast-rise function generator, a tee coupler, and an oscilloscope connected to the probing branch of the coupler.

3.1.22 return loss: The ratio, in dB, of the power incident upon the discontinuity to the power reflected from the discontinuity.

NOTE—This ratio is also the square of the reciprocal of the magnitude of the reflection coefficient.

3.1.23 scattering matrix: An $n \times n$ (square) matrix used to relate incident waves and reflected waves for an n -port network.

3.1.24 semianechoic absorber-lined chamber (SALC): A room or enclosure (either shielded or unshielded) with all its surfaces, except the floor, lined with radio-frequency (RF) absorber material. The floor is covered with a good conductor.

3.1.25 site attenuation: a) The ratio of the power input to a matched, balanced, lossless, tuned dipole radiator to that at the output of a similarly matched, balanced, lossless, tuned dipole receiving antenna for specified polarization, separation, and heights above a flat reflecting surface. It is a measure of the transmission path loss between two antennas.

NOTE—The above is the classical definition of site attenuation. In ANSI C63.4-1992, the definition is extended to cover broadband antennas as well as tuned dipole antennas.

b) The ratio of the power input to a matched, balanced, lossless, wideband dipole radiator to that at the output of a similarly balanced, matched, lossless, wideband dipole receiving antenna for specified polarization, separation, and heights above a flat reflecting surface.

3.1.26 site-attenuation deviation (SAD): The difference, in dB, of the site attenuation and the free-space distance attenuation between the transmit and receive antennas in an open-area test site (OATS), absorber-lined open-area test site (ATS), semianechoic chamber, or anechoic chamber. *See also:* **absorber-lined open-area test site (ATS)** and **open-area test site (OATS)**.

3.1.27 specular reflection: The reflection of a wave when incident on an infinite planar surface. The angle of incidence is equal to the angle of reflection.

3.1.28 standing wave: A wave in which, for any component of the field, the ratio of its instantaneous value at one point to that at any other point does not vary with time. A pure standing wave results from the interference of two oppositely directed traveling waves of the same frequency and amplitude.

3.1.29 time domain: A function in which the signals are represented as a function of time.

3.1.30 transverse electromagnetic wave (TEW): An electromagnetic wave in which both the electric and magnetic field vectors are perpendicular everywhere to the direction of propagation.

3.2 Acronyms

AF	antenna factor
ALC	absorber-lined chamber
ATS	absorber-lined open-area test site
BPF	bandpass filter
CRT	cathode ray tube

CW	continuous wave
DFT	Discrete Fourier Transform
DUT	device under test
FM	frequency modulation
EMC	electromagnetic compatibility
EMI	electromagnetic interference
ERC	equivalent reflection coefficient
EUT	equipment under test
FFT	Fast Fourier Transform
IF	intermediate frequency
LCR	low-frequency coaxial reflectometer
OATS	open-area test site
OSAD	open-site-attenuation deviation
RAM	radar absorber material
RBW	resolution bandwidth
RF	radio frequency
SAD	site-attenuation deviation
SALC	semianechoic absorber-lined chamber
TDR	time-domain reflectometer
TE	transverse electric
TEM	transverse electromagnetic
TEW	transverse electromagnetic wave
TM	transverse magnetic
VBW	video bandwidth
VSWR	voltage standing wave ratio

4. Measurement instrumentation

4.1 Spectrum analyzers

4.1.1 Introduction

Superheterodyne spectrum analyzers are widely used in applications that are electromagnetic compatibility (EMC) related. Other spectrum analyzer architectures, such as Fast Fourier Transform (FFT) analyzers, do have some limitations relative to the superheterodyne spectrum analyzers in the areas of frequency range, sensitivity, and dynamic range. The ability of the FFT analyzer, however, to characterize single-shot phenomena and measure both the magnitude and phase of an emission often makes EMC trouble-shooting much easier or even possible. See [B3]³ and [B4].

Figure 1 shows a simplified block diagram of a superheterodyne spectrum analyzer. An input signal fed into the instrument's RF input passes through an RF attenuator to a mixer, where it mixes with a signal from the local oscillator. Because the mixer is a nonlinear device, its output includes not only the two original signals, but also their harmonics and the sums and differences of the original frequencies and their harmonics. If any of the mixed signals falls within the passband of the intermediate-frequency (IF) filter, it is further amplified, detected by an envelope detector, digitized, and displayed either graphically on a digital display or numerically on a numeric readout. A scan generator generates a ramp voltage, which deflects the cathode ray tube (CRT) beam horizontally across an analog screen and tunes the local oscillator so that its frequency changes in proportion to the ramp voltage. The horizontal axis of the spectrum analyzer display is calibrated in frequency. The vertical axis is calibrated in amplitude. Virtually all analyzers offer the choice of a linear scale, calibrated in V, or a logarithmic scale, calibrated in dB (e.g., referenced to V, mV, μ V, or mW). The

³The numbers in brackets preceded by the letter B correspond to those of the bibliography in Clause 10.

spectrum analyzer often has more than one mixer stage. This second mixing has a constant-frequency local oscillator that converts the first IF frequency to a lower IF. The reason for multiple conversions is to improve image rejection.

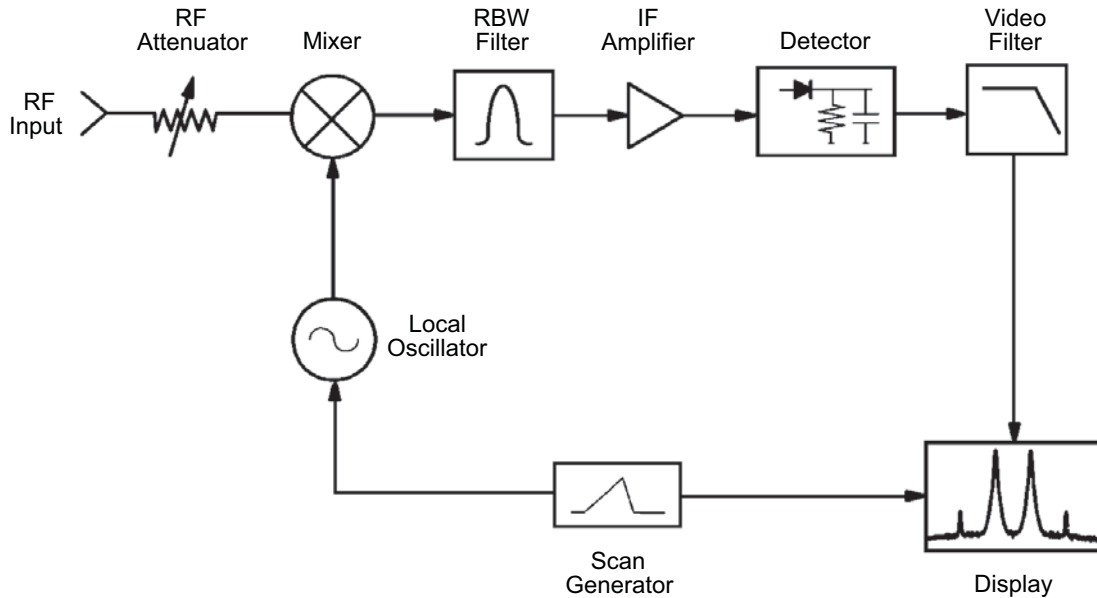


Figure 1—Block diagram of a superheterodyne spectrum analyzer

4.1.2 Input attenuation

The RF attenuator, which can usually be set in 10 dB steps from 0–50 dB (or even higher), is used to condition the amplitude of the input signal in order to avoid mixer saturation and the generation of internal distortion signals, which might also be displayed and mistaken as true signals. The displayed signal-to-noise-floor ratio, the level of the effective noise floor at the input of the analyzer, and the sensitivity of the analyzer are also affected by the RF attenuator setting.

4.1.3 Signal mixing

The mixer is used, along with the local oscillator, to convert the input signal frequency to a fixed IF. Of all the products emerging from the mixer, the two with the greatest amplitudes and, therefore, the two that are most desirable are those created from the sum and the difference of the local oscillator and the input signal. If the frequency of the signal to be examined is either above or below the local oscillator frequency by the IF, one of the desired mixing products will fall within the passband of the IF filter and will appear on the display. The local oscillator frequency is chosen often to produce an IF above the highest tuning frequency. In this case, the tuning equation is

$$f_{\text{sig}} = f_{\text{LO}} - f_{\text{IF}} \quad (1)$$

where

- f_{sig} is the signal frequency (in Hz).
- f_{LO} is the local oscillator frequency (in Hz).
- f_{IF} is the intermediate frequency (in Hz).

The stability of the spectrum analyzer's local oscillator, particularly its first local oscillator, affects the resolution of the instrument. The residual frequency modulation (FM) of the local oscillator is transferred to any mixing product that results from the local oscillator and incoming signals. Therefore, it is not possible to determine whether the signal or the local oscillator is the source of instability. The effects of local oscillator residual FM are not visible in wide resolution bandwidths. Only when the bandwidth approximates the peak-to-peak excursion of the FM does this effect become apparent. For this reason, the minimum bandwidth typically found in a spectrum analyzer is determined at least in part by the local oscillator stability. Another local oscillator attribute, phase noise, also determines the resolution in yet a different manner. Since local oscillators are not perfectly stable, their signals are always frequency or phase modulated to some extent by random noise. As noted before, all instabilities in the local oscillator are transferred to any mixing products; therefore, phase-noise modulation sidebands appear around any spectral component on the display that is far enough above the broadband noise floor of the instrument. The amplitude difference between the displayed spectral component and the phase noise is a function of the stability of the local oscillator as well as the resolution bandwidth. A reduction of the IF filter bandwidth by a factor of 10 will result in a 10 dB decrease of phase-noise level on the display.

4.1.4 IF signal filtering

The IF of a superheterodyne spectrum analyzer is determined by a bandpass filter. This filter selects the desired mixing products (e.g., the sum of the local oscillator and input signal) and rejects all other signals. Because the input signal is fixed and the local oscillator is swept, the products from the mixer are also swept. If a mixing product sweeps past the IF, the characteristics of the bandpass filter are traced on the display. Unless two signals are far enough apart, the traces they cause will fall on top of each other and look like only one response. In this case, individual signals cannot be resolved. Spectrum analyzers, however, have selectable IF filters (e.g., 10 Hz to 3 MHz in a 1-3-10 sequence), so it is usually possible to select one narrow enough to resolve closely spaced signals. Most often, the 3 dB bandwidth of the IF filters are specified, indicating how close together equal amplitude sinusoids can be resolved as two separate signals. The resolution of two signals with unequal amplitude is affected by the filter's shape factor, which is determined by the ratio of the 60 dB bandwidth to the 3 dB bandwidth. Most analog filters in spectrum analyzers are synchronously tuned, have four or five poles, and are nearly Gaussian in shape, which leads to shape factors between 15:1 to 11:1 for narrower filters.

4.1.5 Sweeptime

The selected IF filter also determines the sweeptime, which, in turn, affects the overall measurement time. The bandpass filters are band-limited circuits that require finite times for the filtered signals to reach their maximum amplitude. If the mixing products are swept too quickly, there will be a loss of displayed amplitude and a shift in frequency. The following equation can be used to determine the appropriate sweeptime required to make calibrated measurements (see [B1]):

$$ST = \frac{k \times \text{Span}}{\text{RBW}^2} \quad (2)$$

where

- k is the constant of proportionality (2–3 for synchronously tuned near gaussian filters).
- Span is the displayed frequency range (in Hz).
- RBW is the selected IF bandwidth (in Hz).

4.1.6 IF signal amplification and detection

The IF amplifier boosts the fixed IF signal, according to the current reference level setting (either linearly or logarithmically) and based on the selected display mode, before it is processed further by the detector. Spectrum analyzers typically convert the IF signal to video with an envelope detector. In its simplest form, an envelope detector is a diode followed by a parallel resistor capacitor (RC) combination. The time constants

of the detector are such that the voltage across the capacitor equals the peak value of the IF signal at all times (i.e., the detector can follow the fastest possible changes in the envelope of the IF signal but not the instantaneous value of the IF signal itself). The maximum rate at which the envelope of the IF signal can change is determined by the IF filter bandwidth, as discussed in 4.1.4.

4.1.7 Video filtering

The video filter of the spectrum analyzer is a lowpass filter that follows the detector. As its cutoff frequency is reduced to the point at which it becomes equal to or less than the bandwidth of the IF filter, the high-frequency spectral components of the IF signal's envelope are suppressed, resulting in an averaging or smoothing effect on the displayed signal. This effect is most noticeable in measuring noise, particularly when a wide IF bandwidth is used. The displayed amplitude of broadband coherent signals (e.g., pulses), however, is also affected by the video filter bandwidth.

It should be noted that the video filter has its own response time. When the video bandwidth is equal to or less than the IF bandwidth, the sweep time equation becomes (from [B1])

$$ST = \frac{k \times \text{Span}}{\text{RBW} \times \text{VBW}} \quad (3)$$

where

VBW is the video bandwidth.

4.1.8 Display

Most of the modern spectrum analyzers have a built-in digital display that allows fast data updates at a flicker-free rate without the blooming or fading that is common for analog displays. Once the data has been digitized and stored in display memory, it is updated at the sweep rate of the spectrum analyzer, thus allowing the observation of the actual data update on the display as the instrument is sweeping through the specified frequency range.

Independent of the number of digital points of the display (e.g., 401 or 1001), each point represents a special amplitude value that was detected over some frequency range and some period of time. One display method used is to digitize the instantaneous value of a signal at the end of a digitization interval. This is usually called "sample detector" or "sample mode." Using this mode, the signal variation between individual sweeps is retained, which can be used to identify signal characteristics. Signals, however, might not be displayed at all in the case of wide frequency measurements. In such cases, another method called "peak mode" is used to display the maximum value encountered in each digitization interval to avoid missing signals. A frequency error is usually introduced by this method because the maximum amplitude might be found at some other frequency in the digitization interval. To correctly display both noise and coherent signals, an algorithm is used to determine if the signal rose and fell within the interval represented by the data point. If the signal both rises and falls, then the algorithm classifies the signal as noise (Rosenfell detector). In that case, an odd-numbered data point indicates the maximum value encountered during the digitization interval; whereas an even-numbered point indicates the minimum amplitude.

4.2 Spectrum analyzer and tracking generator

4.2.1 Introduction

A tracking generator is a special type of swept source that is used with a spectrum analyzer to make amplitude and/or precise frequency measurements. The tracking generator has a stable, fixed local oscillator that generates a signal at the IF frequency, f_{IF} , of the spectrum analyzer. Hence, the tracking generator's output

frequency, f_{TG} , can be made to track precisely the spectrum analyzer's input frequency, f_{SA} , since both are effectively tuned by the same local oscillator. This precision tracking exists in a swept-measurement mode and in a fixed-tuned mode, where the output of the tracking generator is simply a continuous wave (CW) signal. Since a flat output level is necessary for swept-frequency applications, the tracking generator generally has an internal leveling loop that ensures a flat output level over the entire frequency range of the spectrum analyzer (see [B4]).

This tracking action allows measurement of the transmitted or reflected amplitude responses of a device (e.g., site attenuation involving two antennas). Using a signal source and spectrum analyzer, the tracking generator allows high-dynamic-range transmission or reflection measurements with fast, continuous sweeps. Furthermore, a spectrum analyzer/tracking generator combination can be used to determine precisely the frequency of unknown signals where the signals to be measured are fed into the spectrum analyzer's input and the tracking generator output is connected to a counter. Most modern spectrum analyzers have a built-in precision counter that provides precision frequency measurement capability.

As shown in Figure 2, the device under test (DUT) can be placed between the tracking generator's output and the spectrum analyzer's input for transmission measurements. Performing reflection measurements, such as to determine the voltage standing wave ratio (VSWR) of a DUT, requires an additional directional coupler or bridge to separate the incident tracking generator signal from the signal reflected by the DUT. Both configurations are used for swept amplitude measurements. No phase information can be obtained with these setups. The spectrum analyzer/tracking generator has a large dynamic range and is capable of measuring very narrowband DUTs (e.g., 20 Hz crystal filters) that are not possible with other swept systems, such as the scalar and vector network analyzers.

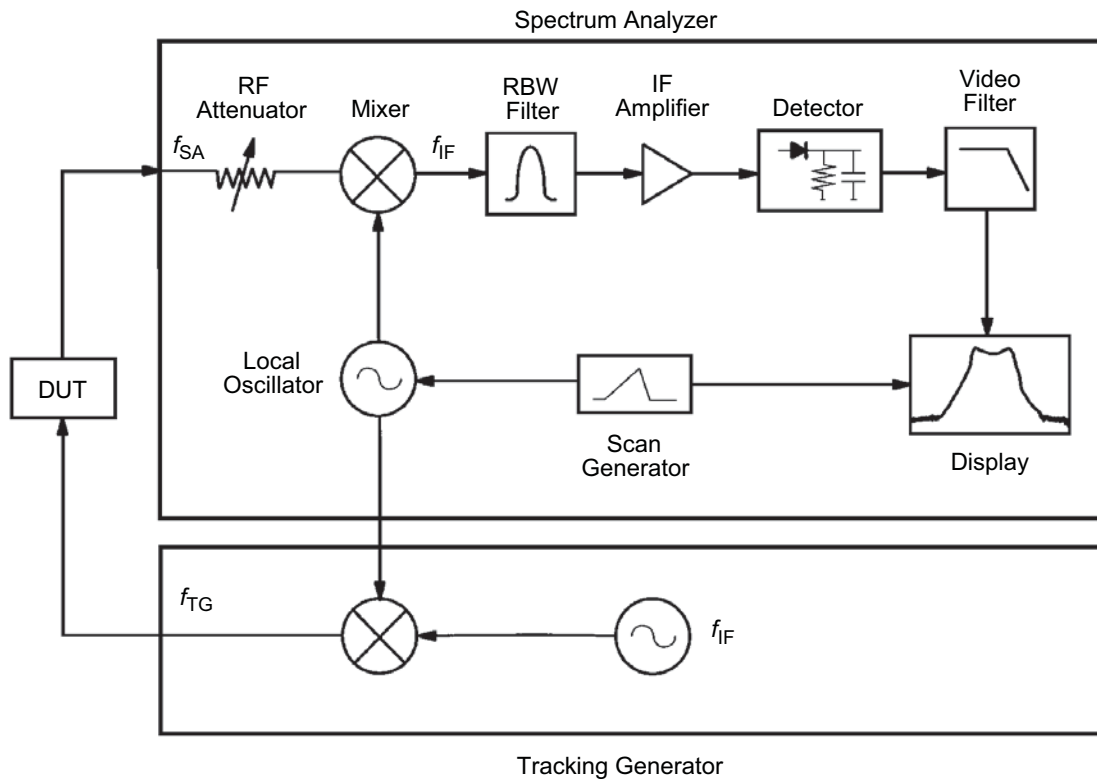


Figure 2—Block diagram of a superheterodyne spectrum analyzer and tracking generator

4.2.2 Dynamic range

The measurement dynamic range of the spectrum analyzer/tracking generator may exceed 120 dB. The key to this large dynamic range is the highly stable and precise tracking of the spectrum analyzer and the tracking generator, which permits overdriving the mixer to the 1 dB compression level while keeping the analyzer distortion products off the display. Furthermore, the spectrum analyzer's lowest IF bandwidth (e.g., 10 Hz or 100 Hz) can be used to reduce the displayed average noise level. Both factors provide a large dynamic range for amplitude measurements.

Precision tracking means that, at every instant of time, the generator fundamental frequency is in the center of the analyzer passband, and all generator harmonics, whether they are produced in the analyzer or generated in the tracking generator itself, are outside the passband. Thus, only the tracking generator fundamental frequency is displayed on the analyzer screen. While these distortion products may exist in the measurement setup, they are completely eliminated from the spectrum analyzer display.

4.2.3 Frequency accuracy

The frequency accuracy of a spectrum analyzer/tracking generator system is dependent upon the frequency tracking between the two instruments. When the tracking is degraded, the tracking generator frequency shifts from the center of the IF bandwidth, and the analyzer response decreases in amplitude and shifts in frequency. This frequency shift is a result of tracking error, and is typically negligible when measuring over wide frequency spans using wide IF filter bandwidths. When measuring narrowband DUTs, however, precise tracking is mandatory to avoid erroneous measurement results.

Measurements of DUTs of very narrow bandwidth (e.g., less than 20 Hz) are potentially limited by the tracking generator's residual FM. The ability to use a very small spectrum analyzer IF bandwidth (e.g., 10 Hz) results in filtering out those components of the residual FM whose fluctuation rates are greater than approximately half of the used IF bandwidth (e.g., 5 Hz), thus leaving only a small fraction of the total residual FM.

4.2.4 Measurement normalization

Normalization is a technique to remove certain components of the absolute system amplitude uncertainty from the measurement result. The procedures for transmission and reflection measurements are different, and the errors being eliminated by normalizing are different as well.

A transmission measurement requires a direct connection that replaces the DUT during the normalization measurement. A sweep is executed over the frequency range in which the actual DUT is to be tested, and the trace is stored in memory. The DUT is then connected in place, and the measurement is made by subtracting the normalization trace from the current trace. This, in effect, removes the system frequency response uncertainty. The measurement errors left are due to display accuracy (e.g., ± 0.5 – 0.8 dB full screen) and the mismatch uncertainties at the input and output of the DUT.

When reflection measurements are made, a different uncertainty calculation, which uses another normalization technique, applies. The reflection measurement amplitude uncertainty can be estimated by the following equation:

$$\Delta\rho = A + B\rho_L + C\rho_L^2 \quad (4)$$

where

- A is the directivity of the coupler.
- B is the frequency response.
- C is the effective source match.
- ρ_L is the reflection coefficient of the DUT (see [B12]).

If the quantities used in this equation are expressed in dB, as they normally are, they should be converted to linear units before using the equation. For example, a frequency response of -20 dB should be 0.1. The term $B\rho_L$ can be eliminated by normalization. This is done by connecting an open circuit ($\rho = 1$) in place of the DUT and storing the trace with all desired measurement settings. Then a short circuit ($\rho = -1$) is connected in place of the open circuit, and another trace is taken and averaged with the open-circuit trace. Next, the DUT is connected, and the averaged normalization trace is subtracted from the current trace. Since the open circuit and the short circuit both have reflection coefficients of magnitude one (0 dB), ideally, either could have been used as a reference for normalization. However, since the directional coupler is not perfectly directional, and since there exists mismatch between the tracking generator and the coupler, a single normalization trace would include information about errors associated with reflections from internal components of the measurement system, not just from the open-circuit or short-circuit reference, as desired. The open-circuit and short-circuit traces are averaged in order to remove this undesired internal reflection component from the reference data. The effective source match, as well as the coupler directivity, cannot be eliminated with normalization.

4.3 Electromagnetic interference (EMI) receiver

4.3.1 Introduction

Modern EMI receivers are based typically on the superheterodyne principle with one to three frequency conversion stages, just like a spectrum analyzer. Figure 3 is a simplified block diagram of an EMI receiver that shows the commonalities with the spectrum analyzer block diagram in Figure 1. The EMI receiver, however, has additional components, such as a preselector, a preamplifier, specialized IF bandwidths, and detector responses, in order to meet IEC/CISPR 16-1 (1993-08)⁴ requirements. Therefore, a spectrum analyzer alone cannot be used for EMI compliance measurements unless additional equipment is used to satisfy the CISPR requirements. The following paragraphs only describe those blocks in Figure 3 that are specific to the EMI receiver. All others are covered in 4.2.

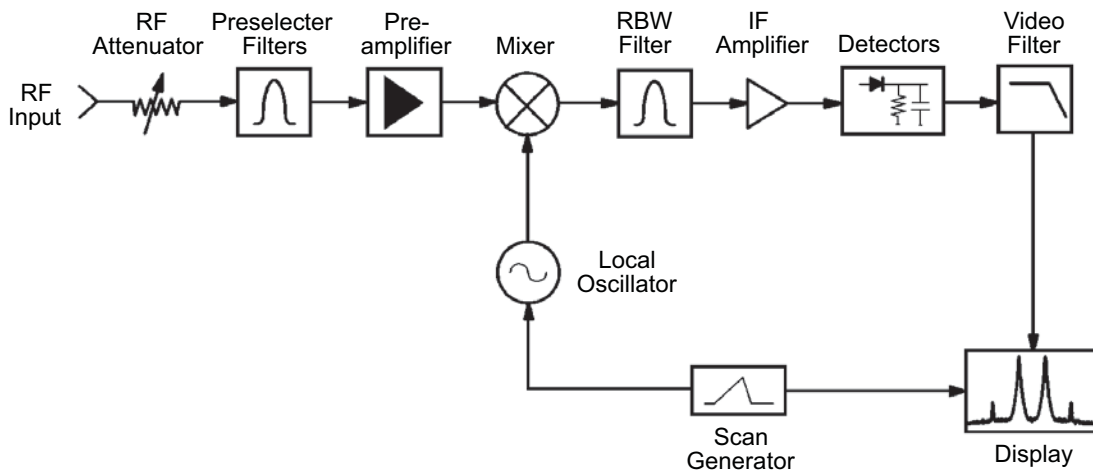


Figure 3—Block diagram of an EMI receiver

4.3.2 RF preselection and preamplification

Both spectrum analyzers and EMI receivers use one or more mixers to convert the unknown signal frequency to the IF frequency. Mixers go into saturation when the input signal exceeds certain levels, as discussed with spectrum analyzers in 4.2. One solution for preventing nonlinear operation is to increase the

⁴Information on references can be found in Clause 2.

input attenuation, which, in turn, reduces the available dynamic range, thus limiting the ability to measure low-level emissions. A better method for measuring broadband signals is to limit the signal spectrum that reaches the mixer to around the desired frequency in order to ensure linear operation. This is accomplished by introducing a preselector filter before the mixer input using either fixed-tuned or variable lowpass and bandpass filters to cover the whole measurement frequency range. The preselection filter passband insertion loss is accounted for by using calibration procedures. Therefore, RF preselection at the input of an EMI receiver enhances the receiver's ability to handle wide dynamic ranges of coherent broadband signals without degrading the dynamic range. Preselection does not prevent the EMI receiver from being overloaded by a signal that happens to be in the passband of a preselector filter. In this case, additional input attenuation needs to be used to avoid mixer saturation.

A low-noise preamplifier, placed after the preselector filter, can be used to improve the EMI receiver's overall system sensitivity. This is particularly useful for radiated EMI measurements in which the test system sensitivity is essentially degraded by the antenna factors of broadband antennas commonly being used.

4.3.3 Specialized IF bandwidths

IEC/CISPR 16-1 (1993-08), specifies IF filter shapes and 6 dB bandwidths that are significantly different from the gaussian shaped filters implemented in most spectrum analyzers. The specialized bandwidths listed in Table 1 should be used during a commercial compliance measurement of DUTs.

Table 1—Specialized IF bandwidths

Characteristic	10–150 kHz	150 kHz to 30 MHz	30 MHz to 1 GHz
6 dB bandwidth	200 Hz	9 kHz	120 kHz
Charge constant (quasi-peak detector)	45 ms	1 ms	1 ms
Discharge constant (quasi-peak detector)	500 ms	160 ms	550 ms
Meter constant (quasi-peak detector)	160 ms	160 ms	100 ms

4.3.4 Specialized detectors

In addition to peak detection, IEC/CISPR 16-1 (1993-08), requires quasi-peak as well as average detection to be used in commercial EMI measurements. The quasi-peak detector was developed to give a reading proportional to the annoyance effect of interference on listeners to broadcast radio. This is accomplished by a circuit that exhibits a time constant and a meter constant, thus simulating the inertia of an analog meter, which provides some smoothing of the readout. These values are listed in Table 1 and are different for the frequency ranges shown. The output of a quasi-peak detector will always decrease with the decrease in the repetition rate of the pulsed emission to be measured. The peak detector output is independent of the repetition rate. Furthermore, the peak detector will always capture the highest signal amplitude, indicating the worst-case value of an emission. The output of a quasi-peak detector might be lower when a broadband signal is measured.

The average detector consists of a peak detector followed by a series-resistor, shunt capacitor averaging network that produces the average of the detected envelope over a certain integration period. An unmodulated sinusoidal signal will produce an average reading proportional to its peak value. For pulsed signals, the average detector produces readings proportional to the duty factor of the signal.

4.4 Vector network analyzers

The minimum network analyzer measurement system consists of a source, a test set, a vector signal processor, and a display. Together, these components comprise a complete excitation/response test system that provides excitation to the DUT and measures the signal transmitted through the device or reflected from its input. The system then processes this data to provide various displays that show the magnitude and phase of these responses. Accuracy enhancement techniques permit measurement calibration at the interface to the DUT, thus minimizing the effect of systematic measurement errors. Figure 4 shows a block diagram of a vector network analyzer system with a swept source providing the excitation to the DUT. A test set provides the points at which the DUT is connected, signal separation devices to measure the four *S*-parameters, and possibly the first frequency conversion stage. Vector network analyzers usually are heterodyne receivers with multiple frequency conversion. Subsequent filtering allows for reducing the processing bandwidth and, therefore, improving the signal to noise ratio, which ultimately leads to improved sensitivity and dynamic range. Furthermore, the narrowband receiver characteristic suppresses harmonic and spurious signals at other frequencies. The signal processor then provides the amplitude and phase of the desired outputs in amplitude and phase. This information allows the application of sophisticated error-correction techniques that dramatically reduce the measurement ambiguities (see [B13]).

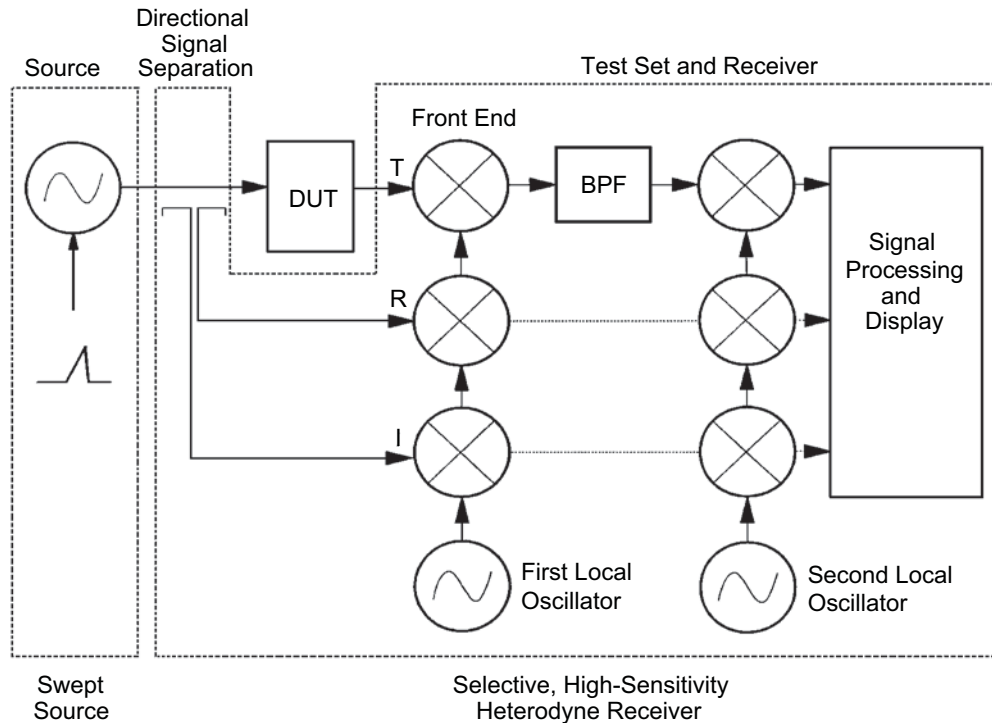


Figure 4—Block diagram of a vector network analyzer

4.5 Scaler network analyzers

The scaler network analyzer, as depicted in Figure 5, measures the magnitude of a microwave test signal by converting it into a low-frequency ac or dc signal by means of a thermoelectric effect or a diode homodyne process. Scaler analyzers with diode detectors as frequency-down converters are inherently broadband receivers. This gives them the capability of measuring any signal in the entire frequency band instantaneously. This feature is mandatory when frequency translating components like mixers have to be characterized, or when high-frequency agility is required. In contrast to a vector network analyzer system, scaler

analyzers offer less sensitivity mainly because of the broadband noise and lower conversion efficiency of the diode converter. Furthermore, there is limited rejection of undesirable signal components, which might lead to erroneous interpretations of measurement results (see [B33]).

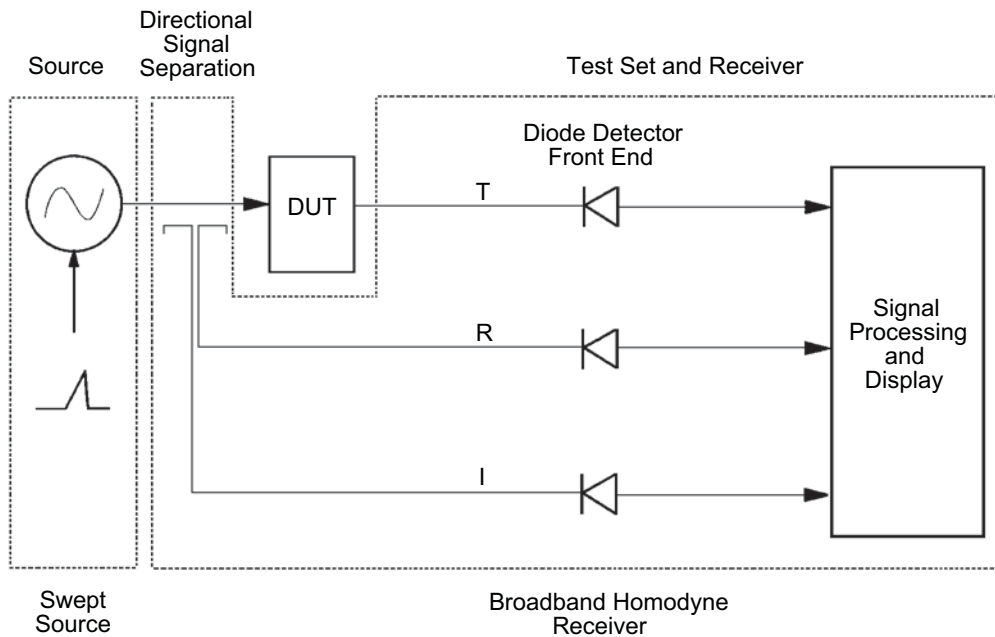


Figure 5—Block diagram of a scalar network analyzer

4.6 Vector voltmeter

4.6.1 Introduction

A vector voltmeter is a dual-channel, autoranging receiver that measures the voltages of two CW signals and the phase difference between them. Any unmodulated RF signal in the frequency range covered by the probes can be used as a source for these measurements, including a source that is part of a DUT. The vector voltmeter's narrowband measuring technique ensures high sensitivity and high dynamic range. The measurements are either of a single channel or of the ratio between the two channels, and the results displayed are as voltage or power, normalized magnitude and phase angle, or real and imaginary components. Measurements can be made either from the input to the output of the DUT or by probing within the device (see [B27]).

4.6.2 Measurement setup

A typical setup for a vector voltmeter measurement is shown in Figure 6. It includes a source (which may be part of the DUT), a reference path, and a measurement path. In order for the source to be suitable for use with a vector voltmeter, it must produce a stable CW signal at the frequency of interest with no modulation. This source signal is fed into a splitter to separate it into a reference signal (channel A) and the excitation for the DUT. The desired DUT response (transmitted or reflected signal) is routed to channel B, which is much more sensitive than channel A. The A input provides the signal to which the instrument is locked, thus serving as a reference to be present at all times for the vector voltmeter to function. Single-channel measurements can be made using the B channel, leaving the A probe in place as a reference. Dual-channel measurements are made by specifying the B/A magnitude ratio or the B – A phase difference as the test parameter. It should be noted that no swept measurements are possible with this setup, since no frequency information is retained along with the actual measurement data by the vector voltmeter itself.

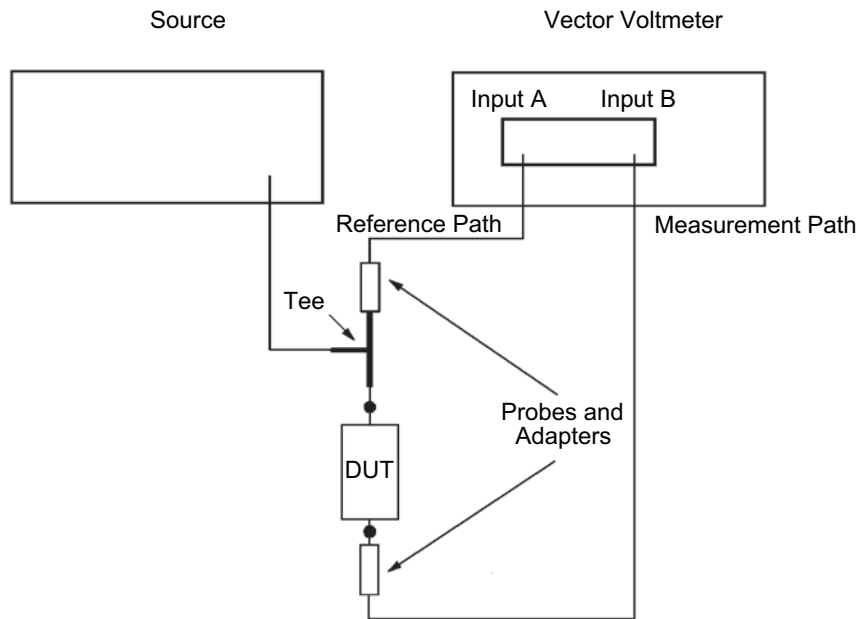


Figure 6—Block diagram of a vector voltmeter test setup

4.7 Time-domain reflectometer

4.7.1 Introduction

Figure 7 shows the basic block diagram of a time-domain reflectometer (TDR). It consists of a very-fast-rise-time pulse generator, an oscilloscope, and a bridging tee with a high-impedance arm toward the oscilloscope. The pulse generator must be well matched at the bridging tee to eliminate reflections back to the signal generator. These reflections would produce a delayed version of the original pulse that would clutter the display if they were to pass again in the forward direction through the bridging tee. There are no directional bridges or couplers to separate incident and reflected waves because they are already separated by time.

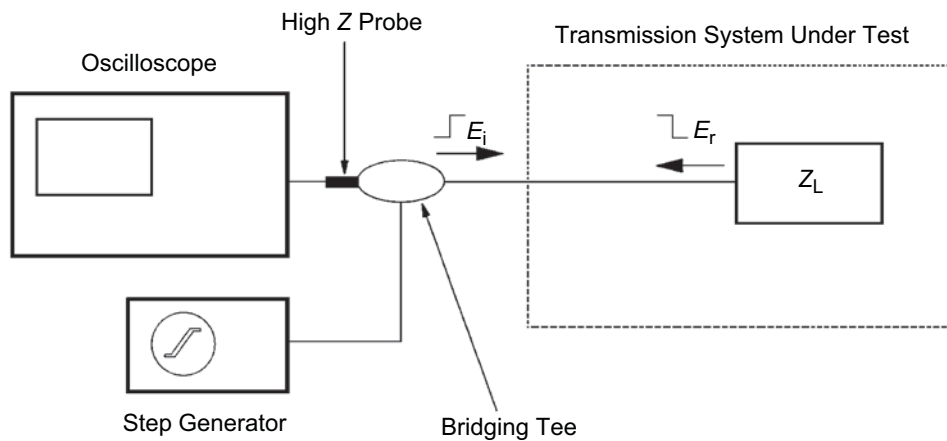


Figure 7—Block diagram of a basic time-domain reflectometer setup

4.7.2 Resolution considerations

The difference in time, t (in s), between two successive echoes is $2s/v$, where s is the distance, in m, between the two discontinuities that produce the echoes, and v is the velocity, in m/s, of propagation. If τ is the pulse rise time, in s, then the echoes can be resolved if $t > \tau/2$. Therefore, the minimum separation that provides accurate measurement is given by

$$s = v\frac{\tau}{2} \quad (5)$$

State of the art systems provide a minimum resolution on the order of 1–2 mm. If discontinuities are closer than this, then the reflected signals will be overlapping, thus preventing an accurate estimate of the discontinuities' separation. Since the horizontal reflection's repetition rate is identical to the pulse repetition rate of the pulse generator, it provides a time scale in the horizontal scale of the scope. This scale can be calibrated in distance if the velocity of propagation in the DUT is known.

4.7.3 Time-domain mode of vector network analyzers

The relationship between the frequency and time-domain response of a DUT is described mathematically by the Fourier Transform, and the response of a device may be completely defined in either domain. In other words, the DUT may be measured in the time domain, and the frequency-domain response may be calculated using the Fourier Transform. Otherwise, the DUT may be measured in the frequency domain, and the time-domain response may be calculated using the Inverse Fourier Transform. State of the art vector network analyzers make measurements in the frequency domain and then calculate the Inverse Fourier Transform to determine the time-domain response. This computational technique benefits from the wide dynamic range and the error correction of the frequency-domain data. These measurement systems mathematically generate either a step function or an impulse as the excitation for time-domain measurements. The reflected or transmitted response of the DUT to either excitation is calculated from frequency-domain data and is displayed in various formats. An additional benefit of this mathematical conversion of frequency to time-domain measurements is the ability to measure DUTs, which have bandpass characteristics and, therefore, do not operate down to dc. Traditional TDR systems require a dc path to be operational that excludes the measurement of bandpass devices (see [B2] and [B13]).

4.8 EMC antennas

4.8.1 Introduction

Many of the EMC measurements require the use of antennas to produce the incident fields (radiated susceptibility measurements tests) or to pick up the radiation from EUTs (radiated emissions). The antennas for both of these measurements vary widely with the frequency and the measurement bandwidth. The antennas can be classified broadly as narrowband or wideband antennas.

4.8.1.1 Narrowband antennas

The most common narrowband antenna is the thin half-wave dipole. It is a dipole that is tuned to the desired frequency by changing the length of its arms to be approximately one-half wavelength at the desired frequency. The arms of these dipoles are telescopic, so that their lengths can be adjusted for the desired frequency. For frequencies above 1 GHz, the antennas of choice usually are horns, which are inherently broadband. The dipole is a linear-polarized antenna that picks up an electric field that is parallel to the antenna wire. Therefore, care must be exercised in aligning the antenna properly with the desired polarization.

4.8.1.2 Wideband antennas

For the frequency range up to 200 MHz, specially designed thick broadband dipoles usually are used. For higher frequencies, an array of thin dipoles that vary in length according to the log of the frequency, called a log-periodic antenna, can be used to cover very wide bands of frequency. These are the antennas of choice for swept measurements from 200 MHz to the 1 GHz range. For the frequency range of 1–5 GHz, horns and log-periodic antennas can be used.

4.8.2 Antenna factor

Antennas used for EMC measurements are characterized by their antenna factor (AF). This factor is defined as the ratio of the incident electric-field magnitude, E (in V/m), to the voltage, V (in V), at the antenna terminals when terminated by the standard impedance of 50Ω . The AF assumes that the antenna is oriented for maximum reception. For a linear-polarized plane-wave dipole antenna, the antenna wire is parallel to the incident E-field. The AF should be furnished by the antenna manufacturer with a complete specification of how it was measured. The AF should be checked periodically, since shock and vibration may affect its value. Note that the antenna factor is only defined for a receive antenna. The radiated field of an antenna can be calculated from its gain and input power. For circular-polarized antennas, such as the conical-helical antenna, the AF is defined in a similar way, and assumes that the antenna has the correct polarization rotation for the incident field. If the incident field is linearly polarized, the AF gives the correct electric-field magnitude, regardless of the antenna orientation, as long as the axis of the conical-helical antenna is in the direction of propagation (see [B16] and [B25]).

5. Test environment parameter guidelines

Unless otherwise specified by the procuring or specifying document, the following guidelines specify the recommended, but not mandatory, test environment parameters for RF absorbers:

- a) The frequency range from 30 MHz to 5 GHz may have to be subdivided into two or more subranges (e.g., low, medium, and high frequencies).
- b) If time-domain solutions are sought, pulse rise time shall be investigated down to 100 ps.
- c) Tests should be performed at field intensities that are representative of the intensities over which the RF absorbers can be expected to be exposed.
- d) Measurement, using both parallel and perpendicular-polarized incident waves over a wide range of angles of incidence, is important to describe fully the RF absorber performance characteristics. A range of incidence angles from as close as possible to 0° to as close as possible to 90° is strongly suggested.
- e) Temperature and humidity conditioning of the RF absorber, before and during testing, is essential. Sufficient time should be allowed to ensure the stability and uniformity of temperature and humidity throughout the sample under test. Suggested temperature limits are $23^\circ\text{C} \pm 3^\circ\text{C}$, with a relative humidity of $50\% \pm 10\%$. This is especially critical for the RF absorber materials that use salts as fire retardants.

6. Material bulk-parameter evaluation

RF absorbers for absorber-lined chambers (ALC) and absorber-lined open-area test sites (ATS) can have many practical implementations. The various RF absorbing materials and combinations thereof can be formed into flat or ridged surfaces, and conical or pyramidal shapes. The RF absorber performance in an actual application will be related to four primary factors. These factors are

- a) The RF properties of the bulk material
- b) The shape of the implementation of the basic RF absorber tile or blanket
- c) The arrangement of the basic RF absorber shapes into arrays
- d) The process used in mounting the shapes over the conducting surface

6.1 Background

The reflection coefficients of multilayer planar RF absorbing materials can be calculated if the complex permittivities and permeabilities, as well as the conductivities of their materials, are known. For the case of conical or pyramidal RF absorbing materials, since the cross-section is not homogeneous, equivalent bulk parameter values can be used (see [B5], [B7], [B17], [B18], [B23], and [B26]). For the case of homogeneous multilayer RF absorbing materials, the layer parameters can be measured or obtained from manufacturers. Since the RF absorbing material usually is illuminated from many different angles, it is necessary to use equations that take the angle of incidence and the polarization of the incident wave into account. These equations are available in the literature (see [B26] and [B40]), and are not difficult to implement.

The parallel polarization occurs when the E-field is in the plane of incidence. The perpendicular polarization occurs when the E-field is perpendicular to the plane of incidence. This plane is defined by the direction of the incident wave and the normal to the layered media as shown in Figure 8. Figure 8 shows a layered media that is being illuminated by a plane wave with the E-field in the plane of incidence (parallel polarization), arriving at an angle, θ , from the normal. The plane of incidence coincides with the (x,z) plane as shown. The H-field is then along the y -axis (out of the paper). Each layer is characterized by four parameters:

- a) The thickness, h
- b) The conductivity, σ
- c) The complex relative permittivity, $\epsilon_r = \epsilon_r' - j\epsilon_r''$
- d) The complex relative permeability, $\mu_r = \mu_r' - j\mu_r''$

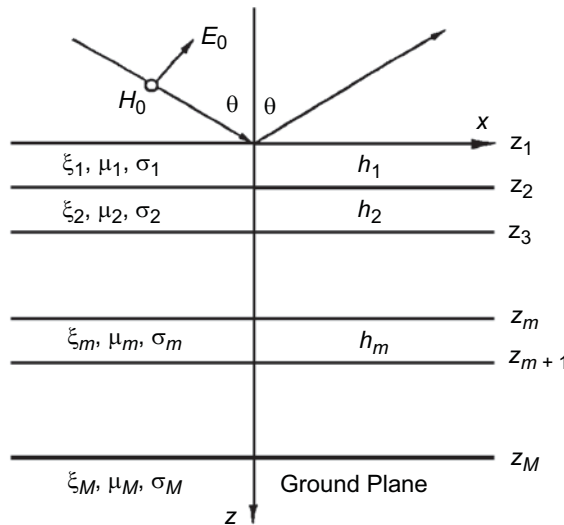


Figure 8— M layers of RF absorbing material—incident wave with parallel polarization

The primed parts of the last two parameters correspond to the usual relative permittivity and permeability, while the double-primed parts correspond to the dielectric and magnetic losses in the material. When complex relative permittivity is used, then $\sigma/\omega\epsilon_0$ can be included in ϵ_r'' . As will be seen later, some measurement procedures of bulk parameters do not measure conductivity as a separate parameter, thus including its effect

in ϵ_r'' . The real part of the relative permittivity is sometimes referred to as the dielectric constant. The actual permittivity and permeability are obtained from ϵ_r and μ_r by multiplying them by ϵ_0 and μ_0 , respectively. All the RF absorbing materials bulk parameters are frequency dependent and, therefore, should be measured over the frequencies of 30 MHz to 5 GHz.

The RF absorbing material of Figure 8 has $M + 1$ layers. $m = 0$ corresponds to the incident medium, usually free space, and $m = M$ is the media behind the RF absorbing material, usually a conductor. For the equations presented here, each layer is assumed to be of infinite extent in the X and Y directions, and the RAM illumination is by a plane wave. This is equivalent to neglecting the diffraction from the edges of finite extent layers. The value of the wave impedance, Z_1 , at the $z = 0$ interface, between the free-space incidence media and the first layer of the layered media, can be calculated by the recurrent formula (see [B26] and [B40]):

$$\begin{aligned} Z_1 &= K_1 \left[\frac{Z_2 + K_1 \tanh(U_1 h_1)}{K_1 + Z_2 \tanh(U_1 h_1)} \right] \\ Z_2 &= K_2 \left[\frac{Z_3 + K_2 \tanh(U_2 h_2)}{K_2 + Z_3 \tanh(U_2 h_2)} \right] \end{aligned} \quad (6)$$

etc...

$$Z_{M-1} = K_{M-1} \left[\frac{Z_M + K_{M-1} \tanh(U_{M-1} h_{M-1})}{K_{M-1} + Z_M \tanh(U_{M-1} h_{M-1})} \right]$$

The general recurrence formula for a layer, m , can be obtained from the last portion of Equation (6) by replacing M with m . K_m is the wave impedance of layer m , and is given by

$$K_m = \frac{U_m}{\sigma_m + j\omega\epsilon_m} \quad (7)$$

where

$$\omega = 2\pi f, \text{ the radian frequency.}$$

U_m is the propagation constant of layer m , given by

$$U_m = (\delta^2 + \gamma_m^2)^{1/2} \quad (8)$$

with

$$\delta = j\gamma_0 \sin(\theta) \quad (9)$$

and

$$\gamma_m^2 = -\mu_m \epsilon_m \omega^2 + j\sigma_m \mu_m \omega \quad (10)$$

Note that, from the denominator of Equation (7), $\sigma_m/\omega\epsilon_0$ can be absorbed by the imaginary part of the complex permittivity, ϵ''_{tm} .

The RF absorbing material reflection coefficient can be calculated from Z_1 using the equation

$$R_0^{\parallel} = \frac{K_0 - Z_1}{K_0 + Z_1} \quad (11)$$

where

$$K_0 \text{ is the wave impedance of the incidence region for the angle of incidence } \theta.$$

K_0 is obtained from Equation (7) when $m = 0$, and is given by

$$K_0 = \sqrt{\frac{\mu_0}{\epsilon_0}} \cos(\theta) = 377 \cos(\theta) \quad (12)$$

If the last layer, the M th, is free space, then Z_M will be given by K_0 of Equation (12). If the last layer is a perfect conductor, then $Z_M = 0$ and Z_{M-1} will be given by

$$Z_{M-1} = K_{M-1} \tanh(U_{M-1} h_{M-1}) \quad (13)$$

If the RF absorbing material has only one layer, on top of a perfect conductor (ground plane), then Z_1 is calculated from Equation (13) with $M = 2$. The RF absorbing material reflection coefficient is obtained from Equation (11).

Note the similarities of Equation (6) with those of cascaded transmission lines. These equations give the input impedance, Z_{m-1} , of a section of transmission line of length, h_{m-1} , with a propagation constant of U_{m-1} , and a characteristic impedance of K_{m-1} . Therefore, the M layers are represented by $M-1$ cascaded sections of transmission lines that are terminated by Z_M and connected to a generator with an internal impedance of K_0 .

A similar solution exists (see [B26] and [B40]) for the perpendicular polarization. To modify Figure 8 for this case, E is replaced by H , and H is replaced by $-E$ (negative y -axis, into the paper). The solution is given in terms of admittances, Y , similarly to the previous equations, as

$$Y_1 = N_1 \left[\frac{Y_2 + N_1 \tanh(U_1 h_1)}{N_1 + Y_2 \tanh(U_1 h_1)} \right]$$

$$Y_2 = N_2 \left[\frac{Y_3 + N_2 \tanh(U_2 h_2)}{N_2 + Y_3 \tanh(U_2 h_2)} \right] \quad (14)$$

etc...

$$Y_{M-1} = N_{M-1} \left[\frac{Y_M + N_{M-1} \tanh(U_{M-1} h_{M-1})}{N_{M-1} + Y_M \tanh(U_{M-1} h_{M-1})} \right]$$

where

$$N_m = \frac{U_m}{j\omega\mu_m} \quad (15)$$

This equation and Equations (8)–(10) complete the formulation. Once Y_1 is known, the RF absorbing material reflection coefficient is calculated by

$$R_0^\perp = \frac{N_0 - Y_1}{N_0 + Y_1} \quad (16)$$

where N_0 is the wave admittance for the incidence region, for the angle of incidence θ . This is obtained from Equation (15), for $m = 0$, by

$$N_0 = \sqrt{\frac{\epsilon_0}{\mu_0}} \cos(\theta) = \frac{\cos(\theta)}{377} \quad (17)$$

If the last layer, the M th, is free space, then Y_M will be given by N_0 of Equation (17). If the last medium is a perfect conductor, then Y_M is infinite, and Y_{M-1} will be given by

$$Y_{M-1} = \frac{N_{M-1}}{\tanh(U_{M-1}h_{M-1})} \quad (18)$$

If the RF absorbing material has only one layer on top of a perfect conductor, then the value of Y_1 is calculated by Equation (18) with $M = 2$. The RF absorbing material reflection coefficient is obtained using Equation (16).

6.2 Bulk-parameter measurement procedures

There are many methods to measure RF material bulk parameters. Both time-domain and frequency-domain techniques may be used. Results should include measurements of known materials such as teflon, distilled water, etc., as a means of validating the procedure and the equipment used. Multiple measurements should be performed to ensure the repeatability of the methods.

6.2.1 Frequency-domain bulk-parameters measurement procedure

A convenient fixture for bulk-parameter measurements in the 30 MHz to 1 GHz frequency range is a coaxial sample holder of 16 mm outer diameter, 7 mm inner diameter, and 100 mm length. Typical lengths of the RF absorber material samples are 100 mm for most dielectric materials and 10 mm for ferrites or magnetic materials. The air-filled, coaxial sample holder, transmission-line characteristic impedance is 50 Ω. A coaxial transmission line filled with RF absorber material is shown in Figure 9. There are several commercially available fixtures or fixture designs, as suggested by manufacturers of measurement equipment, that work best with specific equipment. These fixtures depend on the measurement frequency and equipment used (see [B20] and [B28]). The coaxial sample holders have to be designed so that only the transverse electromagnetic (TEM) mode is present. The frequency for which the first higher-order mode is present in circular coaxial lines is when the average circumference, between the inner and outer conductor, is approximately one wavelength in the material being tested (see [B32]). The RF absorber material presence changes the line characteristic impedance, the input reflection coefficient, and the transmission coefficient. These changes can be measured by the line S -parameters, S_{11} and S_{21} , defined in Figure 10.

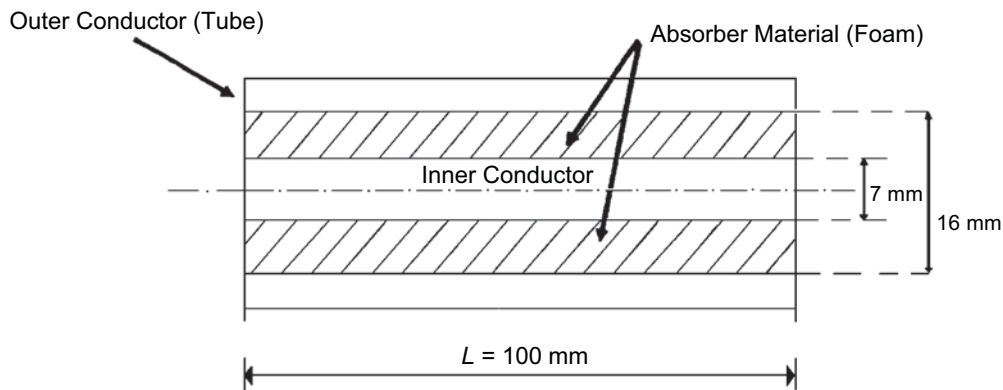


Figure 9—Coaxial fixture to measure bulk parameters of RF absorbing materials

The S -parameters of the fixture, when filled with the RF absorber material, are related to the fixture reflection coefficient, Γ , and transmission coefficient, T , as (from [B28])

$$S_{11} = \frac{(1 - T^2)\Gamma}{1 - T^2\Gamma^2} \quad (19)$$

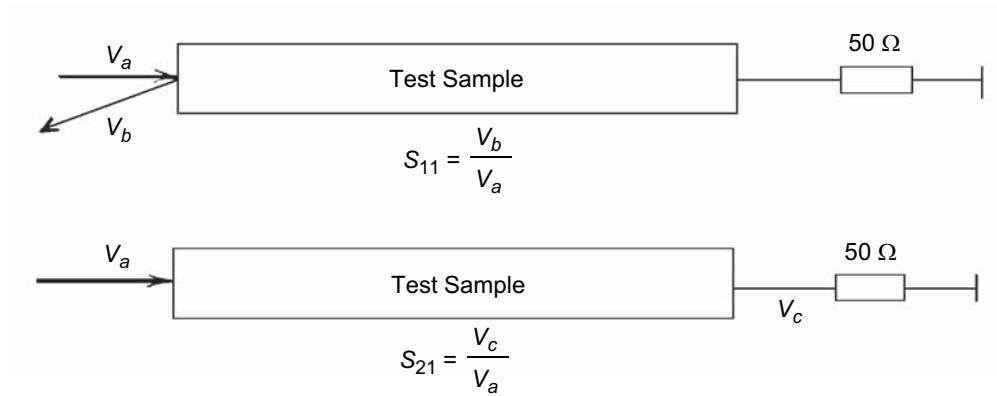


Figure 10—S-Parameter definition

$$S_{21} = \frac{(1 - \Gamma^2)T}{1 - T^2\Gamma^2}$$

The fixture input reflection coefficient, Γ , is related to the bulk parameters by

$$\Gamma = \frac{Z_s - Z_0}{Z_s + Z_0} = \frac{\sqrt{\frac{\mu_r}{\epsilon_r}} - 1}{\sqrt{\frac{\mu_r}{\epsilon_r}} + 1} \quad (20)$$

where

- Z_s is the filled line characteristic impedance.
- ϵ_r is the relative complex permittivity.
- μ_r is the relative complex permeability.

The fixture transmission coefficient, T , is related to the bulk parameters by

$$T = \exp(-j\omega\sqrt{\epsilon\mu}L) = \exp\left(-j\frac{\omega}{c}\sqrt{\epsilon_r\mu_r}L\right) \quad (21)$$

where

- L is the sample length, as shown in Figure 9.

Equations (20) and (21) can be used to obtain the unknown complex, ϵ_r and μ_r . In these types of measurements, $\sigma/\omega\epsilon_0$ is included in the imaginary part of ϵ_r . Since ϵ_r and μ_r are complex numbers, S_{11} and S_{21} have to be measured in amplitude and phase.

6.2.1.1 Test setup

Typical test setups to measure the scattering parameters, using a vector voltmeter, are shown in Figures 11 and 12. Figures 13 and 14 illustrate the test setup and test fixtures when a network analyzer is used in a swept mode. See [B28], for example, for details of the measurement and recommended fixtures.

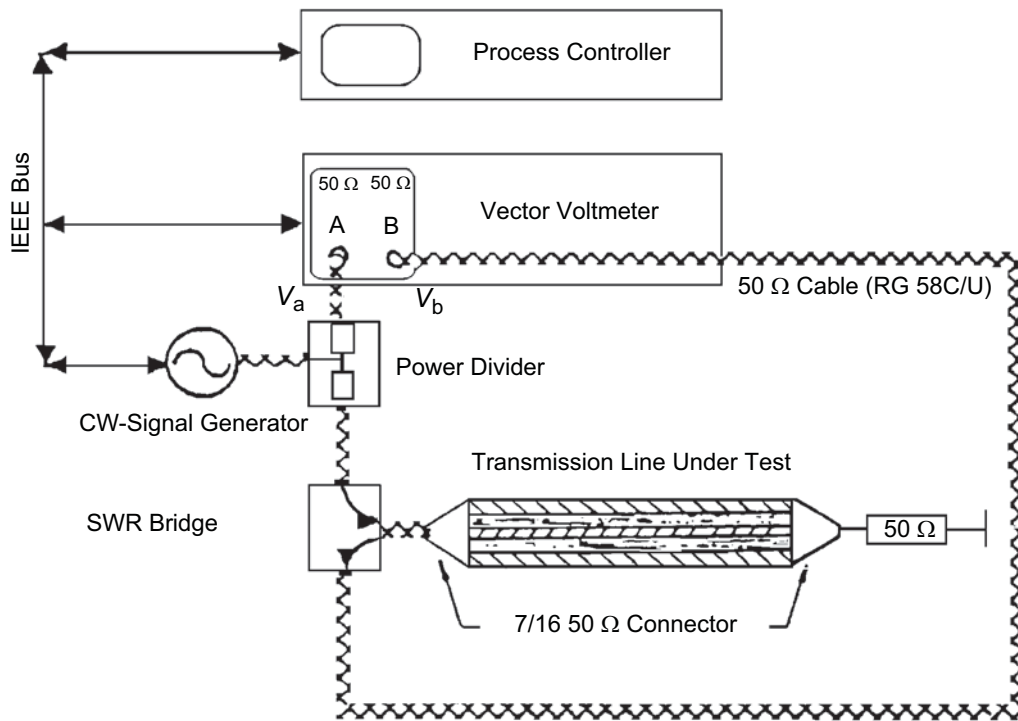


Figure 11—Typical test setup to measure S_{11} using a vector voltmeter

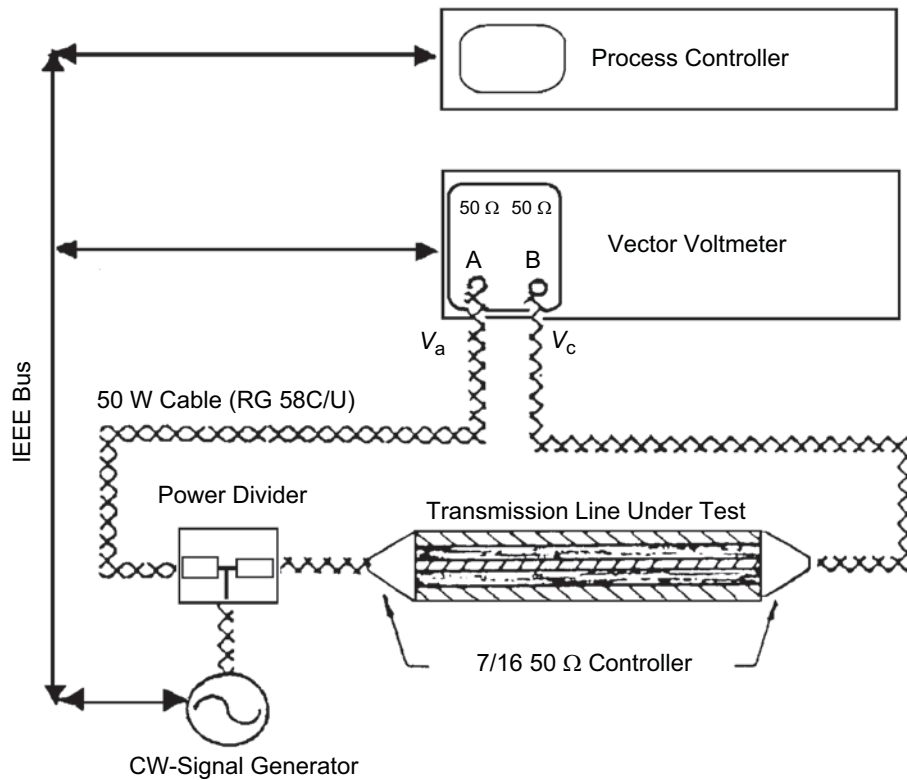


Figure 12—Typical test setup to measure S_{21} using a vector voltmeter

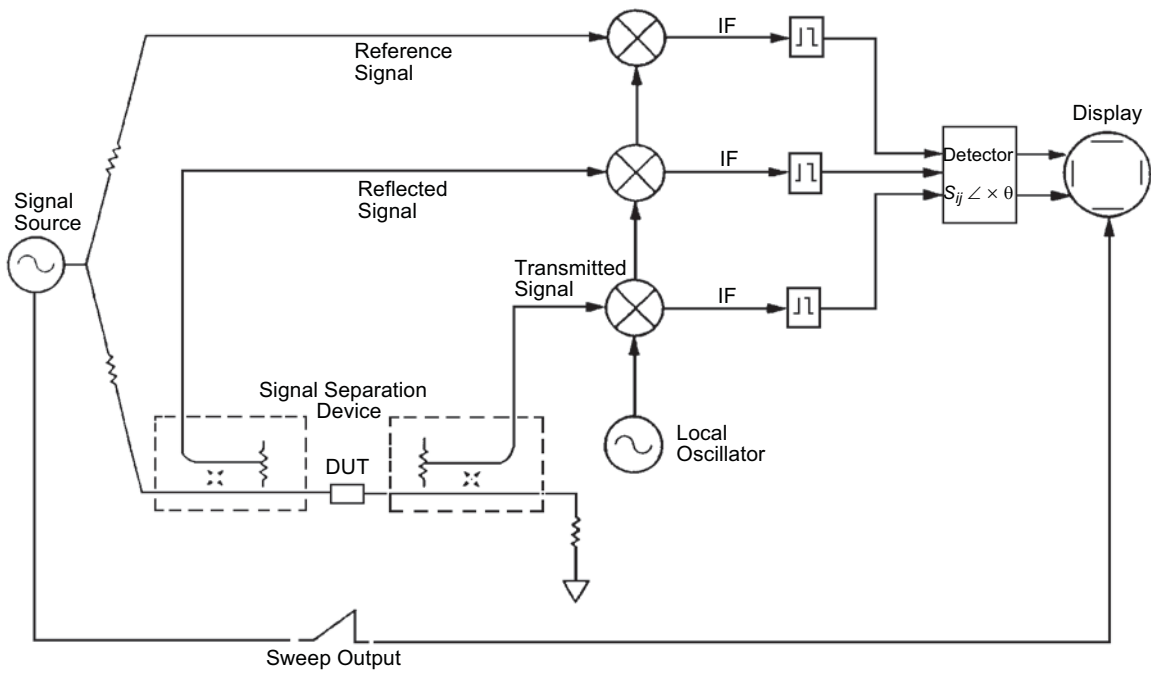


Figure 13—Typical test setup to measure S_{11} and S_{21} using a network analyzer in the swept mode

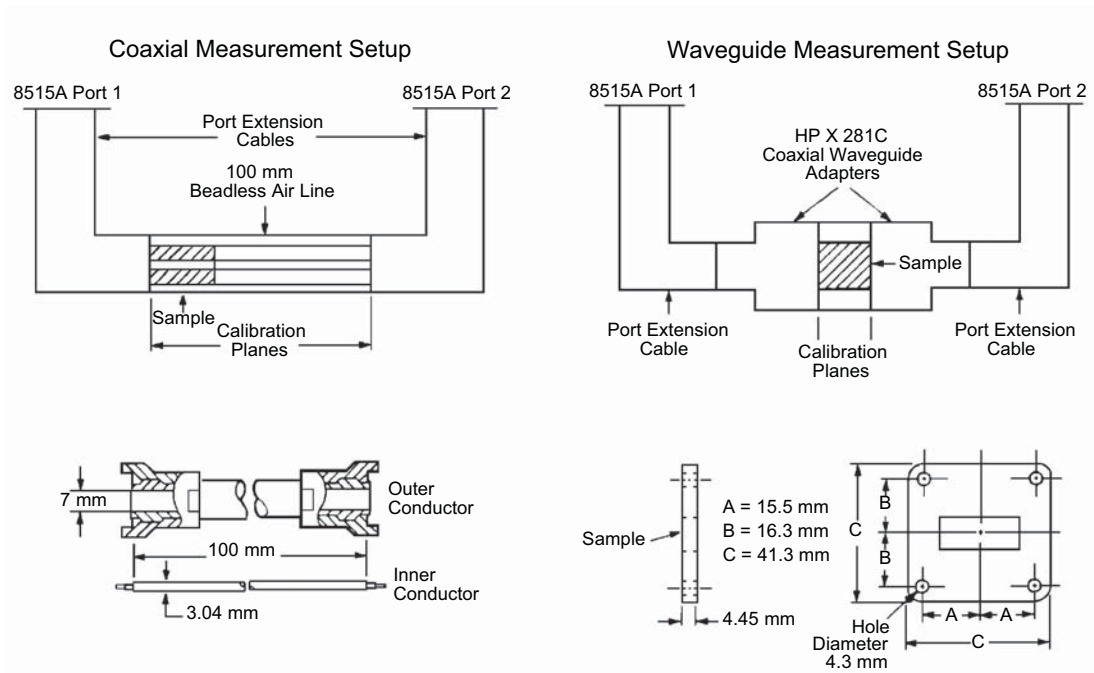


Figure 14—Typical manufacturer suggested fixtures to measure the bulk parameters of RF absorbing materials

6.2.1.2 Test results

Using the vector voltmeter test setup, a pyramidal absorber (1.8 m in length) was tested using samples extracted from several places, as shown in Figure 15. The results for ϵ_r' and σ are shown in Figures 16 and 17. The great variation of the bulk parameters throughout the RF absorber block is clearly shown.

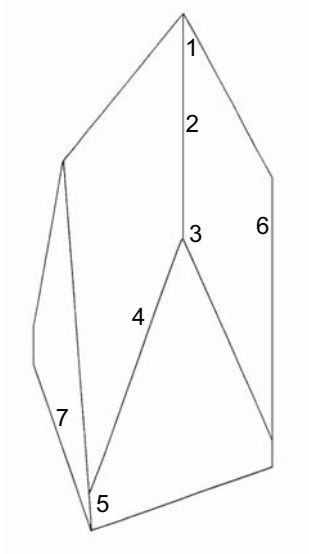


Figure 15—Location of the test samples taken from a pyramidal RF absorber

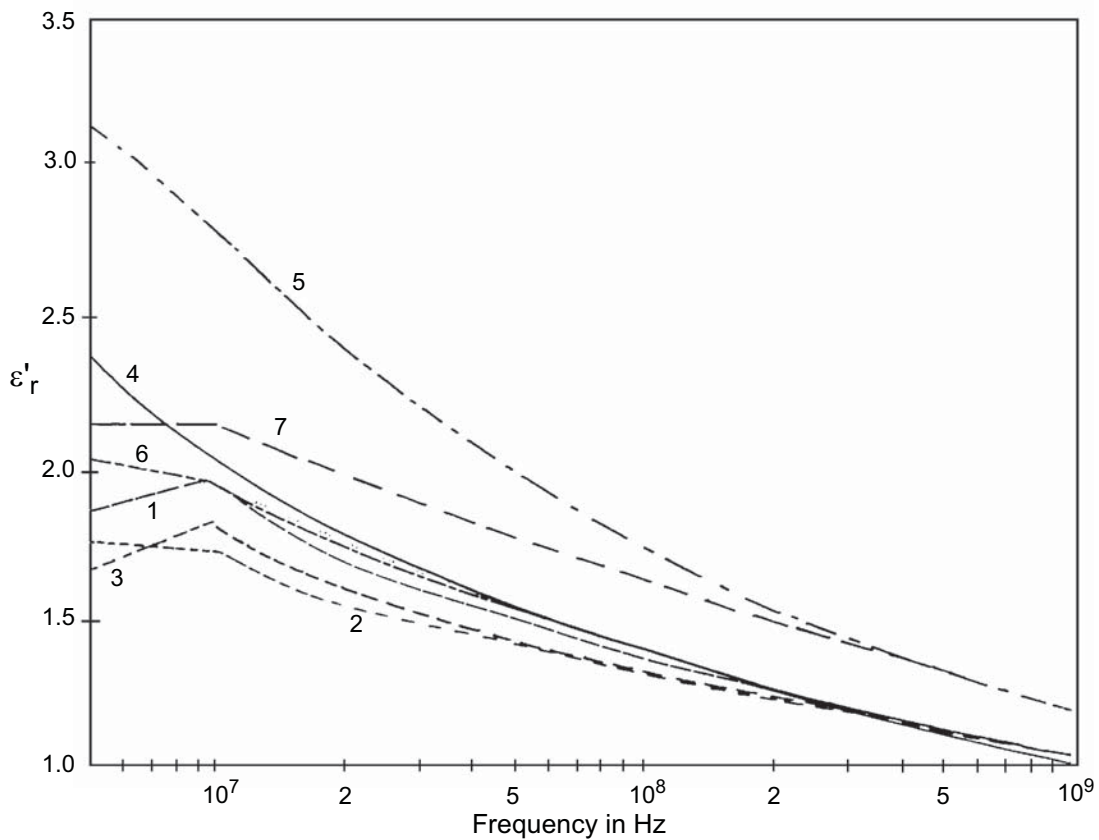


Figure 16—Permittivity of real part ϵ_r' calculated from measured S_{11} and S_{21} for the seven samples of Figure 15

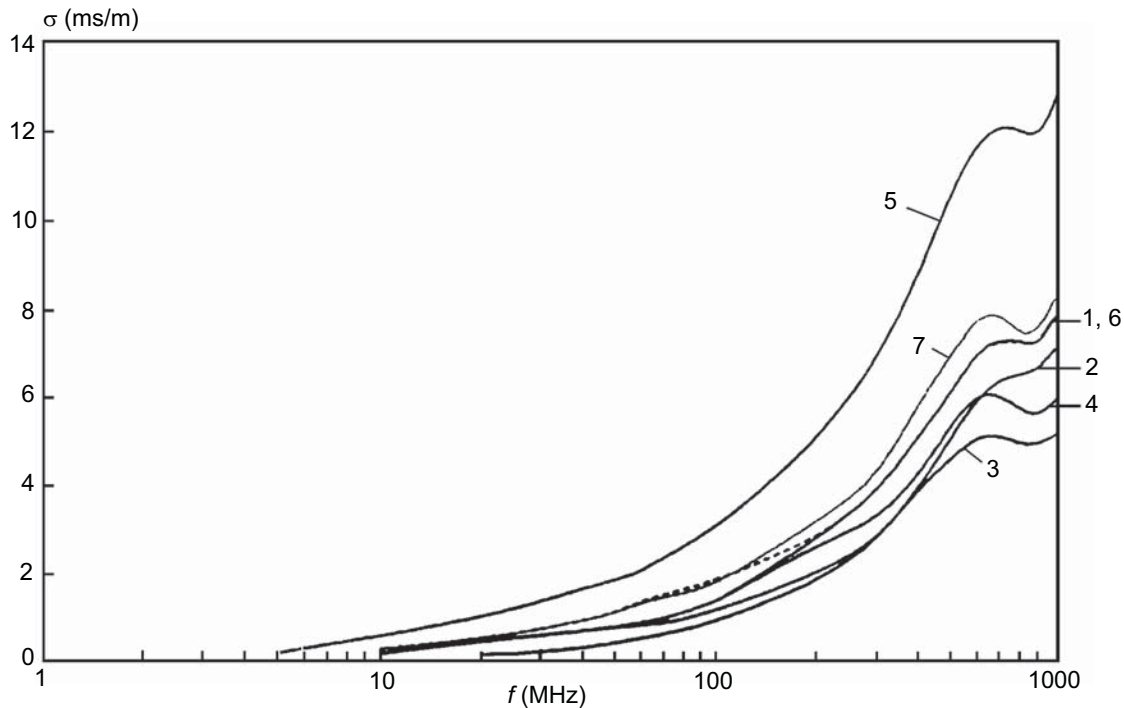


Figure 17—Conductivity calculated from measured S_{11} and S_{21} for the seven samples of Figure 15

A flat ferrite tile RF absorber was also tested (see [B20] and [B21]). The results for μ_r' , μ_r'' , ϵ_r' and ϵ_r'' are shown in Figures 18 and 19.

6.2.2 Time-domain bulk-parameters measurement procedure

The only reference in the literature pertinent to time-domain measurements of bulk parameters, is very old (see [B23]). Apparently, no recent work has been done in this area. Since this technique is very promising, it is hoped that this note will be an incentive to researchers in the field to pursue this matter.

7. Evaluation of the reflectivity of RF absorbers

A lot of progress has been reported in the literature on how to calculate the performance of RF absorbers from bulk parameters (see [B5], [B7], [B17], [B18], [B20], [B21], [B23], [B40], and [B28]). The purpose of this clause is to discuss the techniques for verifying these calculations experimentally.

7.1 Background

The final use of RF absorbers is not as an isolated small piece of material, but rather as a lining applied to reflecting surfaces to control multipath reflections. Examples of such applications are the use of RF absorbers on the walls and ceiling of semianechoic chambers, on all surfaces of fully anechoic chambers, and on the superstructure of ships to eliminate undesired reflections, to mention a few. In order to design for such applications, the engineer has to have information on the performance of RF absorber tiles in typical array configurations. This information should include the reflectivity, in magnitude and phase, for various angles of incidence, from normal to as close to grazing as possible, and for parallel and perpendicular polarizations.

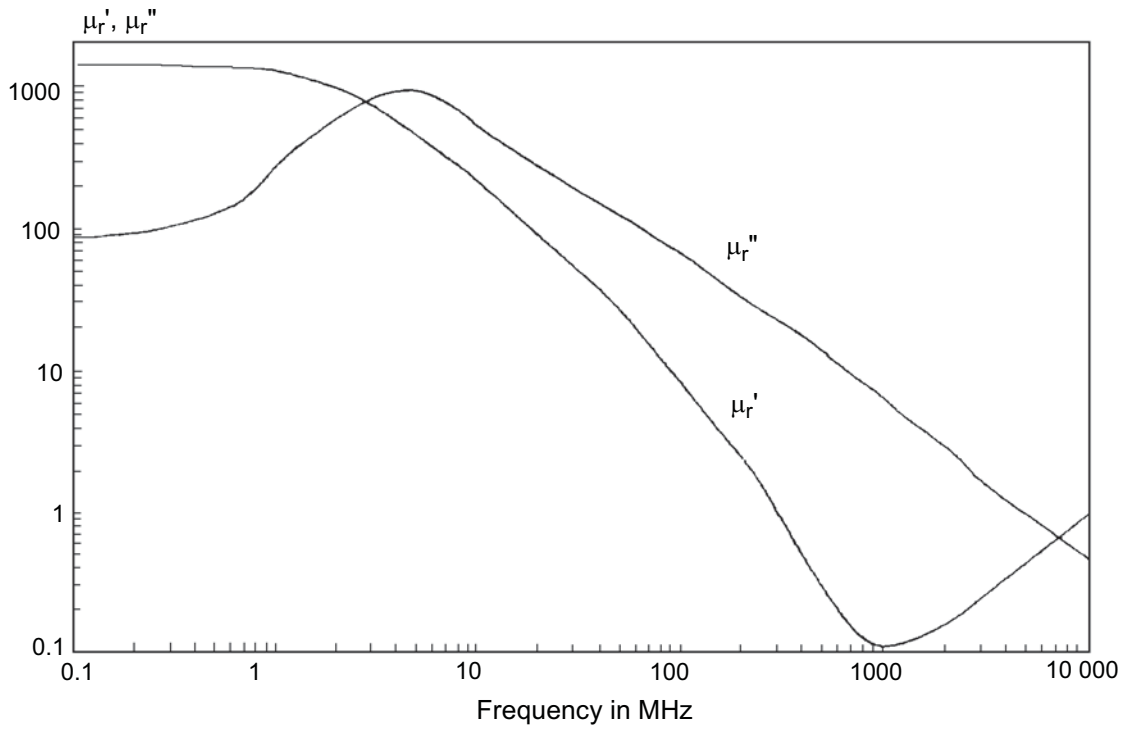


Figure 18—Permeability of real and imaginary parts, μ_r' and μ_r'' , for a flat ferrite RF absorbing material

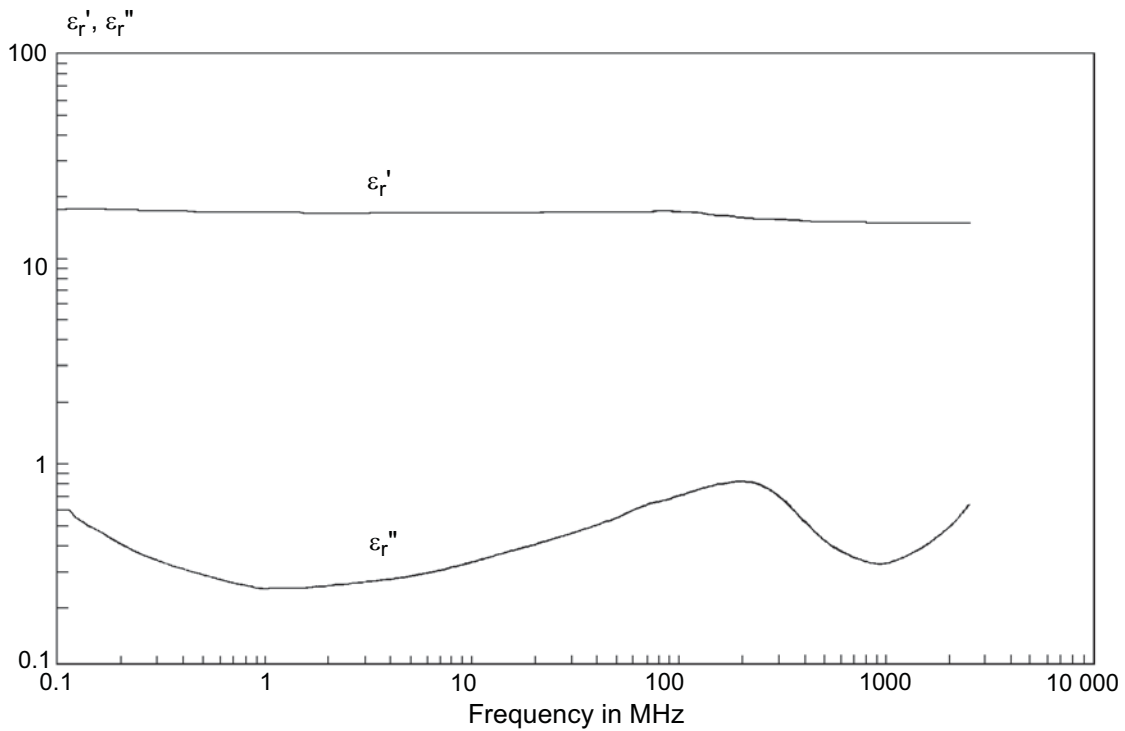


Figure 19—Real and imaginary parts, ϵ_r' and ϵ_r'' , for the same ferrite as in Figure 18

This type of data should be provided by manufacturers. Many manufacturer data sheets, however, fall far short of this, specifying only the magnitude of the RF absorber reflectivity for normal incidence. Since many RF absorbers have high reflectivity when illuminated only a few tens of degrees from normal and are polarization sensitive, this limited information precludes the evaluation of the performance of RF absorbers in actual applications. Without the reflectivity phase information, it is not possible to correctly add the direct signal with the ambient reflections.

7.2 RF absorber reflectivity measurement procedures

There are four techniques currently in use to measure the characteristics of RF absorbing materials.

The first method, called the arch method, uses a transmit and a receive antenna that are mounted on a circular arch that is in a plane perpendicular to the RF absorber surface. The transmit antenna illuminates the RF absorber, and the reflection is picked up by the receive antenna. Reflections from the RF absorber are compared with the reflections from a good conducting surface placed in the same position as the surface of the RF absorber. Different angles of incidence are obtained by moving the transmit antenna along the arch. The receive antenna is also moved to the corresponding angle of reflection. The polarization can be changed by using linear-polarized antennas and by rotating them appropriately.

The second method uses a time-domain approach. The RF absorber is mounted on any wall or on the floor of an enclosed area. The RF absorber is then illuminated by an incident wave, which is produced by a transmit antenna that is excited by a short duration pulse. The reflected wave is picked up by a receive antenna, and is digitally processed to obtain the RF absorber reflectivity over the frequency bandwidth of interest. The presence of the enclosed area walls, floor, and ceiling will produce multiple reflections that can be eliminated by using time windowing and digital signal-processing techniques.

The third method mounts the RF absorber array or tile at the end of a waveguide with a large cross-section and an appropriate length. A tapered waveguide section is used to connect the measurement setup to an excitation probe. The RF absorber reflection coefficient can then be derived from the measurement of the input VSWR at the probe.

The fourth method is based in the same idea as the third method, except that a coaxial line with a large cross-section and an appropriate length is used instead of the waveguide. Again, the RF absorber reflectivity is derived from the system input VSWR.

7.2.1 The arch method measurement procedure

The arch method is an extremely simple and intuitive measurement method. Figure 20 illustrates a typical setup. First, the reflection of a metal plate at the center of the arch is measured. Next, the sample to be evaluated is placed on top of the metallic plate, and its reflection is measured. The ratio of the sample reflection to the metal plate reflection is the reflection coefficient. Theoretically, the arch method may be used at any frequency, although it usually is not used below 1 GHz. For these frequencies, since the sample has to be in the far field, a large arch radius and large samples would be required.

The important physical parameters of this measurement technique are the distance between the transmit and receive antennas (via the reflection from the sample), the sample size, and proper sample illumination for a given geometry of the arch. In addition to these primary parameters, there are several secondary parameters that relate to and interact with the selection of the primary parameters. These secondary parameters include edge diffraction effects from the sample, direct coupling between the measurement antennas, extraneous reflections from the environment, and the fact that the effective plane of reflection of the sample is offset from the metal plate's plane of reflection by virtue of the sample thickness.

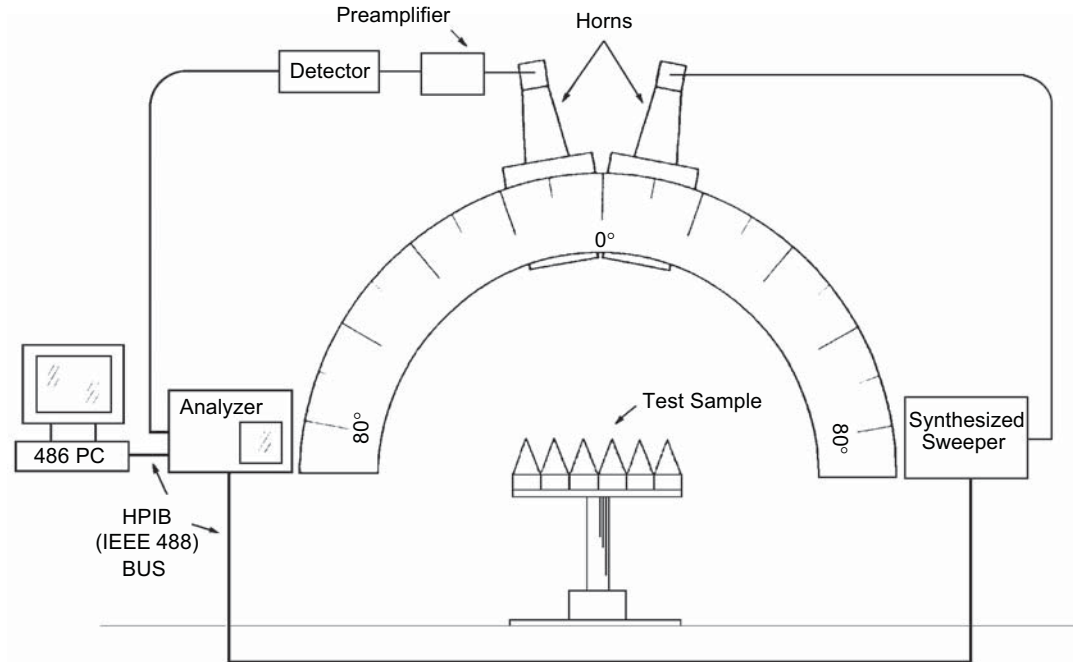


Figure 20—Arch method setup configuration

The first consideration in arch design is the distance between the antennas via the reflecting surface. This should be such that the antennas are in the far field of each other. The far field of an antenna starts at a distance given by

$$r_a = \frac{2D^2}{\lambda} \quad (22)$$

where

- r_a is the distance from transmit antenna phase center to receive antenna phase center via the reflecting plate. The physical radius of the arch is approximately 1/2 this value, in m. It is customary to take this distance as the separation between the near field (Fresnel Zone) and the far field (Fraunhofer Zone) of an antenna (see [B16]).
- D is the aperture of the antennas used, in m. This is usually the largest dimension of the antenna structure.
- λ is the wavelength at the highest frequency of operation for the antennas being used, in m.

The selection of sample size is somewhat more complicated in that it will affect the overall measurement accuracy. If uniform illumination of the sample is used, then it is advisable to make the sample 10λ at the lowest frequency of interest, for an accuracy of ± 1 dB for a reflection coefficient of 20 dB. The accuracy drops to ± 3 dB for a reflection coefficient of 30 dB, and ± 10 dB for a reflection coefficient of 40 dB. An alternative is to change the illumination of the sample. If narrow-beam antennas (high gain) are used with an illumination taper of 10 dB across at the edge of the sample, then the same 10λ sample may be measured to an accuracy of ± 3 dB for a 40 dB reflection coefficient level, and a 30λ sample may be measured to an accuracy of ± 1 dB. When employing tapered illumination, however, the sample must be at least one Fresnel

Zone [the value of r_a in Equation (22)] in dimension at the lowest frequency of interest. Hence, care must be taken in designing an arch, since the aperture of the antennas will determine their directivity and the required range, r_a , which, in turn, will dictate the overall size of the arch and the size of the sample. These requirements are discussed in detail in [B10].

In general, an arch designed for a reasonably accurate measurement of 50 dB reflection coefficients will employ tapered illumination of the sample as well as samples that are several Fresnel Zones in dimension. In any case, sample sizes of less than 20λ should not be considered if one wishes to measure 50 dB reflection coefficients. The edge effects of the sample may be mitigated by the use of similar absorber surrounding the sample.

Consideration of the antenna coupling, extraneous test apparatus reflections, and plane of reflection surface shifts due to sample thickness will be treated in the next clause, as these parameters are of concern during the acquisition and reduction of the measured data.

For more information on the arch method, see [B10] and [B31].

7.2.1.1 Test setup

The usual method of arch measurement uses a fixed-frequency signal source, a detector, and a VSWR meter. The recommended test setup configuration is shown in Figure 20. The receive and transmit antennas move independently on the arch and are directed toward the center of the arch. The metal plate table is designed to move vertically and symmetrically through the center of the arch over a distance of 2λ at the lowest frequency of interest. If reflection coefficient measurements below -50 dB are desired, then it is necessary to place RF absorber around the arch and table structures to reduce any reflections to a level that is below -60 dB. The ambient reflections and the direct coupling between the transmit and receive antennas should also be reduced to these levels. It may be required that the setup be enclosed by an anechoic chamber. The sum of all undesired effects, such as the arch and ambient reflections, the diffraction from the sample edges, and the direct coupling between the transmit and receive antennas, will be referred to henceforth as spurious effects.

7.2.1.2 Test procedure

The method of test can be implemented without the use of computers or expensive signal sources and receiver instrumentation. Data may be reduced by the use of tables or graphs, such as that of Figure 21.

In addition, this test procedure is an excellent double-check on the accuracy and reliability of the more modern, time-domain reflectivity procedure that is described in 7.2.2.

The measurement procedure basically is as follows:

- a) Adjust the signal source and VSWR meter for maximum dynamic range for the equipment being used.
- b) Move the metal plate vertically through a minimum distance of 1λ about the center of the arch. The reason for this procedure is to have an idea of the level of the spurious effects. During the motion of the plate, the level of the plate reflection and of the spurious effects do not change much; however, their relative phase changes a lot. This causes a VSWR to be observed, which is an indication of the relative strength of both signals.
- c) The resulting VSWR (i.e., the signal level at the receive antenna as a function of the table height) is recorded. This VSWR will indicate the minimum reflection coefficient that the arch can measure, since it is related to the reflection coefficient by

$$\rho = \frac{\text{VSWR} - 1}{\text{VSWR} + 1} \quad (23)$$

where

ρ is the magnitude of the reflection coefficient for a given VSWR.

If a smaller reflection coefficient is to be measured, then the spurious effects have to be reduced. A carefully designed arch setup can reduce these effects to -60 dB, which corresponds to a VSWR of 1.002 or a reflection coefficient of .017 dB. This is illustrated in Figure 21, which is a plot of Equation (23) that expresses the variables in dB.

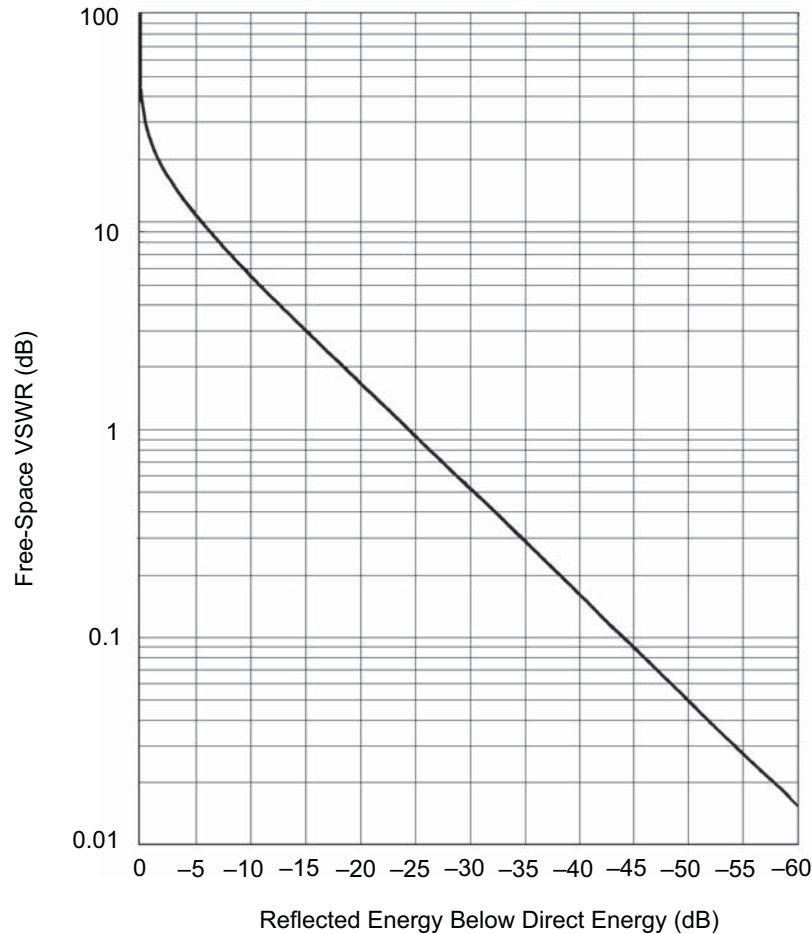


Figure 21—Reflection coefficient vs. VSWR chart

- d) The RF absorber sample is placed on the metal plate, attenuation is removed from the VSWR meter until the sample signal is on scale, and a note is made of the removed attenuation. This attenuation is the sample reflection coefficient. To recheck if the spurious effects are compatible with the measured reflection coefficient, the table is moved again vertically through a minimum distance of 1λ . The observed VSWR during the motion provides an estimate of the relative magnitude of the spurious effects and of the reflected signal from the RF absorber. For example, if the VSWR is 3 dB, Figure 21 indicates that the spurious effects are 15 dB below the RF absorber reflection coefficient.

The interpretation of the result of step d) requires prior knowledge that the spurious effects are below the reflections from the RF absorber. The 3 dB VSWR used previously could also be obtained if the reflection from the RF absorber was 15 dB below the spurious effects. This ambiguity can be removed by using an RF absorber sample of a known reflection coefficient. Once the level of the spurious effects for the particular arch setup and frequency are established, the method does not require the VSWR measurement in step d).

The technique discussed in this subclause measures only the magnitude of the reflection coefficient. Using more sophisticated equipment, such as vector network analyzers, the magnitude and phase of the reflection coefficient can be measured.

7.2.1.3 Test results

The arch method provides an accurate procedure for the measurement of the reflection coefficient of RF absorbers at frequencies above 1 GHz. The reflectivity at frequencies from 30 MHz to approximately 1 GHz cannot be measured by this technique. Refer to the discussion in 7.2.4 on tests using enclosed structures. Figure 22 shows a typical arch measurement result for a 0.6 m (2 ft) pyramidal RF absorber in the frequency range of 6–18 GHz.

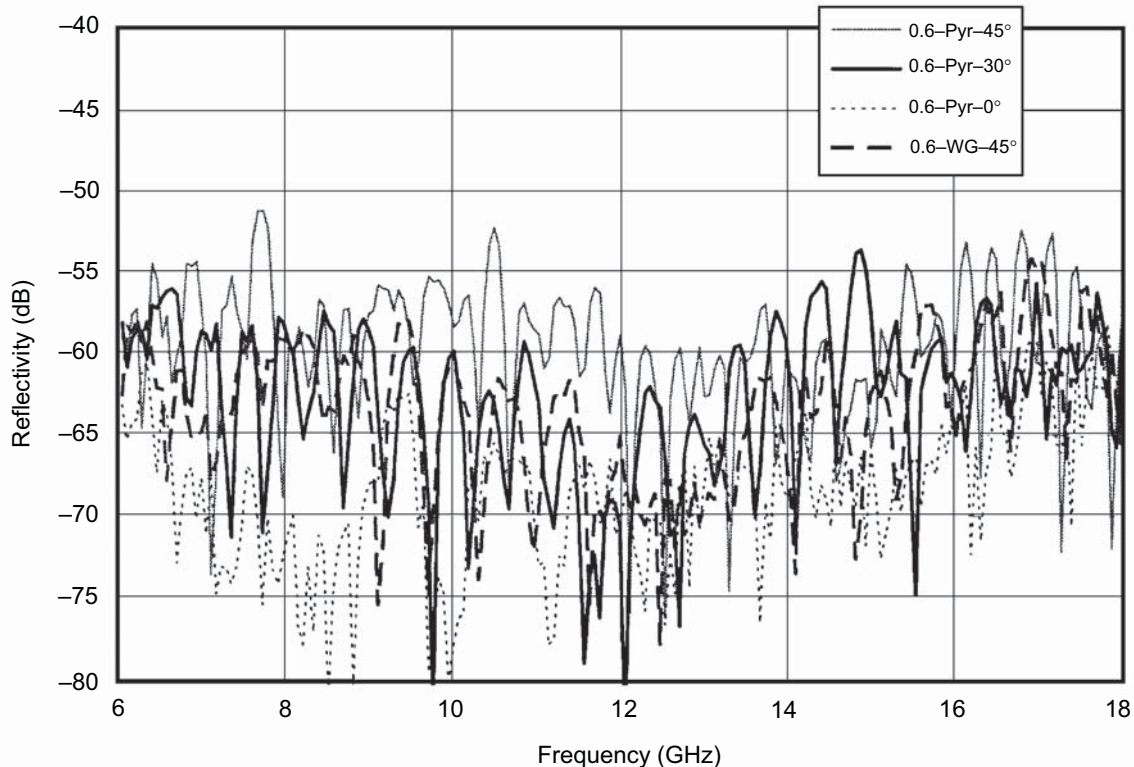


Figure 22—Typical measurement result of the arch method for a 0.6 m (2 ft) pyramidal RF absorber

7.2.2 Time-domain reflectivity measurement procedure

Two time-domain techniques are discussed in this subclause. The first technique addresses the problem of measuring the reflectivity of already installed radar absorber material (RAM) (e.g., the RAM on the walls of an anechoic chamber). The second technique addresses the problem of measuring the reflectivity of RAM tiles.

7.2.2.1 Time-domain reflectivity measurement of large areas of RAM

Measurement of RF absorber reflectivity in an enclosed space is complicated by the fact that RF absorbers usually are quite reflective in the frequency range of 30–100 MHz (see [B15] and [B22]). Carrying out measurements in a space such as an anechoic chamber or shielded room is thwarted by the very-high-level multipath reflections that are present. Even with good-quality RF absorbers, an ordinary anechoic chamber can exhibit resonances and large multipath reflections at low frequencies. The time-domain technique can reduce the errors caused by these reflections. Although it can be used at frequencies as high as 5 GHz, it is particularly well suited for the range from 30 MHz to 1 GHz. Other techniques, such as the arch method, can be successfully used for the range of 1–5 GHz.

The time-domain measurement system is configured so that the transmit and receive antennas are closer to the RF absorber under test than to any other surface in the surrounding space. The transmit and receive antennas are pointed at the RF absorber as shown in Figure 23. Their relative position determines the angle of incidence, as in the arch test. The transmit antenna is excited by a short pulse. The generated field is reflected by the RF absorber and received by the receive antenna. The received voltage is sampled and digitized for subsequent processing. The received waveform can be viewed on an oscilloscope. An example of this is shown in Figure 24. This waveform has several important parts. The earliest part is the signal that coupled directly from the transmit to the receive antenna, since they are closer than any other reflecting surfaces. The next part is the reflection from the RF absorber. The final part of the signal is the other reflections caused by the environment, assuming that these reflection points are further away from the receive antenna than the RF absorber. The operator can estimate the duration of the first two parts of the signal from the measurement setup geometry. As long as the dimensions of the room in which the measurement is being conducted are such that the above conditions are satisfied, it is always possible to separate the first two parts of the waveform from the rest. A simple time window can then eliminate the undesired reflections produced by the ambient.

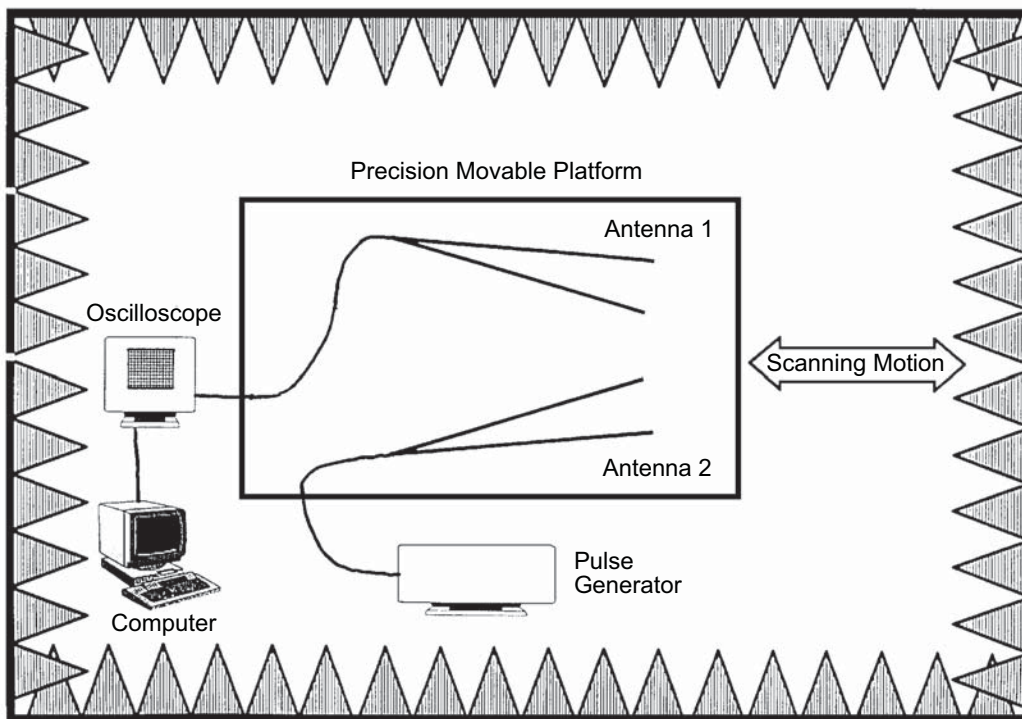


Figure 23—RF absorber reflectivity measurement setup

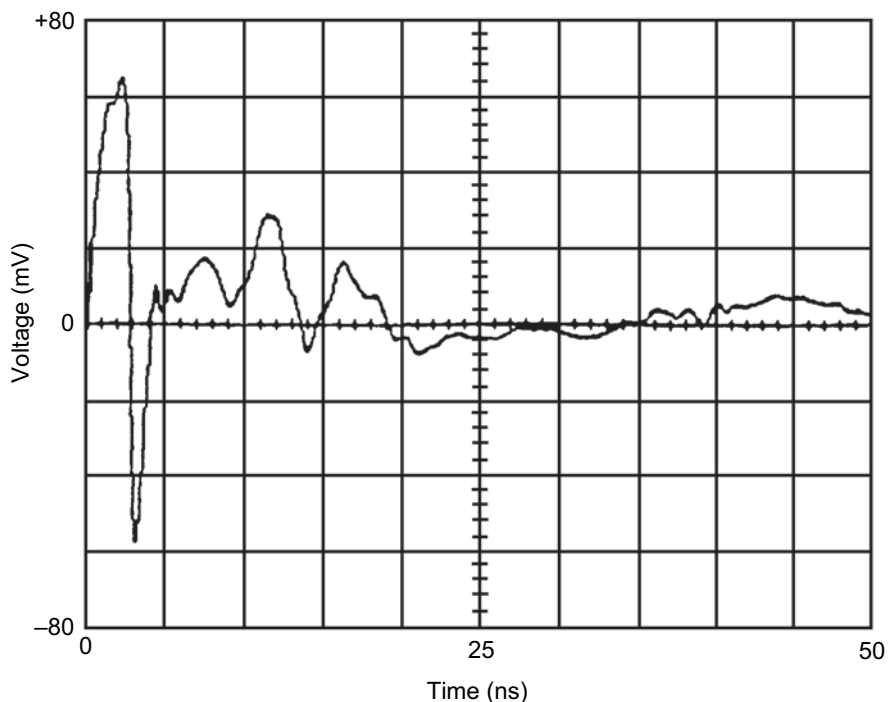


Figure 24—Typical received waveform of a transmitted short pulse

The direct-coupled part of the waveform can be reduced by repeating the reflection measurement at two different distances from the RF absorber. The time of arrival of the direct-coupled part is the same for both measurements, as long as the two antennas are maintained in the same relative position during the two measurements; however, the reflected parts will occur at different times. If the more distant measurement waveform is subtracted from the closer one, the direct-coupled parts are suppressed by as much as 40 dB while the desired parts remain. Any other undesired signal that is independent of the distance to the absorber, such as reflections from the antenna mount, are also reduced appropriately. This is illustrated in Figure 25.

This subtraction process results in a waveform that contains two copies of the reflected signal, the second copy being a delayed and inverted version of the first (due to the subtraction). A reference waveform is measured by replacing the RF absorber wall with a metal reflecting surface. The same sequence of measurements is repeated. This results in a waveform that contains two copies of the reference reflection. A deconvolution process is used to extract the reflection coefficient from these two measurements.

The deconvolution process can be explained in the following way. If a linear time invariant system, having an impulse response of $h(t)$, is excited by an input, $x(t)$, then the response, $y(t)$, is the convolution of $x(t)$ and $h(t)$, which is given by the convolution integral (from [B9]):

$$y(t) = \int_{-\infty}^{+\infty} x(\tau)h(t - \tau)d\tau \quad (24)$$

This integral is usually very difficult to carry out. It also would have to be reevaluated for each desired value of t . This problem is aggravated by the fact that the unknown $h(t)$ is inside the integral. However, the corresponding operation of this process, in the frequency domain, is a simple multiplication. If $H(\omega)$ is the Fourier Transform of $h(t)$, $X(\omega)$ is the Fourier Transform of $x(t)$, and $Y(\omega)$ is the Fourier Transform of $y(t)$, then

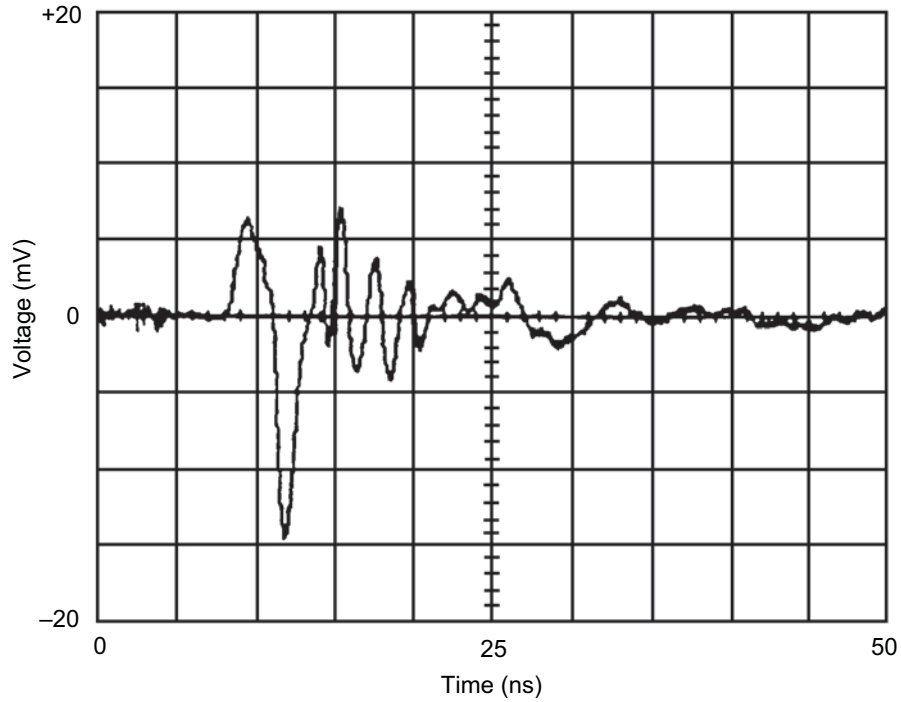


Figure 25—Received waveform after the subtraction process

$$Y(\omega) = X(\omega)H(\omega) \tag{25}$$

From this, $H(\omega)$ can be “deconvolved” (solved for) as

$$H(\omega) = \frac{Y(\omega)}{X(\omega)} \tag{26}$$

$h(t)$ is then the Inverse Fourier Transform of $H(\omega)$.

In the RF absorber measurement, $x(t)$ is the signal incident on the metallic surface or the RF absorber placed on the metallic surface, and $y(t)$ is the reflected signal received by the receive antenna. Therefore, $y(t)$ is an attenuated and delayed version of the transmitted signal, $x(t)$, when no RF absorber is present, thus indicating that no absorption was caused by the metallic surface. The attenuation and delay of $x(t)$ is due to the free-space attenuation between the receive and transmit antennas. When the RF absorber is placed on the metallic surface, $x(t)$ is the excitation of the linear system (RF absorber on the metallic surface), and $y(t)$ is the response, which has information on the RF absorber reflectivity. If the transmit and receive antennas are in the same position for both measurements, then the excitation, $x(t)$, is the same, and the response, $y(t)$, has the same free-space attenuation and delay as in the first measurement. If the excitation, $x(t)$, is an impulse, $\delta(t)$, then the response, $y(t)$, will be $h(t)$, which is the metallic plate time-domain reflection coefficient in the first case, and the RF absorber time-domain reflection coefficient in the second case. If, instead of $\delta(t)$, a signal, $x(t)$, is used, then the response, $y(t)$, will be produced. $x(t)$, $h(t)$, and $y(t)$ are related by the convolution integral of Equation (24) in the time domain, or Equation (25) in the frequency domain.

Instead of using the continuous frequency spectrum, ω , of the Fourier Transform to obtain $H(\omega)$, as suggested in Equation (26), a discrete approach is used. The Fourier Transform is replaced by the Discrete Fou-

rier Transform (DFT). The numerical implementation of the DFT is the algorithm called Fast Fourier Transform (FFT) (see [B24]). The DFT is essentially a truncated Fourier series that is suitable to represent band-limited signals. All the Fourier series terms beyond the signal upper frequency limit, f_u , are zero, since these frequencies are not present. In sampling band-limited signals, no information is lost if the sampling frequency, f_s , is at a rate higher than twice f_u . This is the Nyquist criteria. Using a sampling interval of $\Delta t = 1/f_s$ to sample the signals, $x(t)$ and $y(t)$, and the impulse response, $h(t)$, these continuous functions will become the sequences $x(n)$, $y(n)$ and $h(n)$, $n = 0, 1, 2, \dots, N - 1$. The DFTs of these sequences, calculated by the FFT, are $X(k)$, $Y(k)$ and $H(k)$, $k = 0, 1, 2, \dots, N - 1$. N is the length of the DFT and the FFT algorithm. It is determined by Δt and the length, T , of the time signals by the relation $N = T/\Delta t$. The frequency, $f_0 = 1/T$, is the separation of the spectral lines (fundamental frequency of the truncated Fourier series) of the DFT. The impulse response, $H(k)$, for each value of k corresponding to the frequency kf_0 , is just a division of $Y(k)$ by $X(k)$, as indicated by the simple operation in Equation (26). $H(k)$ is already the frequency-domain reflection coefficient of the RF absorber, in amplitude and phase, since $H(k)$ is a complex number.

The time-domain procedure can measure RF absorber reflectivity at very low frequencies without the problems of edge diffraction. These reflections can be eliminated from the measurements by time windowing and signal-processing techniques. This is possible because the antennas are positioned close to the target area being measured, and the reflections from the edges appear later in the received waveform.

7.2.2.1.1 Test setup

The RF absorber that is being measured can be the material already in place in an anechoic chamber, a sample of material mounted on a free-standing wall, or RF absorber arranged on the floor of an enclosure. Any additional anechoic materials covering the walls or other surfaces are not needed, but they do not interfere. The sample of material to be measured should be at least 3 m \times 3 m, although measurements have been made on smaller samples with reduced accuracy. The antennas used for these very broadband impulsive signals should have a response with constant amplitude and linear phase for all frequencies of interest between 30 MHz and 1 GHz. Other antenna responses will make data processing more difficult. The TEM horn antenna with resistively loaded aperture is recommended, see Figure 26 and [B19].

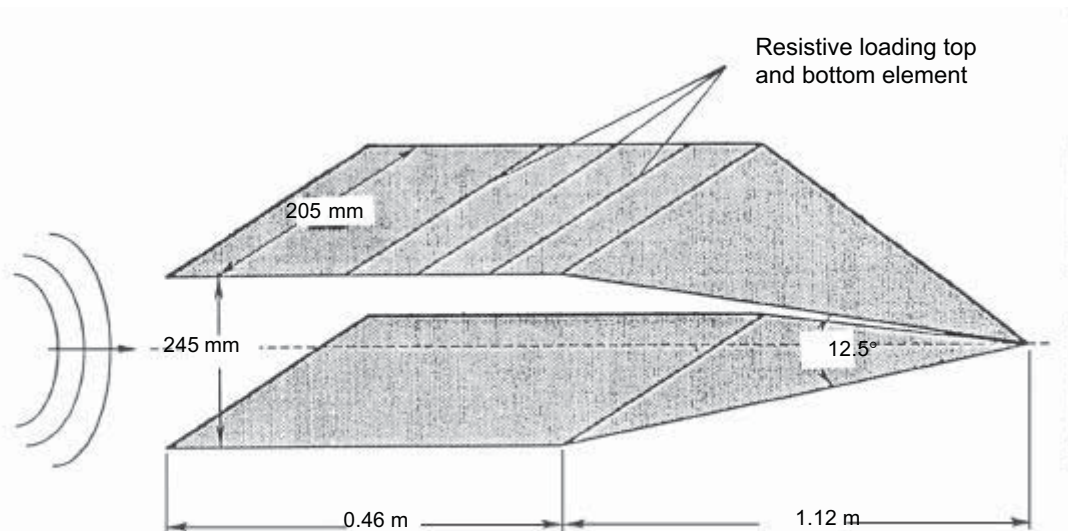


Figure 26—Typical TEM horn antenna used to measure RF absorber reflectivity

7.2.2.1.2 Test procedure

The transmit and receive antennas are positioned side by side, facing the wall under test, in such a manner that their relative positions remain fixed during the measurement. This antenna assembly is mounted on a platform that can be moved in a direction perpendicular to the surface being measured. For example, a vertical test wall will need a horizontal movement of the platform. In this case, the movable platform indicated in Figure 23, can be a cart rolling on tracks or an antenna positioner capable of the proper motion. If the RF absorber to be measured is arranged on the floor, the antenna assembly will have to move vertically above it. For measurements up to 1 GHz, the position of the platform should be repeatable to at least 10 mm. Above 1 GHz, the repeatability must be reduced to 2 mm.

The two antennas can be separated by a metal or RF absorber partition to reduce the effect of the direct coupling as long as the barrier moves with the antenna assembly on the platform. Figure 23 shows an impulse generator driving the transmit antenna. For measurements up to 1 GHz, this impulse should be at least 40 V in amplitude and no wider than 500 ps. For reliable measurements above 1 GHz, the impulse duration should be 100 ps or less. The output of the receiving antenna is digitized in an oscilloscope that has the required bandwidth.

7.2.2.1.3 Test results

The waveform shown in Figure 24 was obtained with the platform close to the RF absorber, approximately 1 m. This waveform includes the direct-coupled signal (large pulse in the first 5 ns), the desired reflection, and all other room reflections. A second measurement was taken at 1.5 m and subtracted from the first, giving the waveform in Figure 25. Notice that the direct-coupled part of the waveform has been suppressed at least 40 dB. Two similar measurements were made of a metal reflector, and those were also subtracted from each other.

This subtraction may not remove enough of the unwanted signals. If the waveforms have not been time-windowed previously, the operator can calculate the time of arrival of the desired signal and set the rest of the waveform to zero. The direct-coupling error can be separated adequately in time from the desired signal after it has been suppressed by the subtraction.

A computer can then be used to deconvolve the reference signal from the absorber reflection. The program for deconvolution uses standard FFT routines in which the number of data points are a power of two (see [B22]). The output of the FFTs are complex numbers because they carry information on the amplitude and phase of the reflection coefficient. The deconvolution is simply a division of each RF absorber spectral component by the corresponding reference component, done in complex arithmetic to retain the phase information. A typical set of results for a 0.6 m (2 ft) pyramidal absorber are shown in Figure 27. For the low frequencies, the reflection coefficient is slightly positive after the signal processing. The explanation for this is that the reflectivity from the tiles is larger than the reflection from the reference metallic wall. This may be due to the fact that the measurement is being performed in the near field, and the metallic wall is surrounded by absorber material.

7.2.2.2 Time-domain reflectivity measurement of RAM tiles

From the RAM manufacturer's point of view, it is important that only a small amount of absorber material be required by the evaluation technique. Such a measurement capability would be practical for monitoring the quality of the product during the manufacturing process. The technique discussed in this subclause, although still in the research stages, is capable of fulfilling this requirement.

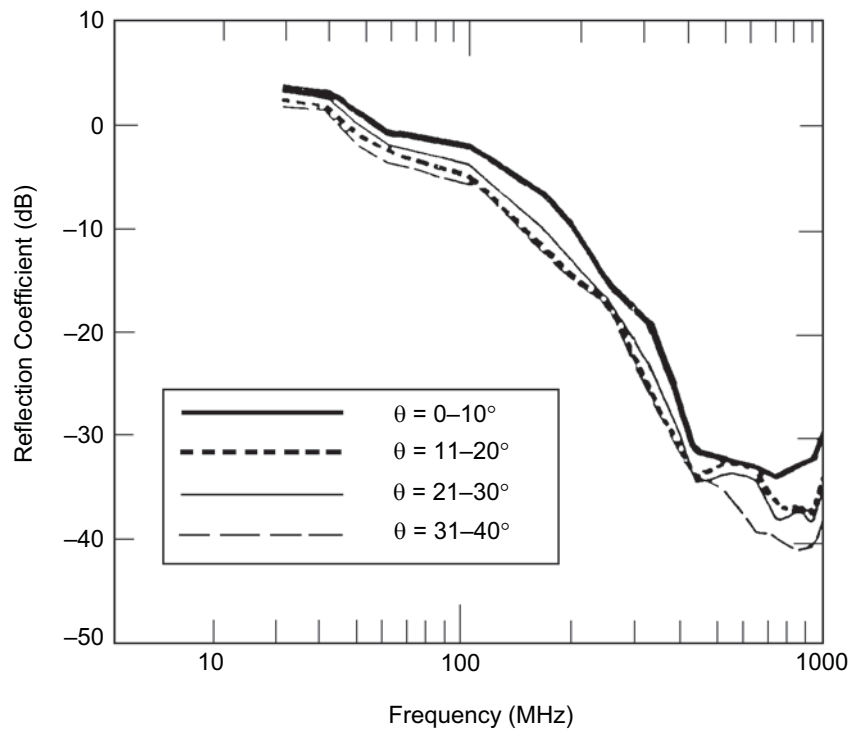


Figure 27—Time-domain measured reflectivity of a RF absorber as a function of frequency and angle of incidence

7.2.2.2.1 Test setup

The experimental setup and the associated instrumentation are depicted in Figure 28. The instrumentation consists of an impulse generator that delivers a 42 V, 400 ps wide Gaussian pulse-type waveform at a repetition rate of 50 kHz, two wideband TEM horns (see [B15]) with a wideband frequency response of 25–1000 MHz, a wideband hybrid coupler with a frequency response of 20–2000 MHz, a 14 GHz bandwidth digitizing sampling oscilloscope, and a personal computer (see [B14]).

The operation of the system is straightforward. The impulse generator transmits a pulse directly to the hybrid coupler, which splits the waveform equally between the two TEM horn antennas. The two antennas, therefore, transmit the same waveform into the chamber. Substantial reflections occur with the arrival of the transmitted waveforms, at the horns' aperture planes, due to the large electrical discontinuities present there. A significant portion of the waveform energy is reflected back into the hybrid, and the remaining waveform energy is transmitted into the environment containing the absorber sample. The energy that is backscattered from the target sample, as well as other objects in the measurement environment, is received by both antennas and fed directly back into the hybrid, which feeds the difference of the two antenna outputs into the sampling head of the digitizing oscilloscope. Once the received data waveforms are sampled and digitized, the results are then transferred to the PC for signal processing in accordance with the procedures discussed in 7.2.2.2.2.

The reason that the system requires two antennas as well as a hybrid coupler is for the protection of the oscilloscope sampling head. Most sampling heads contain delicate switching diodes that can withstand only a few volts before severe nonlinear distortion or burnout occur. The amplitude of the reflected pulses from the apertures of the TEM horns is approximately 40 V, which would destroy the sampling diodes if applied

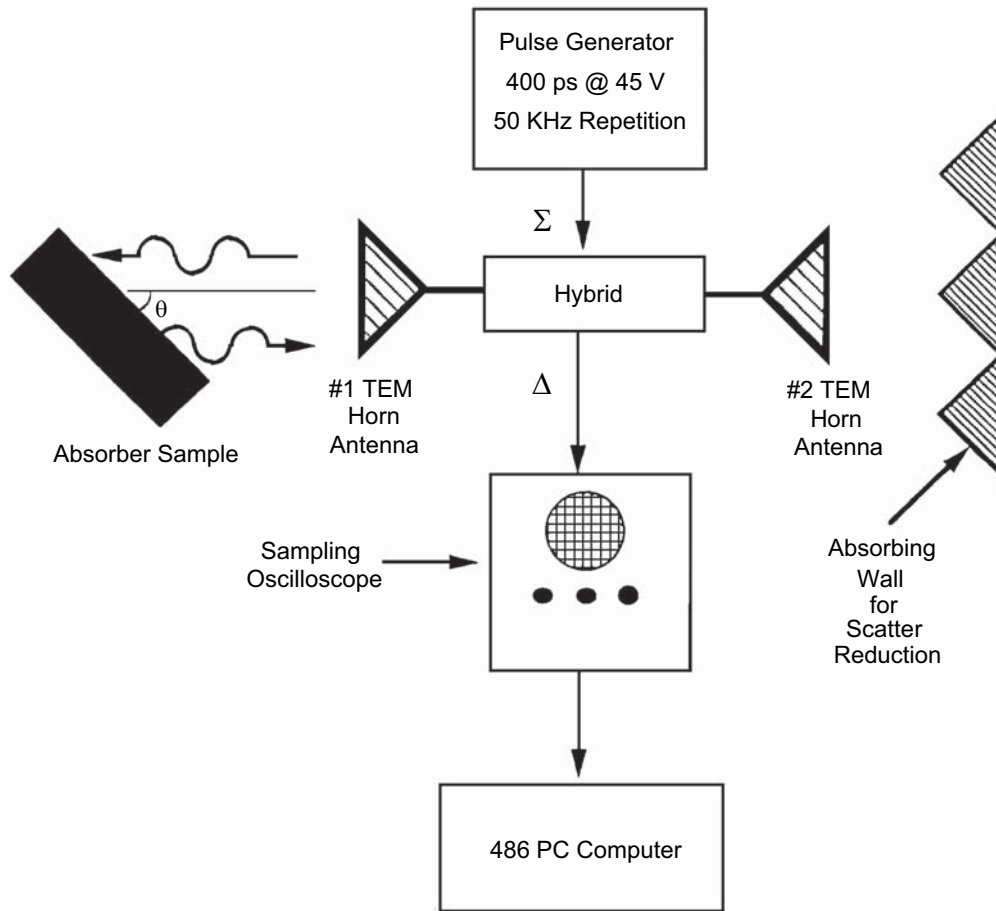


Figure 28—Time-domain tile measurement setup

directly to them. Since the two antennas are fed with transmission lines of the same length, equal signals are reflected back to the hybrid coupler which, in turn, feeds the difference of these two signals to the sampling head at an acceptable peak voltage amplitude of less than 1 V. For this process to be effective, the reflected waveforms must be nearly identical, which requires the use of two similar TEM horns.

TEM horn #2 in the test setup is strictly for the purpose of ambient reflection reduction. This antenna plays no essential role in the detection or sensing of backscattered signals from the sample. TEM horn #2 should be placed as far away from the absorber sample as the measurement setup conveniently permits. A separation of 2 m or more was found to be satisfactory. The sample backscatter sensing is performed by TEM horn #1, which is placed in close proximity to the absorber sample under evaluation.

7.2.2.2.2 Test procedure

The test procedure that is used consists of the following steps (see [B14]):

- a) With no sample present, the resulting waveform is captured on the sampling oscilloscope and is stored on the computer. This waveform is referred to as the background waveform, and it contains reflections from the walls, ceiling, and floor of the room, as well as other objects that are contained within the immediate vicinity of the measurement system. This waveform, as well as all of the subsequent waveforms that are described here, also contains system imperfections due to the antennas, cables, connectors, pulse generator, and the oscilloscope sampling head.

- b) Immediately after the background waveform is recorded, the absorber sample is placed on the holder platform, and the resulting waveform is recorded on the computer. This waveform contains contributions from the absorber sample along with a multitude of other room reflections.
- c) In order to eliminate the bulk of the room reflection effects, the background waveform of step a) is subtracted from the waveform with the sample of step b). At this point, the waveform primarily consists of the sample backscatter plus a component due to the shadow region directly behind the absorber sample.
- d) In order to isolate the backscatter response of the absorber sample, a time gating and averaging procedure is applied to the waveform of step c) (see [B22]). This waveform still contains the effects of the measurement system that are later calibrated out.
- e) The gated absorber response of step d) is converted to the frequency domain using the FFT algorithm, and the resulting amplitude spectrum is stored in the computer. The phase of the response is also available at this step. In the present implementation of the technique, only the amplitude is considered.
- f) The absorber sample is removed from the measurement fixture.
- g) Using a 2.7 m × 2.7 m metal reference plate in place of the absorber sample, steps a) through f) are repeated in precisely the same sequence. The end result of this process is the amplitude spectrum of the measurement system response with a perfect reflector in place of the absorber. Initially, this metallic plate was the same size as the absorber. It was observed that using the 2.7 m × 2.7 m plate resulted in better correlation with calculated results.
- h) The ratio of the amplitude spectra obtained in step e) to that of step g) is computed to obtain the absorber reflectivity. The reflectivity measured with this system is only approximately related to the plane-wave reflection coefficient of the absorber material. It is *not* the same quantity as the plane-wave reflection coefficient that is obtained using TEM measurement fixtures or certain modelling techniques (see [B11]). Plane-wave absorber modelling and measurement methodologies typically assume an infinite slab of absorber with a plane electromagnetic wave incident on it, while this time-domain measurement procedure involves a spherical wave incident on a finite material sample. Since the dimensions of the sample are small in respect to the wavelengths for the frequencies of interest, the phase and amplitude do not change appreciably over the sample, especially for near normal incidence.

7.2.2.3 Test results

Reflectivity measurements were performed on ferrite tiles with ground plane and urethane absorber attached to ferrite tiles.

Figure 29 shows the first configuration used. A 1 m × 1 m ferrite tile panel is backed by a 1 m × 1 m plywood-aluminum ground-plane combination. The reflectivity results obtained are shown in Figure 30, where the plot corresponds to results obtained with the transmitted and received field oriented vertically (vertical polarization). The most salient feature of the results is the deep notch tuning that is predicted by a plane-wave reflection coefficient modelling procedure (see [B11]). Clearly, the ground-plane plywood combination provides the proper tuning to achieve desired broadband behavior.

Next, a section of urethane absorber was mounted on top of the previous ferrite absorber. Reflectivity results are depicted in Figure 31. As can be seen readily, the urethane absorber provides a significant reduction on the reflectivity above 600 MHz.

7.2.3 Enclosed measurement procedure

7.2.3.1 Background

The measurement techniques discussed previously, with the exception of the time-domain technique, cannot measure the reflectivity of RF absorbers at frequencies below 200 MHz, in the best of circumstances, because of the reflections from the edges of the RF absorber. These reflections on a standard 0.6 m × 0.6 m

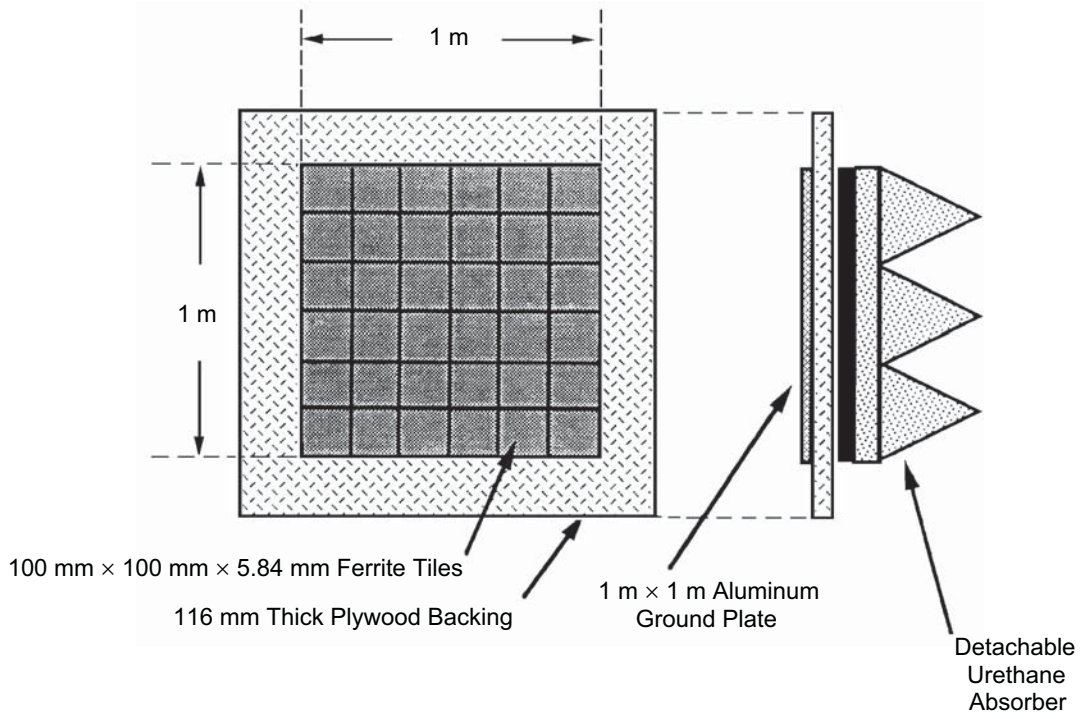


Figure 29—Ferrite tile/urethane hybrid RF absorber structure

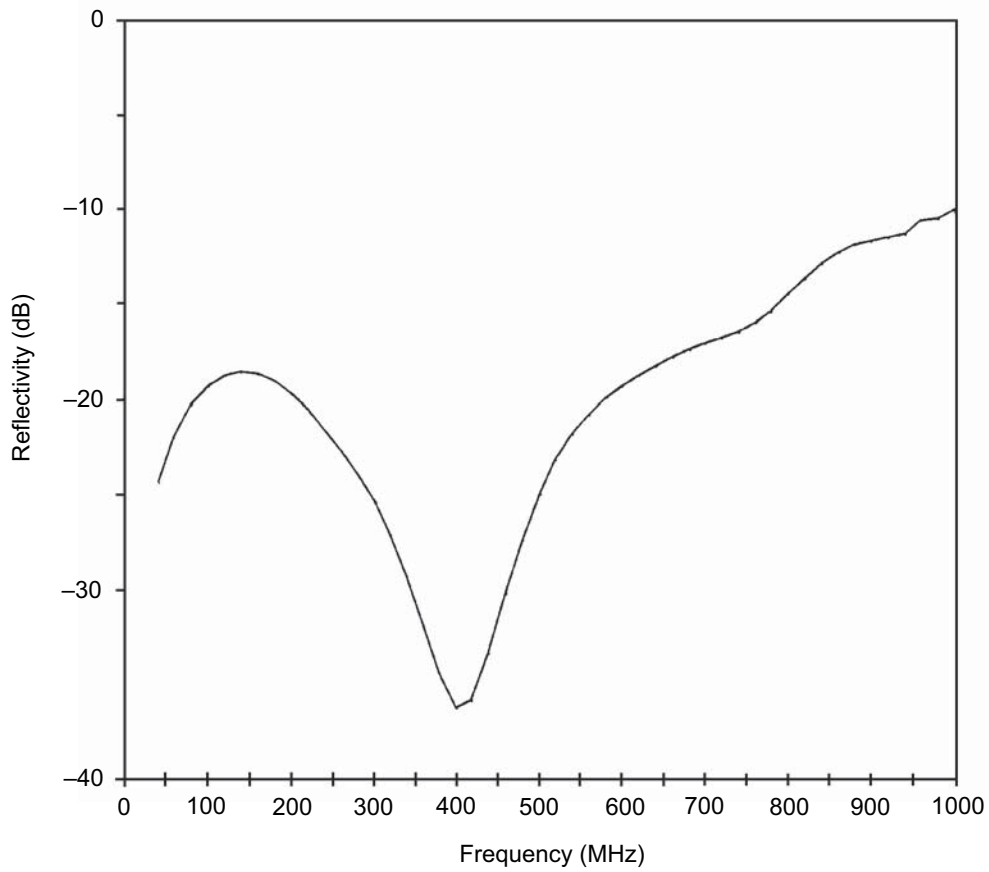


Figure 30—Reflection coefficient of ferrite tile only

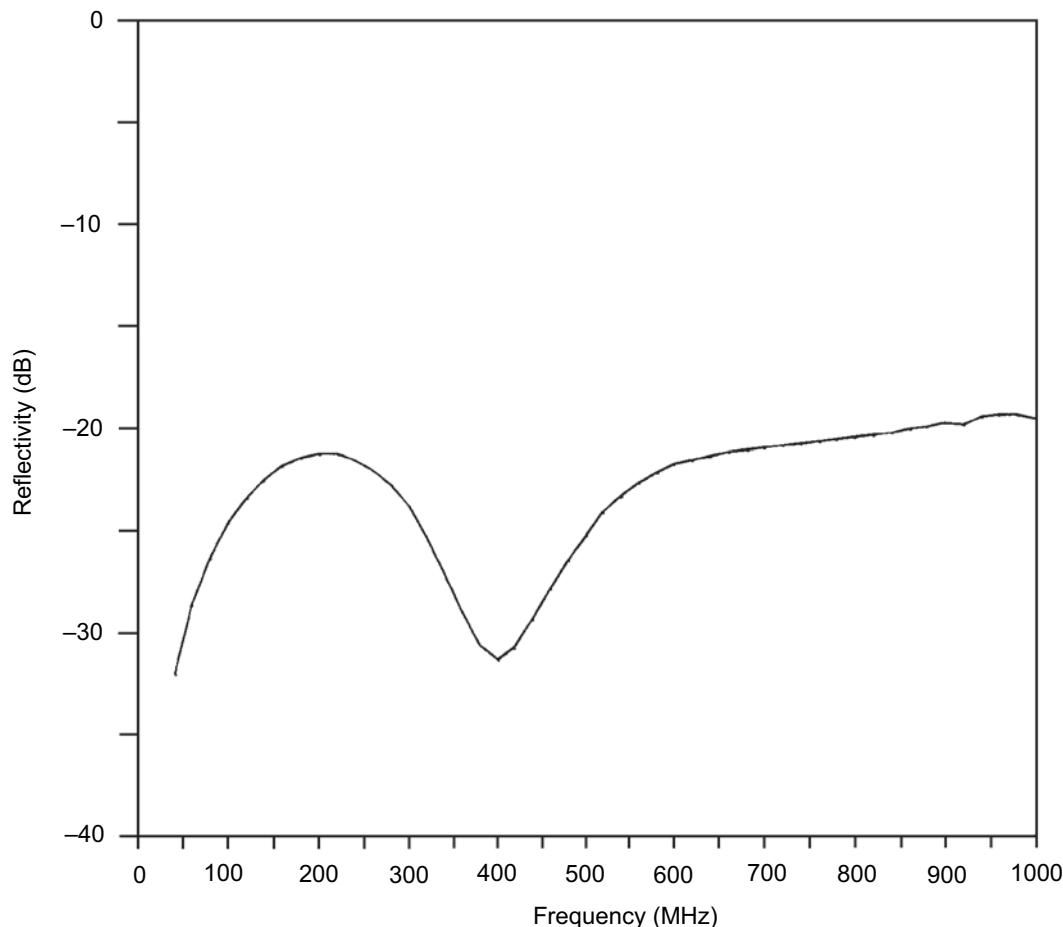


Figure 31—Reflection coefficient of ferrite/urethane of Figure 29

(2 ft × 2 ft) tile, or even a square array of 16 tiles, can easily exceed 20 dB, thus precluding the accurate measurement of high-performance RF absorbers. The arch method, with antennas that can taper its illumination of the sample edges by about 10 dB, still requires that the sample be at least 4 wavelengths in size (see [B10]). At 30 MHz, this would require a square of about 40 m (132 ft) on each side, requiring 4356 standard size tiles. The fields inside a waveguide or coaxial transmission line are relatively uniform, and are confined to small regions of space, even at low frequencies. This suggests that such devices could be used to measure the reflectivity of RF absorbers using much smaller sample sizes since the diffraction from the edges is not a factor.

7.2.3.2 The enclosed-waveguide measurement procedure

The enclosed-waveguide measurement procedure, also known as the flared-waveguide measurement procedure, uses a length of waveguide with a cross-section the size of the standard RF absorber tile or of a small array of them. The waveguide is excited at one end with a probe that is designed to excite only the TE_{10} mode. The other end is closed by the RF absorber under test as shown in Figure 32. The energy propagates from the probe to the RF absorber, where a portion of it is absorbed and the rest is reflected. If the waveguide is assumed to be lossless, then the ratio of the reflected to the incident energy, at the input probe, is the same as at the surface of the RF absorber. The system input reflection coefficient, or VSWR, is therefore a measure of the reflectivity of the RF absorber. The only problem is that the impedance of the wave propagating inside of the waveguide is not the same as free space and, therefore, the reflection coefficient is

measured with the wrong reference impedance. From waveguide theory (see [B8]), the waveguide impedance is given by

$$Z_{mn} = \frac{Z_0}{\sqrt{1 - \left(\frac{k_{mn}}{k}\right)^2}} \tag{27}$$

where

$$k_{mn}^2 = \left(\frac{m\pi}{a}\right)^2 + \left(\frac{n\pi}{b}\right)^2 .$$

$$k = \frac{2\pi}{\lambda} .$$

- λ is the free-space wavelength.
- Z_0 is the free-space intrinsic impedance.
- a is the width of the waveguide.
- b is the the height of the waveguide.
- m and n are the mode-order indices.

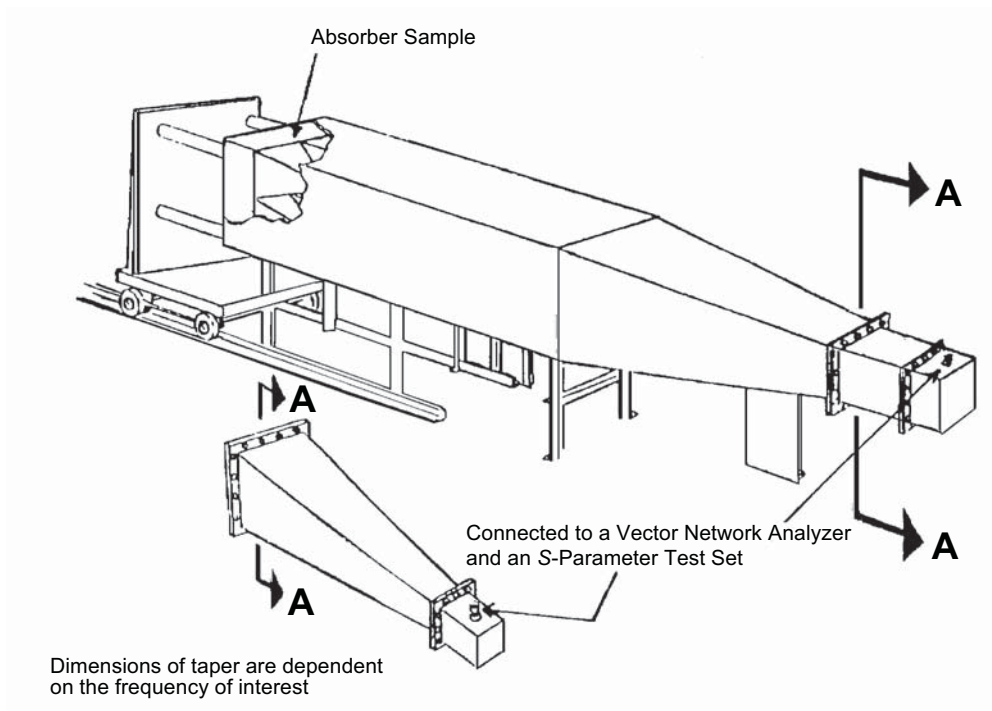


Figure 32—Flared waveguide measurement procedure test setup

For the fundamental mode, TE₁₀, Equation (27) reduces to

$$Z_{10} = \frac{Z_0}{\sqrt{1 - \left(\frac{\lambda}{2a}\right)^2}} \tag{28}$$

Note that for Z_{10} to be real, a has to be greater than half the wavelength. The closer a is to this, the larger the difference between Z_0 and Z_{10} becomes. So, for these two impedances to be close, a has to be large. For example, for $a = \lambda$, $Z_{10} = 1.15 Z_0$. This gives an idea of the minimum size of the sample as a function of frequency. For 30 MHz, $\lambda = 10$ m (33 ft). An array of this size would require at least 17 tiles for a waveguide height of up to 0.6 m (2 ft) [the standard RF absorber tile is 0.6 m \times 0.6 m (2 ft \times 2 ft)].

A detailed study of this is presented in [B10]. It is shown there that, for an error of 2 dB, when measuring a 30 dB RF absorber, a is required to be at least 2λ .

For higher frequencies, the TE_{10} mode is excited in a waveguide whose dimensions are smaller than a standard tile of 0.6 m \times 0.6 m (2 ft \times 2 ft), or a small array of them. In such cases, a “flared-out” waveguide is used. The flaring is carried out slowly so as to reduce the direct excitation of the higher-order modes. When interpreting the measured values of the VSWR, it is assumed that the field incident on the material is still the dominant mode alone, despite the increased dimensions of the guide in the region where the sample is placed. According to [B10], the larger the dimension of the flared-out guide, the closer the measured reflection coefficient is to free space.

7.2.3.2.1 Test setup

The test setup for the enclosed waveguide measurement test is shown in Figure 32. The metallic waveguide consists of the following three sections:

- a) A 0.6 m \times 0.6 m (2 ft \times 2 ft) square metallic tube that is approximately 4.8 m (16 ft) long (roughly 4λ). This will accommodate one sample up to 1.8 m (6 ft) in thickness.
- b) A flat metal rear plate upon which the material under test will be mounted. This plate will be fastened securely to the open end of the waveguide such that the plate makes full contact with the edges. RF gasket or fingerstock can be used to ensure full contact. This also minimizes any signal leakage.
- c) The flared signal launch section, which also contains the coaxial to waveguide transition.

All three sections are fastened together, and a 3–6 dB attenuator is attached to the coaxial connector. This will minimize any VSWRs that may result from any mismatches from the system.

A cable of known loss is then connected to the attenuator and to a vector network analyzer. At this point, it is important to ensure that the waveguide is empty so that a reference measurement can be recorded as described in 7.2.3.2.2. This level is what the absorber material will be compared against.

Once the reference level is recorded, the rear plate is removed and the absorber sample is mounted on it. The sample is then inserted into the waveguide and the level is recorded again. The algebraic difference between the levels of the flat plate alone and the absorber sample is the magnitude of the reflection coefficient of the absorber. It should be noted here that the base sides and bottom of the samples must have very good contact with the waveguide interior. This will provide an accurate measurement by ensuring that all the energy passes through the absorber.

7.2.3.2.2 Test procedure

The measurement of reflectivity of a 0.6 m \times 0.6 m (2 ft \times 2 ft) piece of RF absorber in the enclosed waveguide method proceeds as follows:

- a) The frequency band of the waveguide is selected for use on a vector network analyzer and its S -parameter test set. Within that band, 201 sample points are chosen for measurement.
- b) One-port calibration for S_{11} is performed on the network analyzer (accounting for directivity, frequency response, and port mismatch of the system).
- c) The network analyzer is connected to the waveguide via coaxial cable to the feed end of the guide.

- d) A 0.6 m × 0.6 m (2 ft × 2 ft) piece of RF absorber is then placed in the guide. See Figure 32.
- e) The time-domain gating function on the analyzer is turned on, and the gate is set around the area where the sample under test is placed in the guide. This is an important step because it eliminates from the measurement undesired reflections caused by imperfections in the waveguide and the interconnecting cables.
- f) The reflection coefficient is then measured directly from S_{11} .

For a discussion of this test procedure, refer to [B29].

7.2.3.2.3 Test results

The results of RF absorber measurement in an enclosed waveguide are essentially a flat trace over the frequency band of the guide. A typical 0.6 m (2 ft) pyramidal RF absorber would have the reflection coefficient performance shown in Figures 33 and 34 for the frequency bands of 20–120 MHz and 450–600 MHz, respectively.

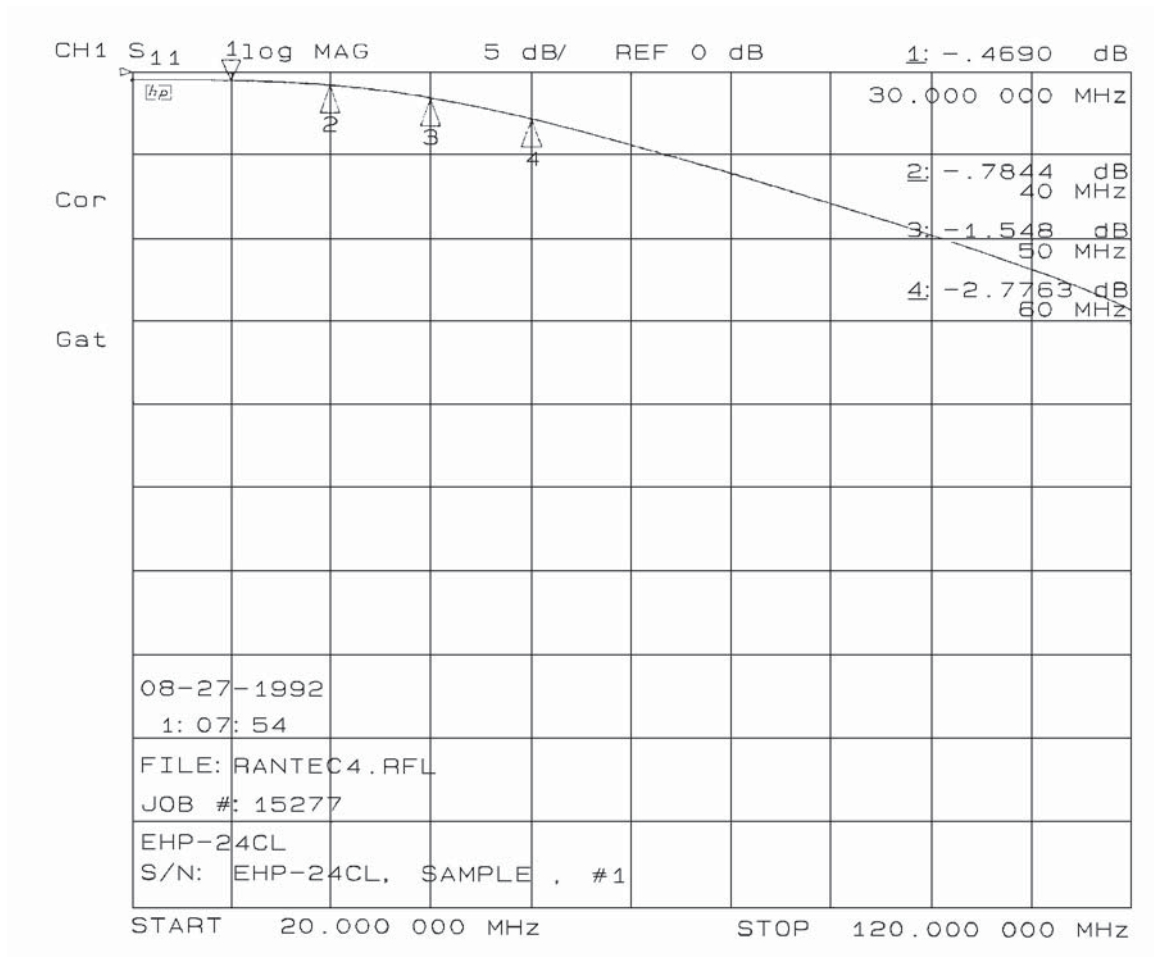


Figure 33—0.6 m (2 ft) pyramidal RF absorber in the 20–120 MHz band

7.2.3.3 Low-frequency coaxial reflectometer measurement procedure

A variation of the enclosed waveguide test method uses a special coaxial air-filled line. This is commonly referred to as the low-frequency coaxial reflectometer (LCR) method.

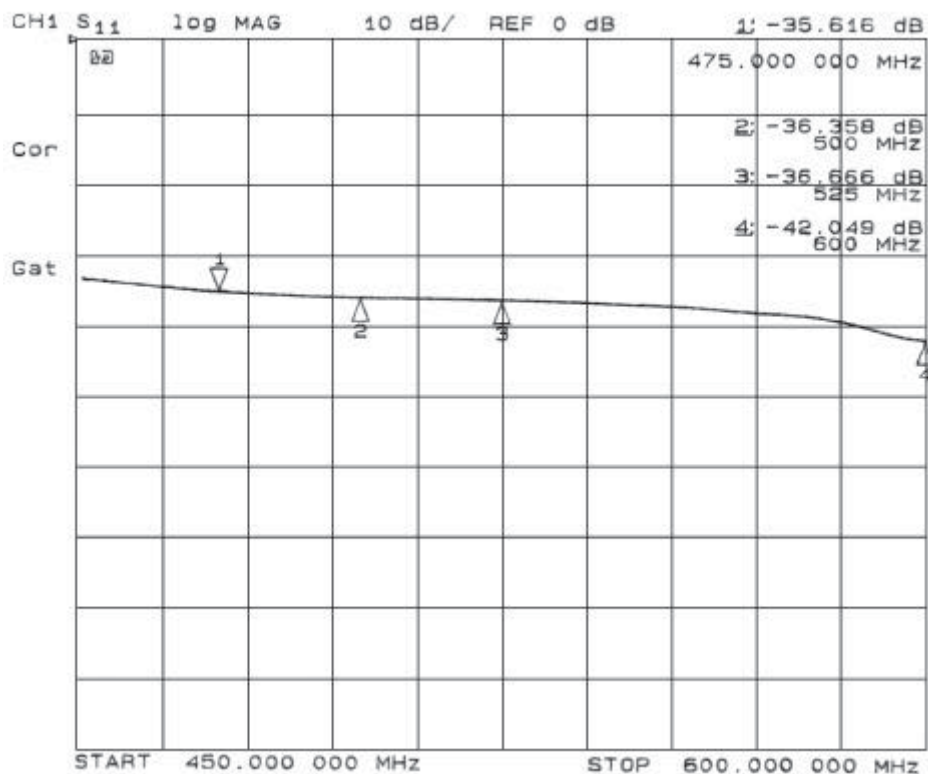


Figure 34—0.6 m (2 ft) pyramidal RF absorber in the 450–600 MHz band

A coaxial line, supporting a TEM wave, simulates the free-space wave incident on RF absorbers and does not have a low-frequency cutoff. The high-frequency limitation of this line is due to the generation of high-order modes. As a rule of thumb, for circular coaxial lines, higher-order modes will be generated when the frequency is such that its wavelength is shorter than the circumference of a circle with a radius that is equal to the average of the radii of the inner and outer conductors (see [B10]).

Figure 35 shows the three basic cross-section designs used to construct LCRs:

- Design 1:* Square inner conductor with a square outer conductor that is three times the size of the inner conductor. This configuration will take eight 0.6 m × 0.6 m (2 ft × 2 ft) RF absorber tiles to conduct a reflectivity measurement.
- Design 2:* Thin circular-wire inner conductor with a square outer conductor. This configuration will take four 0.6 m × 0.6 m (2 ft × 2 ft) RF absorber tiles to conduct a reflectivity measurement.
- Design 3:* Thin-septum inner conductor with a square outer conductor. This configuration will also take four 0.6 m × 0.6 m (2 ft × 2 ft) RF absorber tiles to conduct a reflectivity measurement.

Design 2 is the least desirable configuration, since the coaxial line has a high characteristic impedance. This would put severe demands on the matching device between the LCR and the 50 Ω measurement system. In addition, test results may be less repeatable because the gap between the thin wire and the absorber elements, produced when the center conductor is inserted into the absorber, can vary considerably from sample to sample. Designs 1 and 3 have both been constructed by a few absorber manufacturers. The following discussions represent operation experiences from one of the absorber manufacturers who has constructed and operated LCRs of both designs:

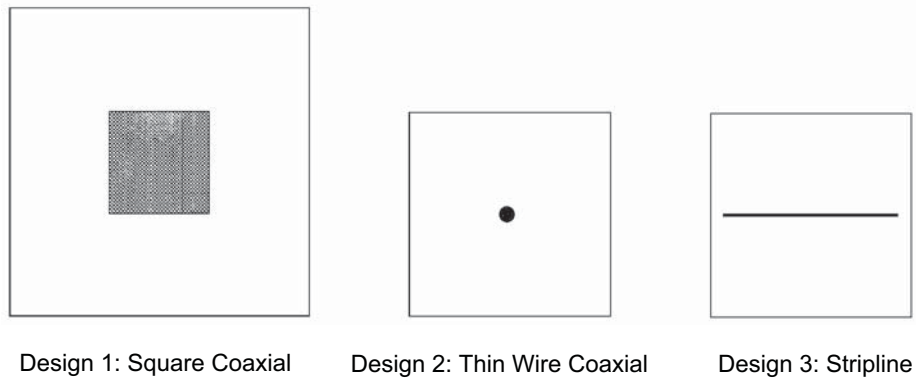


Figure 35—Cross-sections of coaxial lines used in the low-frequency coaxial reflectometer procedure

- a) In order to construct an LCR, using Design 3, with a $50\ \Omega$ characteristic impedance, the width of the septum would have to be only a few inches smaller than the outside conductor. The fringing field generated by this configuration has a very severe impact, especially for nonisotropic absorbers. Its position relative to the fringing field region greatly influences the measured result. In addition, the first higher-order mode, TE_{10} , is excited whenever there is vertical asymmetry in the LCR. The cut-off frequency of the TE_{10} mode is approximately 120 MHz for this type of LCR using four full-size absorber tiles. Due to gravity, a vertical asymmetry usually is present, since the cross-section of the LCR normally is oversized to allow easy handling of the absorber tiles during the test. Measured results using this design indicate the strong presence of the TE_{10} higher-order mode at 120 MHz. This may be observed for frequencies as low as 115 MHz, thus introducing an error of the order of 3 dB. This error is observed in the measurements of both the loaded and unloaded reference metallic plate (as explained in 7.2.3.3.2). Measurements made using this design above 120 MHz have been shown to introduce excessive errors.
- b) Due to the 3:1 ratio of the outer to the inner conductor dimensions in Design 1, the characteristic impedance of the LCR line is approximately $60\ \Omega$. Therefore, there is a $-20\ \text{dB}$ reflection due to the mismatch between the LCR and the $50\ \Omega$ measurement instrumentation. This reflection can be suppressed effectively using the time-domain gating techniques detailed in [B30]. Theoretically, the first higher-order mode is the TE_{11} , which exists at about 84 MHz (using the circular coaxial line mode definition in [B10]). The TE_{11} mode, however, requires that two different geometrical asymmetries exist on the vertical and horizontal axes of the square coaxial cross-section. Experience has shown that this does not usually occur. The measured data for the shorted reference plate, as well as for a variety of absorbers, never indicates any noticeable presence of this high-order mode. The only noticeable high-order mode is at approximately 230 MHz, which is attributed to the TE_{31} mode. The error introduced by this mode on the shorted plate measurement is approximately 0.3 dB, and the error on the absorber-loaded measured data is hardly noticeable. Therefore, the worst-case error due to the TE_{31} mode could be as high as 0.6 dB. This error is well within the precision of RF absorber measurements at any frequency. If higher errors (e.g., 2 dB) are permitted, the LCR system can be used for frequencies as high as 500 MHz. Severe measurement errors will occur, however, if measurements are attempted for frequencies above 600 MHz. The disadvantages of this design are its high construction cost and the complexity of absorber loading to perform the test.

Based on the above analysis, the square coaxial LCR represents the best design, and should be recommended as the preferred low-frequency RF absorber reflectivity measurement fixture. In order to implement the time-domain gating technique to effectively suppress the reflection due to the impedance mismatch, it is recommended that a minimum of 10 m of straight coaxial line section be used in order to allow reliable error suppression. Like all measurements using time-domain gating, the start and stop frequencies should be kept

away from the intended test-frequency range in order to minimize the window-edge effect when time gate is applied. Whenever possible, it is strongly recommended that 10% of the test-frequency range be allocated before the first usable data point at the low-frequency end.

7.2.3.3.1 Test setup

A typical construction and test equipment setup is shown in Figure 36. The approximate dimensions of the LCR are 12 m for the coaxial line section and 4 m for the tapered section. The outer conductor is a square that is 1.8 m (6 ft) on the inside, while the inner conductor is 0.6 m (2 ft) on the outside.

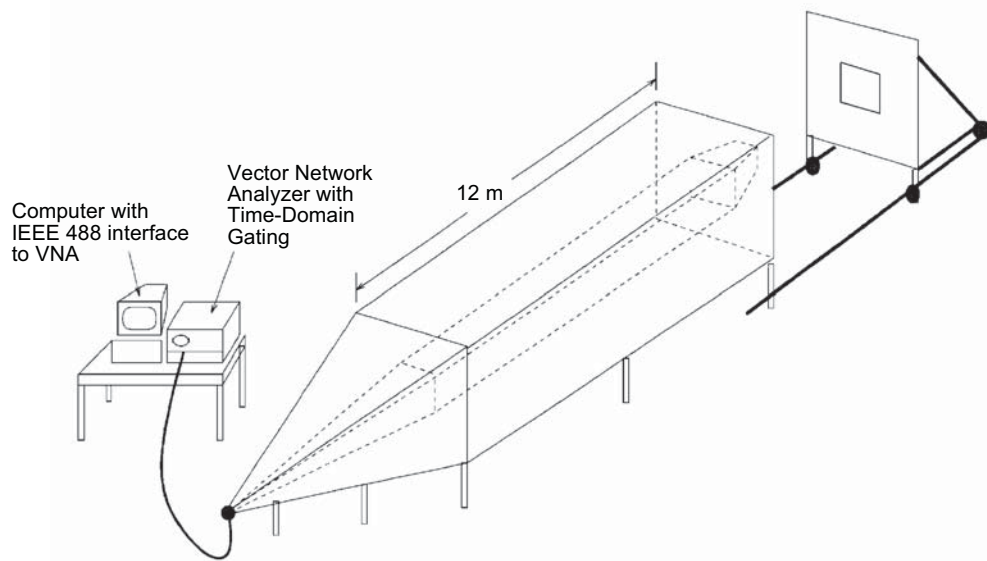


Figure 36—Low-frequency coaxial reflectometer measurement test setup

7.2.3.3.2 Test procedure

A typical procedure for using the LCR for RF absorber measurements can be outlined as follows:

- Turn on the vector network analyzer, and allow it at least 15 min to warm up.
- Set the start and stop frequencies of the vector network analyzer, and select the S_{11} measurement option. When possible, the test start frequency should be chosen so that it is below the lowest frequency to be measured by at least 10% of the measurement frequency range.
- Perform a full one-port S_{11} calibration at the cable connector that connects to the LCR.
- Install the metallic shoring plate to measure the reflection coefficient of the shorted line, with time-domain gating to discriminate the reflection from characteristic impedance mismatch. This trace should be recorded in the computer as the reflectivity reference.
- Load eight pieces of full-size absorber to cover the shoring plate, as shown in Figure 36.
- Measure the reflection coefficient again with the time-domain gating. The time gate settings of the two measurements with the metallic plate and the absorber may or may not be the same.
- The ratio of the reflection coefficients from the two measurements is computed and recorded as the absorber reflectivity, in dB.
- This measurement procedure may be automated by using a computer with an IEEE 488 bus.

7.2.3.3.3 Test results

Figure 37 shows the comparison between the predicted and the measured data obtained with the recommended Design 1 cross-section LCR for a 0.6 m (2 ft) RF absorber. With minor modifications to the inner and outer conductors, the same test fixture is configured to measure reflectivity performance of ferrite tile and hybrid foam-ferrite RF absorbers. Figure 38 shows a sample test result and its comparison to the theoretical prediction for a 1.2 m (4 ft) hybrid RF absorber. As shown in both figures, test results have an excellent correlation with the theoretical predictions.

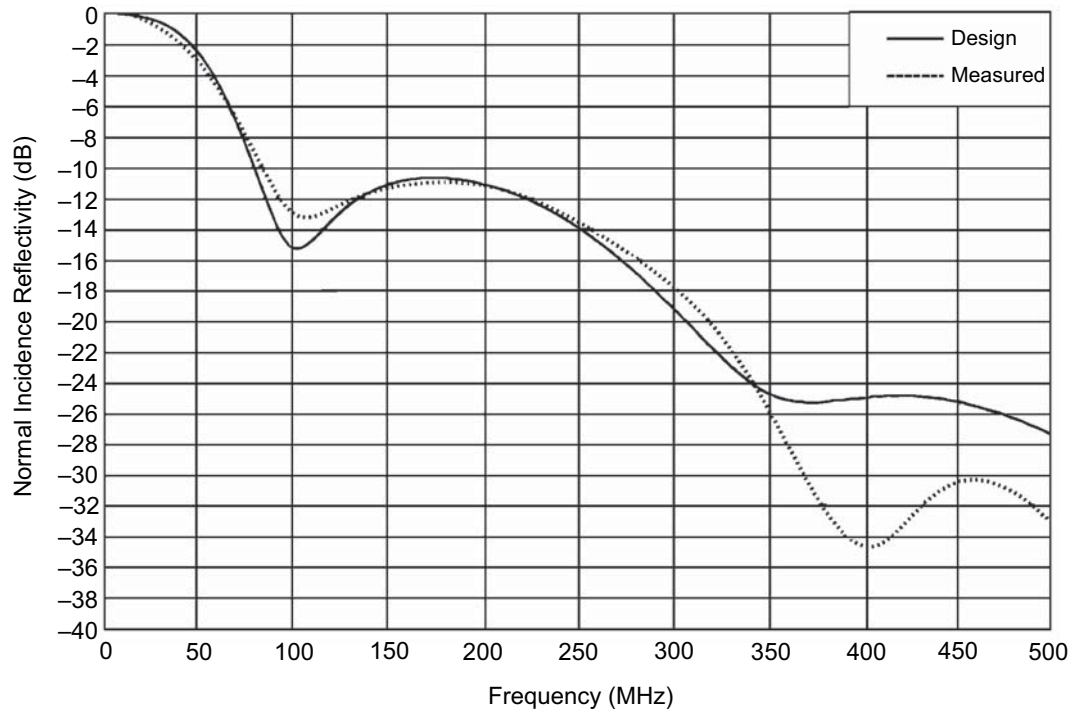


Figure 37—Reflectivity of a 0.6 m (2 ft) pyramidal RF absorber in the frequency range of 30–500 MHz

8. RF absorber performance in ATS, ALC, and semianechoic absorber-lined chambers (SALC)

The final use of the RF absorber characteristics, in the context of this recommended practice, is in the design of actual ATS, ALC, and SALC sites. The development of a methodology to measure the performance of such facilities provides a means not only for assessing the performance of RF absorbers but also for experimentally verifying the design of such facilities.

8.1 Background

For ATS and ALC sites, since they simulate free space, the obvious criterion is to compare the site attenuation with the free-space attenuation. For SALCs, the comparison should be between the site attenuation and the OATS attenuation specified in ANSI C63.4-1992 (see [B30]).

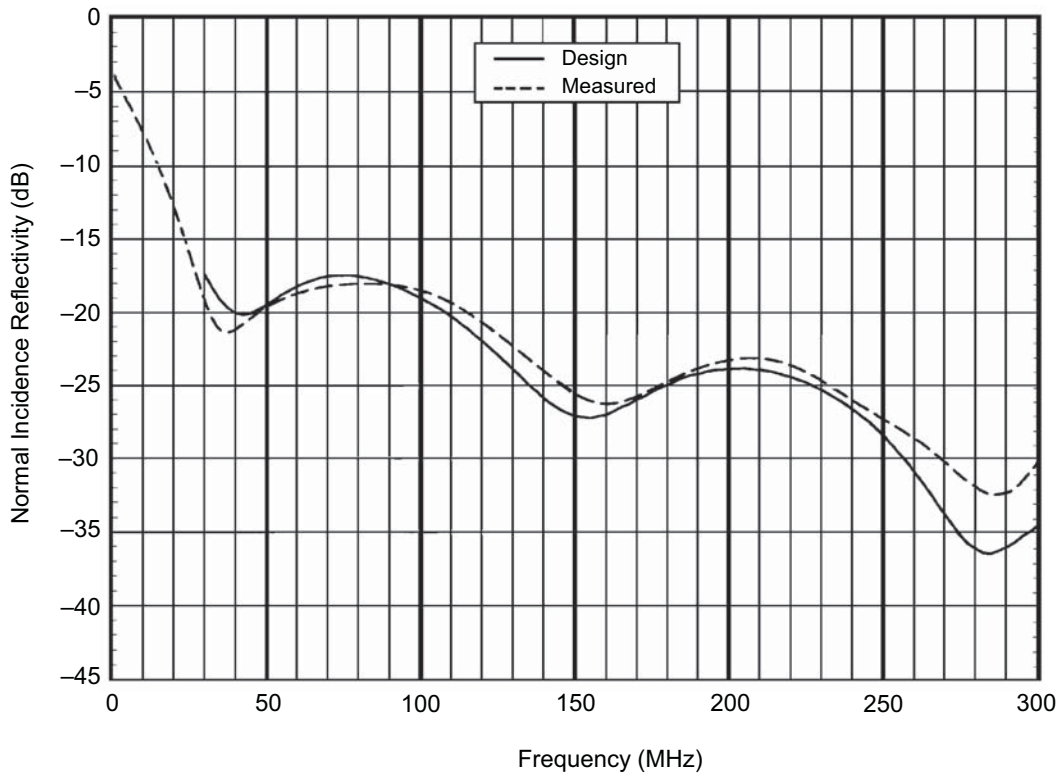


Figure 38—Reflectivity of a 1.2 m (4 ft) pyramidal RF absorber in the frequency range of 30–300 MHz

8.2 ATS and ALC measurement procedure

A figure of merit for evaluating the performance of an ATS and an ALC, which has been used in the literature, is the site-attenuation deviation (SAD). It is defined as the difference, in dB, between the site attenuation measured for a particular receive and transmit antenna position and the attenuation between the same antennas if they were in free space (see [B38]–[B39]). This is a reasonable criterion, since the purpose of the ATS is to simulate free space. To obtain a realistic SAD that reflects the performance of an RF absorber, the RF absorber under test should be mounted on the reflecting surface of an OATS or ALC, in arrays, as normally used (i.e., with the same thicknesses of adhesive, same air gaps between adjacent tiles, same mounting brackets, etc.). These measurements should be performed using both parallel and perpendicular polarizations. The antennas should be positioned at the separation for which the site will be used, such as 3 m, 10 m, or 30 m, and scanned vertically over the ranges specified in ANSI C63.4-1992. As the antennas are scanned vertically, the angles of incidence vary, and can be calculated by the site geometry. Since this method relies on the measurement of the site attenuation, it evaluates the RF absorber over the whole frequency range from 30 MHz to 5 GHz.

Equations are derived to show how the measurement of the performance of an ATS could also be used to calculate the reflectivity of RF absorbers. Since the equations assume that the ground reflections occur in the far field, they are not valid for the low frequencies. This limit is a function of the measurement distance (3 m, 10 m, or 30 m) and the size of the antennas. Since the measurement specified in ANSI C63.4-1992 is specified even though the EUT and the receive antennas are in the near field, the SAD criteria is still valid all the way down to 30 MHz.

In order to derive the equations, the ATS of Figure 39 should be considered. The ground plane is covered with RF absorber material. When calculating the site attenuation, only two waves are considered: the direct

wave and the RF absorber reflected wave, as shown in Figure 39. The site attenuation is given by the following equation:

$$S = V_e - V_i = A - 10\log_{10}|\zeta(\rho, a, G_{eid}, G_{eir})| \tag{29}$$

where

- V_e is the voltage at the transmit (e) antenna terminals.
- V_i is the voltage at the receive (i) antenna terminals.
- A is the test setup transmission factor = $A_{fe} + A_{fi} + A_{cble} + A_{cbli}$.
- A_{fe} is the transmit antenna factor.
- A_{fi} is the receive antenna factor.
- A_{cble} is the transmit antenna cable loss.
- A_{cbli} is the receive antenna cable loss.
- ρ is the magnitude of the equivalent reflection coefficient (ERC).
- a is the angle of the ERC.
- G_{eid} equals $G_{ed}(\theta_{ed}, \phi_{ed})G_{id}(\theta_{id}, \phi_{id})$.
- $G_{ed}(\theta_{ed}, \phi_{ed})$ is the transmit (e) antenna gain for the direct (d) wave.
- θ_{ed}, ϕ_{ed} are the polar angles of the transmit antenna for the direct wave.
- $G_{id}(\theta_{id}, \phi_{id})$ is the receive (i) antenna gain for the direct (d) wave.
- θ_{id}, ϕ_{id} are the polar angles of the receive antenna for the direct wave.
- G_{eir} equals $G_{er}(\theta_{er}, \phi_{er})G_{ir}(\theta_{ir}, \phi_{ir})$.
- $G_{er}(\theta_{er}, \phi_{er})$ is the transmit (e) antenna gain for the reflected (r) wave.
- θ_{er}, ϕ_{er} are the polar angles of the transmit antenna for the reflected wave.
- $G_{ir}(\theta_{ir}, \phi_{ir})$ is the receive (i) antenna gain for the reflected (r) wave.
- θ_{ir}, ϕ_{ir} are the polar angles of the receive antenna for the reflected wave.

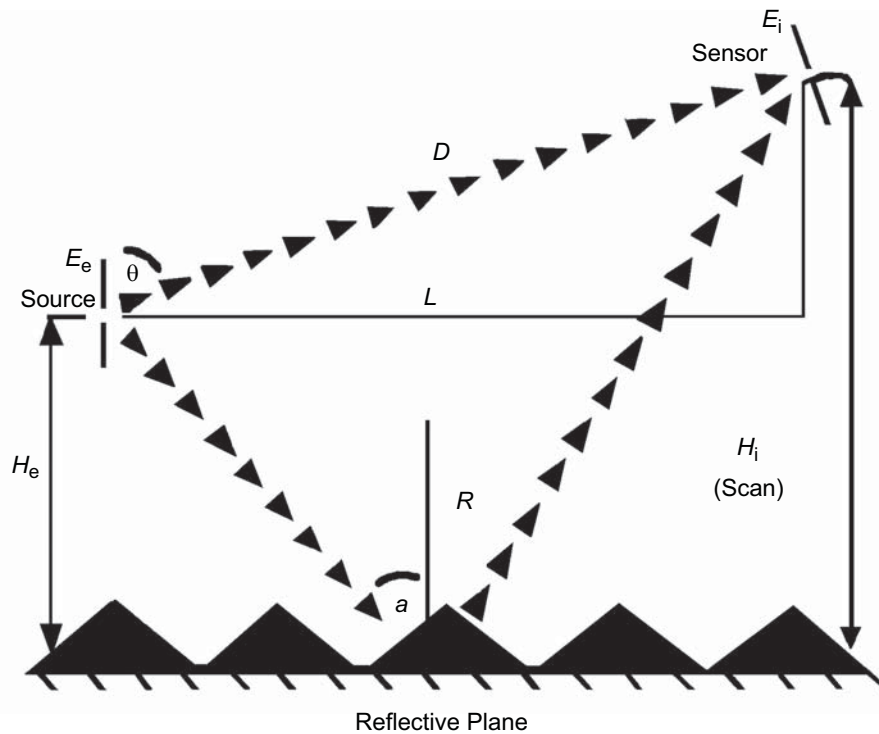


Figure 39—Geometry of the source and sensor on an OATS covered with RF absorber

The RF absorber is characterized by the (complex) ERC,

$$\tau = \rho \varepsilon^{-ja} \quad (30)$$

where

- τ is the complex ERC.
- ρ is the ERC magnitude.
- a is the ERC phase.

The expression under the logarithm in Equation (29) has a modulus of

$$M = |\zeta(\rho, a, G_{\text{eid}}, G_{\text{eir}})|^2 = \left(\frac{G_{\text{eid}}}{D}\right)^2 + \left(\frac{G_{\text{eir}}\rho}{R}\right)^2 + \frac{2\rho G_{\text{eid}}G_{\text{eir}}}{DR} \cos[\beta(R-D) + a] \quad (31)$$

The direct (D) and reflected (R) wave propagation path lengths are given by

$$D = \sqrt{L^2 + (H_i - H_e)^2} \quad (32)$$

$$R = \sqrt{L^2 + (H_i + H_e)^2} \quad (33)$$

where

- L is the horizontal distance between transmit and receive antennas (see Figure 39).
- H_i is the transmit antenna height over the ground plane/RF absorber.
- H_e is the receive antenna height over the ground plane/RF absorber.

The free-space phase constant, β , is given by

$$\beta = \frac{2\pi}{\lambda} = \frac{2\pi f}{3 \cdot 10^8} \quad (34)$$

where

- λ is the wavelength, in m.
- f is the frequency, in Hz.

Equations (29)–(34) can be solved for the unknowns ρ and a , which are the desired parameters. A detailed derivation of these equations is given by Tsaliovich [B38]–[B39].

V_e and V_i are the data obtained during the measurements. The test setup transmission factor, A , can be calculated or measured. In some cases, however, it may be convenient to consider the two antenna factors also as unknowns, and to determine them in the process of obtaining the RF absorber ERC for each particular test configuration. By varying the test conditions, a sufficient number of equations can be obtained to determine all unknown variables. This can be achieved by changing the heights and/or separation distances between the receive and transmit antennas, as well as by replacing the RF absorber of the ATS with a good reflecting ground plane, which is usually already under the RF absorber. By changing simultaneously both the antenna heights and the separation distance, a wide range of angles of incidence can be investigated between 0° and 90° .

There is a hypothesis that only two waves should be considered in the calculation of the site attenuation. For an ATS and layered-type absorbers, this may be a good assumption if diffraction effects from the edges of the site can be neglected or eliminated by the directivity of the antennas used. For pyramidal absorbers, the diffraction from the tips of the pyramids may be significant, especially for high angles of incidence and

high-performance absorbers. For ALC and layered absorbers, there are no diffraction effects from the edge of the site. They are replaced by reflections from all other chamber surfaces, especially the ceiling. The same concern about diffraction from the pyramids of pyramid RF absorbers is still valid, further aggravated by the fact that there are many other surfaces reflecting the incident field. The measurement of the SAD, however, is still a valid criteria to assess the performance of both an ATS and an ALC, since the measurement is done in a realistic setting.

Another hypothesis implicit in the derivation of Equation (29) is that the antennas are in the far field of each other. Clearly, at the low frequency of 30 MHz, this is not true. Therefore, Equation (29) should be considered an approximation. The justification for its use is that actual measurements in ATS and ALC installations are done under the same conditions.

The complex environment of an ALC emphasizes the importance of using simulation tools to make its design more economical. This can only be achieved if the RF absorber's reflectivity contains amplitude and phase information as a function of the angle of incidence, polarization, and frequency.

8.2.1 Test setup

The test setup is the same as for the measurement of the site attenuation for an OATS or ATS. This is specified, in detail, in ANSI C63.4-1992. If other standards are being used, the equivalent procedures apply.

8.2.2 Test procedure

The recommended test configuration is shown in Figure 40. The site-attenuation measurement, S_1 , is performed with the receive antenna at Position 1, with a separation distance of L_1 and an antenna height of H_{i1} , thus providing for the desired angle of incidence, a . From the geometry, the free-space attenuation can be calculated and the SAD can be obtained.

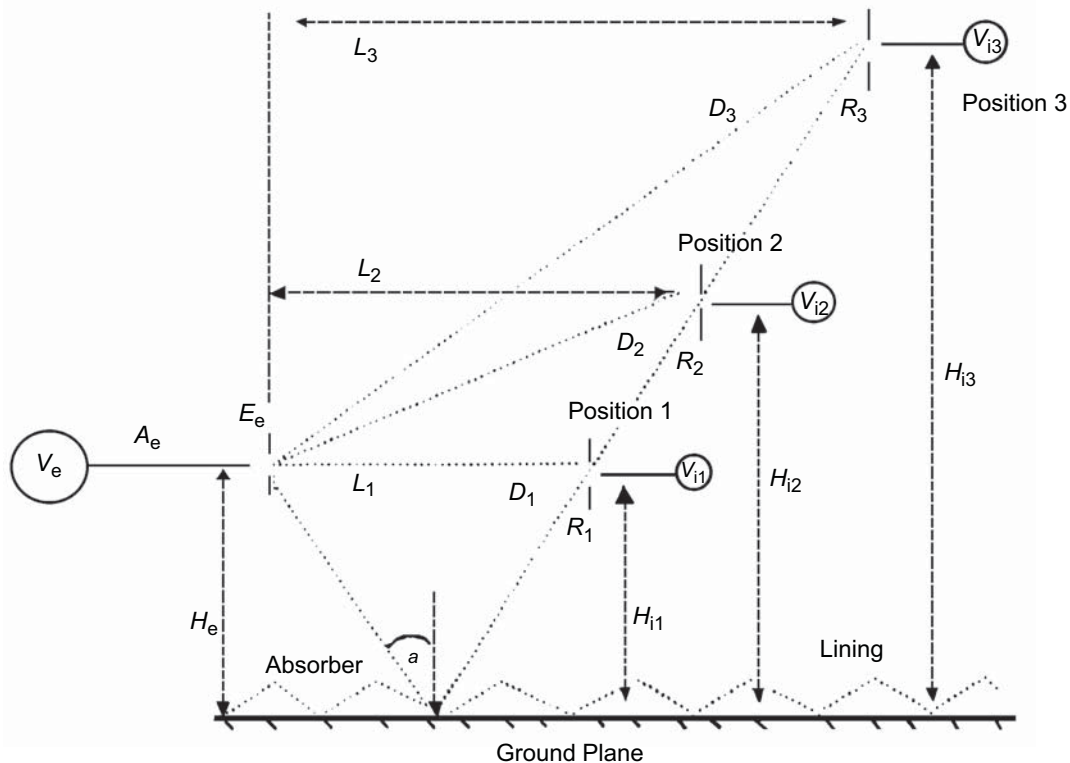


Figure 40—Geometry of the different locations of the source and sensor necessary to obtain enough equations to calculate the complex ERC

To calculate the ERC, more measurements, for the same angle of incidence, α , have to be made to provide enough simultaneous equations. This can be done by repeating the test either with the receive antenna moved to Position 2 or with the receive antenna in the same Position 1, but with the RF absorbers removed (that is, over a metallic ground plane). In the second case, the fact that the ground plane reflection coefficient, τ , is known is used. In the first case, Position 2 is chosen so that the separation distance, L_2 , and antenna height, H_{12} , result in the same angle of incidence, α .

By moving the receive antenna further into a third position, with the same angle of incidence, α , yet another equation can be used, if necessary.

8.2.3 Test results

Figure 41 is an example of measured SAD. The SAD dependence on the receive antenna height is shown for several RF absorber types, measured at 200 MHz. The 0 dB (SAD = 0) dotted horizontal line corresponds to the direct-path, line-of-sight, free-space attenuation obtained by calculation. The tests were performed at a “conventional” OATS, with a metallic ground plane, and at the corresponding ATS, lined with three absorber types: 1.13 m (45 in) pyramids, 0.75 m (30 in) pyramids, and ferrite tiles. The ATS size was 4.1 m × 4.3 m. The site attenuation was measured between two horizontally polarized dipoles with 3 m of separation distance. The transmit antenna was placed at a 2 m height. The site attenuation was measured while the receive antenna height was scanned from 1–4 m over the ground plane. For the specified frequency and test conditions, while the maximum SAD for the OATS is about 10 dB, it is only 3 dB for the 0.75 m (30 in) pyramid-lined ATS, and less than 2 dB for the 1.13 m (45 in) pyramid-lined and ferrite-tile-lined ATS.

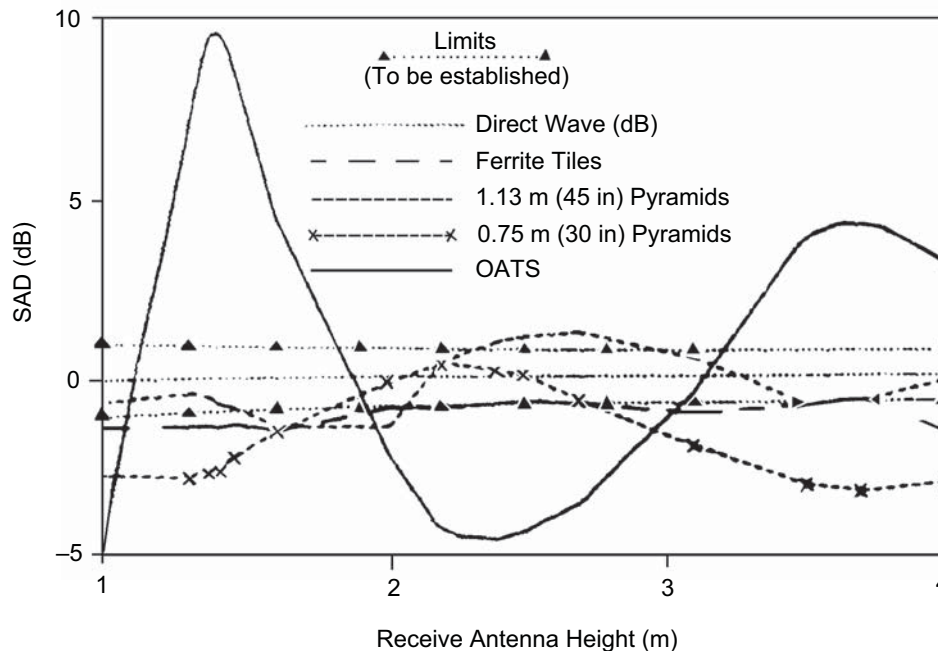


**Figure 41—SAD as a function of the receive antenna height:
 $L = 3$ m, $H_t = 2$ m, and $f = 200$ MHz**

8.3 Semianechoic chamber measurement procedure

For semianechoic chambers, since they simulate an OATS, the proper criteria should be a modified SAD, referred to here as the open-site-attenuation deviation (OSAD). It is defined as the difference, in dB, between the measured site attenuation and the OATS site attenuation specified in ANSI C63.4-1992 (see [B15]) or the standard being used (i.e., CISPR, VDE, etc.).

8.3.1 Test setup

The test setup is the standard setup to measure site attenuation for OATS as specified in ANSI C63.4-1992.

8.3.2 Test procedure

To perform the site-attenuation measurement, the procedure specified in ANSI C63.4-1992 can be followed or an automated procedure can be used (see [B34]). The automated procedure requires the use of broadband antennas for the frequency range of interest, and a spectrum analyzer with a MAX HOLD (store only the maximum reading of all sweeps) capability. The following steps are used:

- a) Set the transmit and receive antennas at the desired antenna separation of 3 m, 10 m, or 30 m.
- b) Set the transmit antenna at the EUT location at 1 m above the ground plane.
- c) Raise the receive antenna to its maximum height, for the antenna separation used, as specified in ANSI C63.4-1992.
- d) Set a spectrum analyzer in the sweep mode over the frequency limits of the measurement bandwidth. The sweep speed should be the highest speed that is compatible with the swept-frequency range. It is generally necessary to use more than one swept-frequency range, and more than one set of broadband antennas, to cover the 30 MHz to 1 GHz frequency range.
- e) Set the spectrum analyzer in MAX HOLD to store only the maximum measured site attenuation.
- f) Lower the transmit antenna slowly to the minimum height specified in ANSI C63.4-1992 for the antenna separation used. The lowering speed of the transmit antenna should be such that the antenna height does not change much on each frequency sweep. Since the site attenuation varies very slowly around its maximum, any error introduced by this procedure should be negligible.

The requirements of steps d) and f) are closely connected. It may be necessary to choose a smaller swept-frequency range to accommodate both requirements.

Step b) should be repeated for different positions on the EUT to cover the volumetric requirements of ANSI C63.4-1992.

8.3.3 Test results

Figure 42 shows the measured site attenuation in the range of 25–200 MHz, using the automated method, for a semianechoic chamber that has a length of 12.8 m, a width of 9.8 m, and a height of 4.5 m. The measurement was conducted using broadband dipoles at a distance of 3 m. The solid line is the measured site attenuation and the dashed line is the calculated ideal OATS site attenuation, as specified in ANSI C63.4-1992, with the antenna factors of the used measurement dipoles included. The difference between the solid and dashed plots is the OSAD. Note that the chamber is within 3 dB of the ANSI C63.4-1992 specified site attenuation above 65 MHz. Below this frequency, the OSAD exceeds ANSI C63.4-1992 by approximately 10 dB, thus showing that the RF absorber is not performing well. Figure 43 shows the same measurements conducted in a factory open area, measuring 32 m × 32 m with a ceiling of 4.5 m, for an antenna separation of 10 m, in the same frequency range. Note the much larger OSAD.

This same technique can be used for fully anechoic chambers. The site attenuation reference to calculate the SAD should be the free-space attenuation instead of ANSI C63.4-1992 for OATS.

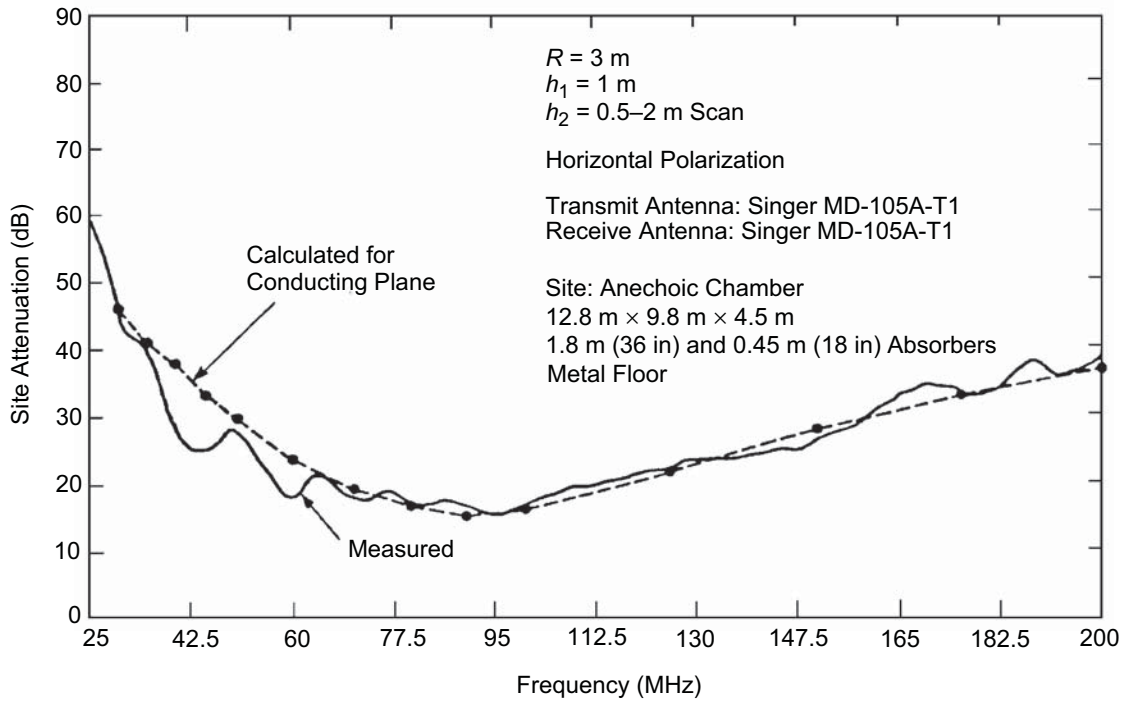


Figure 42—Horizontal polarization site attenuation for 3 m separation in a semianechoic chamber using broadband antennas for 25–200 MHz

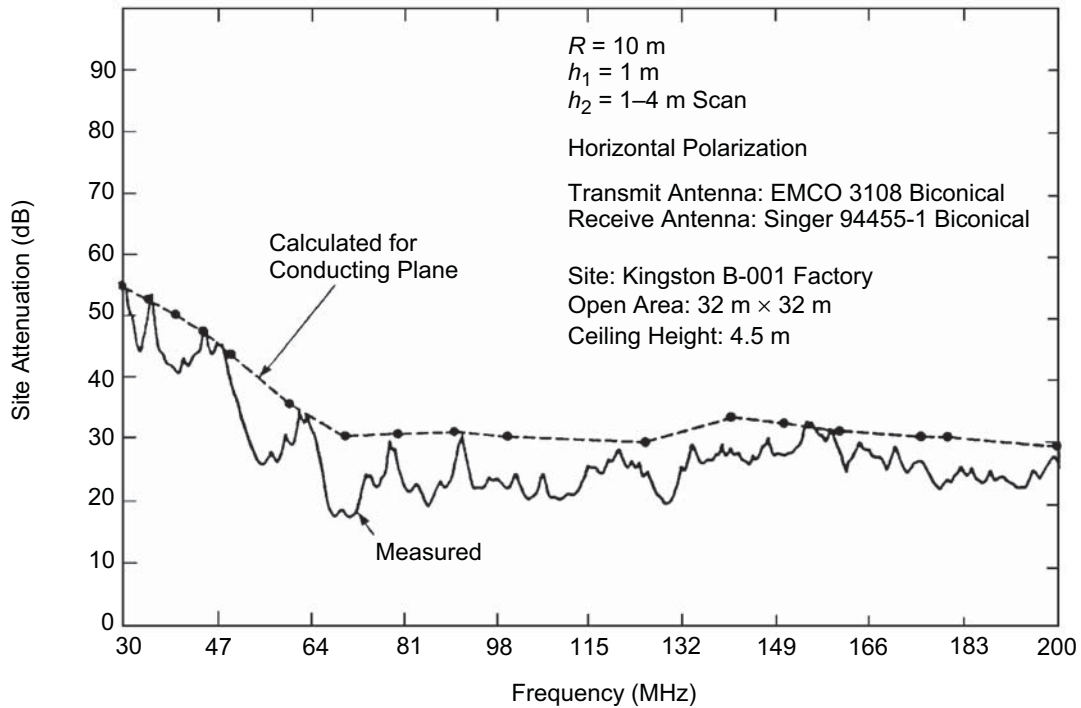


Figure 43—Horizontal polarization site attenuation for 10 m separation in an empty factory using broadband antennas for 30–200 MHz

9. Test reports

9.1 Test report content

Test reports should include all details of the tests performed, so that the tests can be replicated by anyone reasonably skilled in the art. The test report should list all equipment used in making the tests, including model and serial numbers and other identifying features. Drawings or photographs of the test setup are also to be included. Environmental conditions, such as temperature and humidity, should also be noted. The identity of the persons actually making the tests should be noted. Where a manufacturer codifies absorbing material during the various stages of processing, that information should be part of the test report.

9.2 Test report disposition

Test reports should be maintained by the organization that performed the tests for at least ten years after the obsolescence of the product.

10. Bibliography

These publications are for information only and are not essential for application of this recommended practice. They provide further details on the discussed topics.

[B1] Adam, S. F., *Microwave Theory and Applications*. Englewood Cliffs, NJ: Prentice-Hall, 1969, ch. 3, 5, and 6.

[B2] Application Note 62, "TDR Fundamentals," Hewlett-Packard, 1988.

[B3] Application Note 150, "Spectrum Analysis Basics," Hewlett-Packard, 1989.

[B4] Application Note 150-3, "Spectrum Analysis...Swept Frequency Measurements," Hewlett-Packard, 1974.

[B5] Ari, N., Hansen, D., and Garbe, H., "Analysis and Measurement of Electromagnetic Scattering by Pyramidal Absorbers," *Proceedings of the 1989 Zurich International Symposium and Technical Exhibition on EMC*, pp. 301–304.

[B6] Cruzan, O. R., and Garver, R. V., "Characteristic Impedance of Rectangular Coaxial Transmission Lines," *IEEE Transactions on Microwave Theory and Techniques*, vol. MTT-12, no. 5, pp. 488–495, Sept. 1964.

[B7] Hansen, D., Ari, N., and Garbe, H., "An Investigation into the Scattering and Radiation Characteristic of RF-Absorbers," *Proceedings of the 1988 IEEE International Symposium on EMC*, pp. 99–105.

[B8] Harrington, R. F., *Time-Harmonic Electromagnetic Fields*. New York: McGraw-Hill, 1961, ch. 4.

[B9] Haykin, S., *Communication Systems, 2nd Ed.* New York: John Willey & Sons, Inc., 1983, pp. 60–66.

[B10] Hiatt, R. E., Knott, E. F., and Senior, T. B. A., "A Study of VHF Absorbers and Anechoic Rooms," *Report No. 5391-1-F*, The University of Michigan/NASA, Langley Research Center, Langley Station, Hampton, Virginia.

[B11] Holloway, C. F., and Kuester, E. L., "Measurement Techniques for Determining the Reflection Coefficient and Complex Permittivity of Pyramid Cone Absorbers," *Scientific Report No. 101*, University of Colorado Electromagnetics Laboratory, Boulder, CO, Aug. 1990.

[B12] “HP 70300A Tracking Generator: Automatic Stimulus-Response Measurements,” *RF and Microwave Symposium Paper*, Hewlett-Packard, 1986.

[B13] “Introductory User’s Guide—HP 8510C Network Analyzer,” Hewlett-Packard, 1991.

[B14] Johnk, R., Ondrejka, A., Tofani, S., and Kanda, M., “Time-Domain Measurements of the Electromagnetic Backscatter of Pyramidal Absorbers and Metallic Plates,” *IEEE Transactions on Electromagnetic Compatibility*, vol. 35, no. 4, pp. 429–433, Nov. 1993.

[B15] Kanda, M., “Standard Electric Field Strength From an Open-Ended Waveguide in an Anechoic Chamber,” *Workshop on RF Absorber Evaluation Techniques and Application Experience*, Denver, CO, May 1989.

[B16] Krauss, J. D., *Antennas, 2nd Ed.* New York: McGraw Hill, 1988, p. 60.

[B17] Kuester, E. F., and Holloway, C. L., “Improved Low-Frequency Performance of Pyramid-Cone Absorbers for Application in Semi-Anechoic Chambers,” *Proceedings of the 1989 IEEE International Symposium on EMC*, pp. 394–398.

[B18] Kuester, E. F., and Holloway, C. L., “Plane-Wave Reflection from Inhomogeneous Uniaxially Anisotropic Absorbing Dielectric Layers,” *Scientific Report No. 97*, Electromagnetics Laboratory, Department of Electrical and Computer Engineering, University of Colorado, Boulder, CO, May 1989.

[B19] Lawton, R. A., and Ondrejka, A. R., “Antennas and the Associated Time Domain Range for the Measurement of Impulsive Fields,” *NBS Technical Note 1008*, Nov. 1978.

[B20] Mayer, F., and Chaumat, J. P., “Absorptive Dielectromagnetic Materials for RAM and Anechoic Chambers,” *Workshop on Absorptive Evaluation, 1990 IEEE International Symposium on EMC*.

[B21] Mayer, F., and Chaumat, J. P., “Dielectromagnetic Materials for Absorber Lined Chambers,” *Proceedings of the 1991 Zurich International Symposium on EMC*, pp. 107–109, Mar. 1991.

[B22] Nahman, N. S., and Guillaume, M. E., “Deconvolution of Time Domain Waveforms in the Presence of Noise,” *NBS Technical Note 1047*, Oct. 1981.

[B23] Nicholson, A. M., and Ross, G. F., “Measurement of the Intrinsic Properties of Materials by Time-Domain Techniques,” *IEEE Transactions on Instrumentation and Measurements*, vol. IM-19, no. 4, pp. 377–382, Nov. 1970.

[B24] Oppenheim, A. V., and Schaffer, R. W., *Digital Signal Processing*. Englewood Cliffs, NJ: Prentice-Hall, 1975, ch. 3 and 6.

[B25] Paul, C. R., *Introduction to Electromagnetic Compatibility*. New York: John Wiley & Sons, Inc., 1992, ch. 5.

[B26] Perini, J., and Cohen, L. S., “Design of Broad-Band Radar-Absorbing Materials for Large Angles of Incidence,” *IEEE Transactions on Electromagnetic Compatibility*, vol. 35, no. 2, pp. 223-230, May 1993.⁵

[B27] Product Note 8508-1, “Vector Voltmeter User’s Guide,” Hewlett-Packard, 1988.

[B28] Product Note 8510-3, “Materials Measurement,” Hewlett Packard.

⁵The equations on this paper have been programmed in FORTRAN and are available upon request (see J. Perini’s address on the paper, and send a formatted diskette (700K minimum) with a self-addressed, stamped envelope).

- [B29] Pues, H., "Electromagnetic Absorber Measurement in a Large Waveguide," *Proceedings of the 8th International Zurich Symposium on EMC*, pp. 253–258, Mar. 1989.
- [B30] Pues, H., "Electromagnetic Wave Absorber Measurement in a Large Coax," *Proceedings of the 9th International Zurich Symposium on EMC*, pp. 541–546, Mar. 1991.
- [B31] Pues, H., "Error-Corrected Wideband Reflectivity Measurement of Microwave Absorbing Materials Using the Arch Technique," *Mikrowellen Magazin*, vol. 14, no. 6, pp. 524–526, 1988.
- [B32] Ramo, S., Whinnery, J. R., and Van Duzer, T., *Fields and Waves in Communication Electronics*. New York: John Wiley & Sons, Inc., 1965, pp. 446–448.
- [B33] "Scaler Network Analysis: An Attractive and Cost Effective Technique for Testing Microwave Components," *RF and Microwave Symposium Paper*, Hewlett-Packard, 1985.
- [B34] Smith, A. A., German, R. F., and Pate, J. B., "Calculation of Site Attenuation from Antenna Factors," *IEEE Transactions on Electromagnetic Compatibility*, vol. EMC-24, no. 3, pp. 316–322, Aug. 1982.
- [B35] Tofani, S., Ondrejka, A. R., and Kanda, M., "A Time-Domain Method for Characterizing the Reflection Coefficient of Absorbing Materials from 30 to 1000 MHz," *IEEE Transactions on Electromagnetic Compatibility*, vol. 33, no. 3, Aug. 1991.
- [B36] Tofani, S., Ondrejka, A. R., and Kanda, M., "Bistatic Scattering from Absorbing Materials from 30 to 1000 MHz," *IEEE Transactions on Electromagnetic Compatibility*, to be published.
- [B37] Tsaliovich, A., "Absorber-Lined Open-Area Test Site—A New Type of EMC Test Facility," *Proceedings of the 1988 IEEE International Symposium on EMC*, pp. 106–111, 1988.
- [B38] Tsaliovich, A., "Evaluation of RF Anechoic Room Absorbers in the 30–1000 MHz Range," *Proceedings of the 1986 IEEE International Symposium on EMC*, pp. 140–144, 1986.
- [B39] Tsaliovich, A., "RF Absorber Qualification Criteria and Measurement Techniques," *Proceedings of the 1990 IEEE International Symposium on EMC*, 1990.
- [B40] Wait, J. R., *Electromagnetic Waves in Stratified Medium, 2nd Ed.* Oxford: Pergamon, 1970, ch. 2.